

**Enantiomer separation by
ultrafiltration of enantioselective micelles in
multistage systems**

BIJLICHTEK
LANDBOUWUNIVERSITEIT
WAGENINGEN

Promotoren: dr. ir. K. van 't Riet
voormalig hoogleraar levensmiddelenproceskunde
dr. ir. J.T.F. Keurentjes
hoogleraar proces- en apparaatontwerp, Technische Universiteit Eindhoven

Co-promotor: dr. ir. A. van der Padt
universitair docent, verbonden aan het departement
levensmiddelentechnologie, leerstoelgroep levensmiddelenproceskunde

AN08201, 2520

Pieter Overdevest

**Enantiomer separation by
ultrafiltration of enantioselective micelles in
multistage systems**

Proefschrift

ter verkrijging van de graad van doctor op gezag van de rector magnificus
van Wageningen Universiteit, dr. ir. L. Speelman
in het openbaar te verdedigen op maandag 4 september 2000
des namiddags te vier uur in de Aula.

im 929486

DANKWOORD

Wat een tijd! Jaren vlogen voorbij. Met veel plezier heb ik gewerkt aan het onderzoek en dit boekje. Graag wil ik een aantal mensen bedanken voor hun onontbeerlijke hulp.

Albert, veel heb ik aan je te danken. Zonder jou inspirerende begeleiding had ik dit mooie resultaat niet kunnen bereiken. Daarnaast heeft je grote sociale en wetenschappelijke betrokkenheid bij mij en mijn onderzoek ervoor gezorgd dat ik met zeer goede herinneringen terugdenk aan mijn promotietijd.

Jos, bedankt voor je grote enthousiasme tijdens onze vele bijeenkomsten en voor de deuren die dankzij jou opengingen. Daarnaast waardeer ik jouw grote betrokkenheid bij mijn onderzoek. Klaas, ik wil je bedanken voor de grote vrijheid die je me hebt gegeven. Onze bijeenkomsten waren zeer inspirerend en motiverend.

Floor, met veel plezier heb ik vier jaar naast je gezeten en met jou o.a. gebabbeld over oligosacchariden, Björk, de nieuwste bioscoop- en videofilms, Matlab, en enantiomeren. Ondanks dat we in bepaalde opzichten totaal verschillend zijn, ontstond er toch een bijzondere band tussen ons. Ed, ik vond het bijzonder prettig met jou op een kamer te hebben gezeten. Ik waardeer de oprechte interesse die je in andermans werk toont; vaak gaf je mij een andere kijk op mijn resultaten. Erik, vol van hardlopen en wetenschap, over beide nooit zonder gesprekstof. Anneke, samen met onze kamergenoten hebben we een aantal perfecte etentjes gehad; met name Eduard's preitaart is in positieve zin noemenswaardig. Anja, vier jaar lang wist je mijn besprekingen met Albert altijd op een leuke manier te 'verstoren'. Bedankt dat ik altijd mijn verhalen bij jou kwijt kon.

Theo, onze samenwerking was uniek. Met veel plezier kwam ik altijd naar OC om aan ons project te werken, bedankt voor jouw bijdrage aan mijn onderzoek. Ernst, Ton, Han, Arie en Harm, bedankt voor jullie bijdrage aan mijn onderzoek en onze bijeenkomsten. Ik vond het zeer leerzaam om mijn onderzoek vanuit verschillende disciplines te benaderen.

Frans en Martien, bedankt voor jullie enthousiaste bijdrage aan onze besprekingen, waardoor we meer duidelijkheid hebben gekregen in de colloïd-chemische achtergrond van mijn onderzoek. Remko, bedankt voor je hulp bij de lichtverstrooiingsexperimenten.

Mijn onderzoek werd gefinancierd door de NWO-stichting STW, Akzo Nobel, en DSM. Nico Boots (STW), Jos Keurentjes, Karin Dirix, Rob Zsom, Matthias Wessling (Akzo Nobel), Hans Kierkels, Veerle Cauwenberg, Wytze Meindersma, en Wouter Pronk (DSM), bedankt

voor jullie bijdrage aan de gebruikerscommissievergaderingen en voor de hartelijke ontvangst tijdens onze bezoeken aan Akzo Nobel en DSM voor een vergadering of presentatie.

Een zevental studenten heeft mij geholpen bij mijn onderzoek in de vorm van een afstudeervak. Lisette, Joris-Jan, Dick, Leon, Maarten en Mark, bedankt voor jullie geweldige inzet en bijdrage aan dit proefschrift. Angel, thank you very much for your contribution to my research. De verfrissende ideeën waar jullie mee aankwamen, op het tweede bordes en soms zelfs aan de bar, zijn een goede herinnering die ik aan onze samenwerking heb overgehouden. Top!

Al tijdens mijn eigen afstudeervak bij Proceskunde merkte ik dat Proceskunde uit een zeer hechte groep mensen bestaat, die voor elkaar klaar staan. Deze goede verstandhouding haalde mij al snel over de streep toen ik voor de keuze stond om bij Proceskunde een promotieonderzoek te doen. Bedankt voor de gezellige afleiding tijdens en na het werk. Gerrit en Jos, ik heb zelfs goede herinneringen aan die afbeulende fietstochten die jullie organiseerden in de Ardennen. De tocht was altijd een uitdaging om aan te beginnen, maar bijna onmogelijk om uit te fietsen. Dankzij jullie mentale en fysieke steun, ben ik telkens fietsend aangekomen. Jos, ook bedankt voor de eenvoudige oplossingen die je altijd had voor experimentele problemen. Joyce, Hedy, en Lotte, bedankt voor jullie ondersteuning en de plezierige tijd. Wat betreft verdere ondersteuning ben ik veel dank verschuldigd aan de medewerkers van de werkplaats, het magazijn, de mediaservice en I&D.

Harm, bedankt voor je hulp bij het drukklaar maken van dit proefschrift en het samenstellen van de kافت.

Graag wil ik dit dankwoord afsluiten met het danken van een aantal voor mij heel belangrijke mensen. Aad, dat de laatste lootjes het zwaarst wegen, geldt zeker voor dit proefschrift. Dankzij jou hulp is het proefschrift tijdig afgekomen en kan ik het nog voor mijn 30ste verdedigen. Ik heb grote waardering voor jouw hulp. Pa en Ma, jullie hebben mij al bijna 30 jaar met raad en daad bijgestaan. Dankzij jullie steun heb ik deze mijlpaal kunnen bereiken. Ik heb veel geleerd van het enthousiasme waarmee jullie in het leven staan. Ika Mai, bedankt voor je geduld, je steun, en je luisterend oor. Jij bent de zon in mijn leven.

Pieter

ISBN 90-5808-274-1

Stellingen

1. Omdat dimensieloze parameters correlaties aantonen tussen procesparameters, zijn ze een krachtig instrument bij de opschaling van een proces (dit proefschrift).
2. Aangezien een moleculaire scheiding nooit volledig is, is het onduidelijk wat Storti *et al.* bedoelen met *complete separation regions*.
Storti, G.; Mazzotti, M.; Morbidelli, M.; Carrà, S. *AIChE J.* **1993**, *39*, 471.
3. Hoewel de tegenwoordige optimalisatietechnieken het gebruik van extractiefactoren overbodig maken, geven deze factoren wel de noodzakelijke inzichten waarom bepaalde ontwerpen wel of niet succesvol zijn.
4. *Experimental design* ter minimalisering van betrouwbaarheidsintervallen van parameters is onbruikbaar voor niet-lineaire modellen.
5. In tegenstelling tot wat Alper *et al.* schrijven, leiden Monte Carlo simulaties niet altijd tot goede schattingen van betrouwbaarheidsintervallen van afhankelijke parameters; in die gevallen kan reparameterisatie van het model wel leiden tot goede schattingen van betrouwbaarheidsintervallen.
Alper, J.S.; Gelb, R.I. *J. Phys. Chem.* **1990**, *94*, 4747.
6. Het bestaan van een vervolg van een speelfilm pleit meer voor de kwaliteit van de eerste speelfilm dan voor die van de vervolgfilm(s).
7. De ontwikkelingen in de biotechnologie beleven een revolutie. Echter, de maatschappelijke acceptatie van biotechnologie volgt een evolutionair pad.
8. De Nederlandse hyacintenkweek wordt serieus bedreigd door opoffering van, voor Nederland unieke, geestgronden aan verstedelijking en natuurontwikkeling.
9. Aangezien de zuurgraad toeneemt met afnemende getalswaarde (pH), is het beter om van alkaligraad te spreken.
10. Soms lijkt het zo te zijn dat netwerken maar net werken.

Stellingen behorende bij het proefschrift:

Enantiomer separation by ultrafiltration of enantioselective micelles in multistage systems

CONTENTS

Chapter		Page
1	Introduction	1
2	Complexation Modeling	9
3	Complexation and Regeneration	35
4	Complexation Kinetics	51
5	Model Validation	67
6	Concluding Remarks	85
	Summary	109
	Samenvatting	111
	Curriculum vitae	113

Voor mijn ouders

Voor Ika Maí

1

INTRODUCTION

Multidisciplinary research in separation technology development

An increasing demand for optically pure products has intensified the search for new separation processes. At Wageningen University a new separation system is under development that is based on the ultrafiltration of nonionic micelles containing chiral Cu^{II} -amino acid derivative selector molecules. This research focuses on the separation of amino acid enantiomers both at a molecular level and on a process scale. At the Laboratory of Organic Chemistry, molecular interactions taking place in the diastereomeric complex formation are investigated by minor modifications in either the chiral selector or the racemic substrate. Quantum mechanical calculations have been performed on model compounds to study this diastereomeric complex in more detail. At the Food and Bioprocess Engineering Group, the separation performance has been studied as a function of pH which shows that Langmuir isotherms describe the competitive complexation of phenylalanine (Phe) enantiomers by the chiral selector. The validated model has been used to design a cascaded counter-current separation system capable of 99% resolution of racemic mixtures. This cascaded ultrafiltration (UF) system enables enantiomer separation in systems that are essentially aqueous, which may prove to be advantageous for the development of new separation processes preserving the environment. Besides the separation of enantiomers this cascaded system provides a straightforward technology to a 99% separation or removal of aqueous solutes, which are difficult to separate based on size exclusion.

A part of this chapter has been published as part of P.E.M. Overdevest and A. van der Padt, 'Optically pure compounds from ultrafiltration' *CHEMTECH* 1999, 29, no. 12, 17.

An increasing demand for optically pure products

The desired biological activity of chiral compounds is often caused by only one enantiomer of a pair of enantiomers (figure 1). Consequently, use of only the active enantiomer is preferred, since the other one can have no effect, undesired effects, or can even be harmful. In May 1992 the current move to single enantiomer drugs received a push when the FDA issued a policy statement [1], which stimulated pharmaceutical-, food-, and agrochemical industries to develop methods for the production of optically pure compounds.

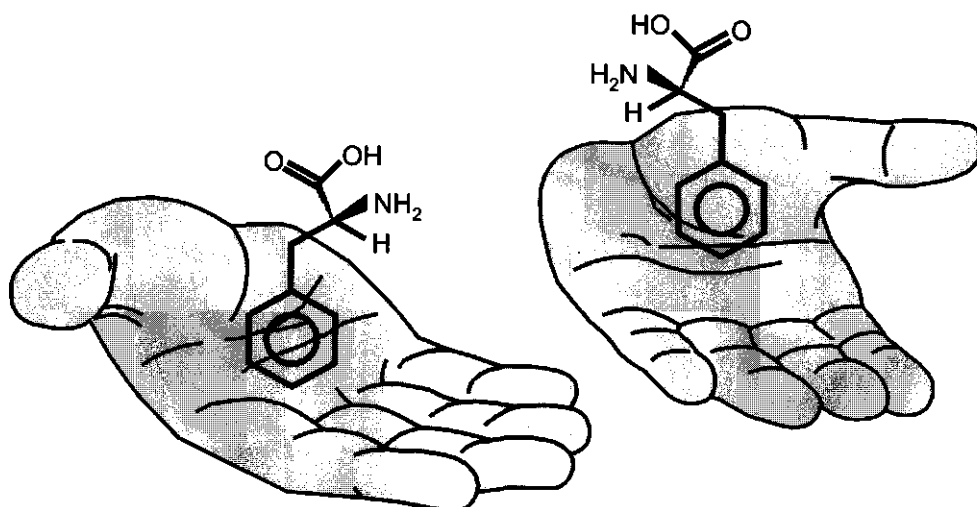


Figure 1. Just like our hands, enantiomers are each others mirror image.

The most obvious source for these compounds is the chiral pool, relatively inexpensive, optically pure natural compounds [2]. However, the limited number of compounds in this pool requires modification or the total synthesis by either an enantioselective chemical or enzymatic route to obtain the desired product. An appropriate route must to be developed for each compound because of substrate specificity, which leads to considerable costs and increased development time [3]. As an alternative, the usually less expensive synthesis of racemic mixtures, followed by a separation step, would isolate both optically pure isomers. Nonchiral (symmetric) synthesis followed by a separation step becomes a more attractive

route if a multistep chiral (asymmetric) synthesis results in very low yields or when there is a market for both isomers.

Various ways to separate racemic mixtures

Although symmetric synthesis is usually less demanding than asymmetric synthesis, separation of enantiomers is frequently not trivial, because their physical properties only differ in chiral media. Conventionally, large scale production of optically pure compounds is based on diastereomeric salt formation [4]. This technique involves many processing steps that result in high energy consumption and significant product losses. An alternative process uses membranes to resolve enantiomers, can be operated continuously at ambient temperatures, and is easily scaled up, making it attractive and cost-efficient. Several kinds of enantioselective membranes can be used to separate enantiomers: membranes containing proteins [5,6] or chiral polymers [7,8], molecular imprinted membranes [9,10], and supported [11,12] or emulsion [13,14] liquid membranes. Non-enantioselective membranes can be used to retain two (im)miscible phases of which at least one is enantioselective [15,16].

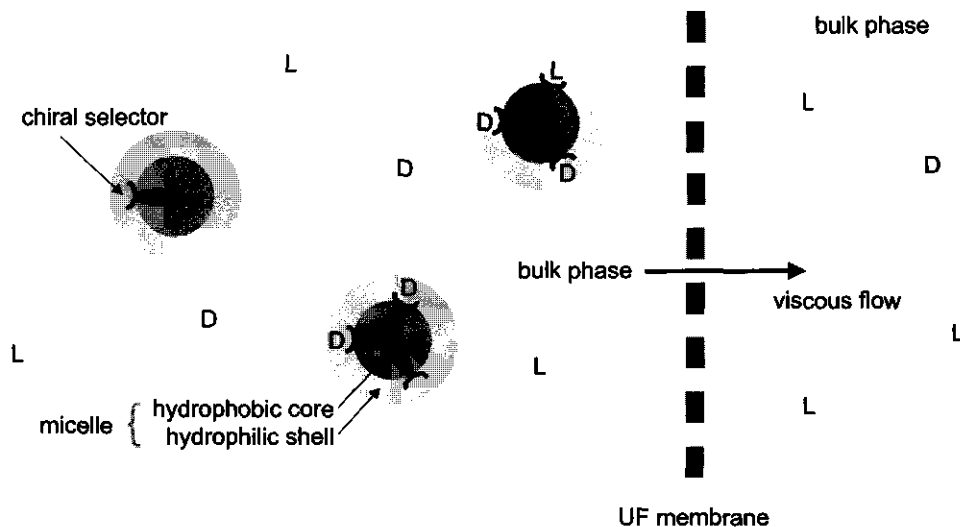


Figure 2. Enantiomer separation by ultrafiltration of enantioselective micelles.

Enantiomer separation by UF of enantioselective micelles

In our research we focus on the second type of membrane application. At Wageningen University the concept of Micelle-Enhanced UltraFiltration (MEUF) is used to separate enantiomers [17]. MEUF combines high permeate flows with the possibility to separate low molecular weight components depending on their affinity for the micelle. MEUF has already been used for the removal of small organic compounds and for the separation and removal of heavy metals from aqueous streams [18,19]. The pore size of the ultrafiltration membrane is small enough to reject the micelles, however, large enough to pass all other unbound aqueous solutes (figure 2).

In our studies, the surfactants forming the microheterogeneous medium (in our case micelles) have been nonionic and achiral; therefore a chiral co-surfactant (chiral selector) is required. The studied chiral selector is cholesteryl-L-glutamate (figure 3). The selector can form ternary chelate complexes with a Cu^{II} ion and a D- or L-amino acid (racemic test compounds). The enantioselectivity of the chiral selector molecules is related to the difference in stability of the two diastereomeric complexes. During filtration the unbound enantiomers pass the membrane, whereas the micelles – including chiral selectors and bound enantiomers – are retained.

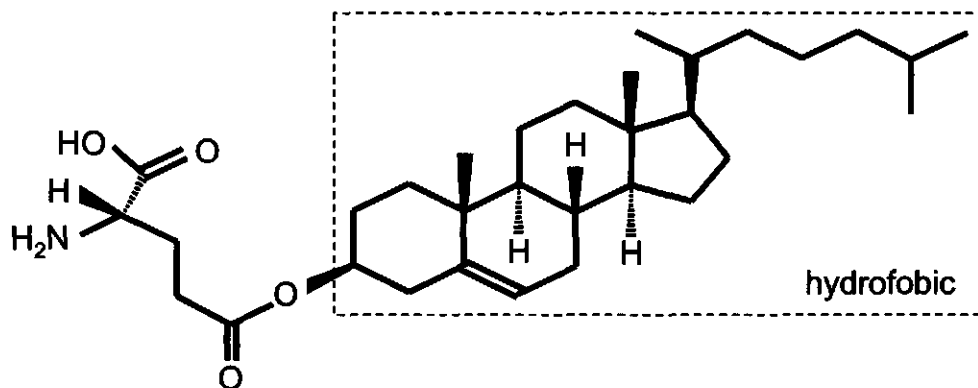


Figure 3. Chiral selector: cholesteryl-L-glutamate.

The separation can be quantified by the enantiomeric excess of the micelles, $ee_{CS} = |q_D - q_L| / (q_D + q_L) \cdot 100\%$ and of the aqueous bulk phase, $ee_B = |c_D - c_L| / (c_D + c_L) \cdot 100\%$, where c and q are the unbound and bound concentrations, respectively. Two aspects of this system should be distinguished: the affinity of the selector for the enantiomers K_D and K_L , and the enantioselectivity of the selector for the enantiomers. The operational enantioselectivity $\alpha_{D/L,op}$ is defined as follows:

$$\alpha_{D/L,op} = \frac{q_D / c_D}{q_L / c_L} \quad (-) \quad (1)$$

According to Langmuir isotherms, the operational enantioselectivity can be rewritten into the intrinsic enantioselectivity, $\alpha_{D/L,int} = K_D / K_L$. Thus, an enantioselectivity larger than one defines a preference of the selector for the D-enantiomer.

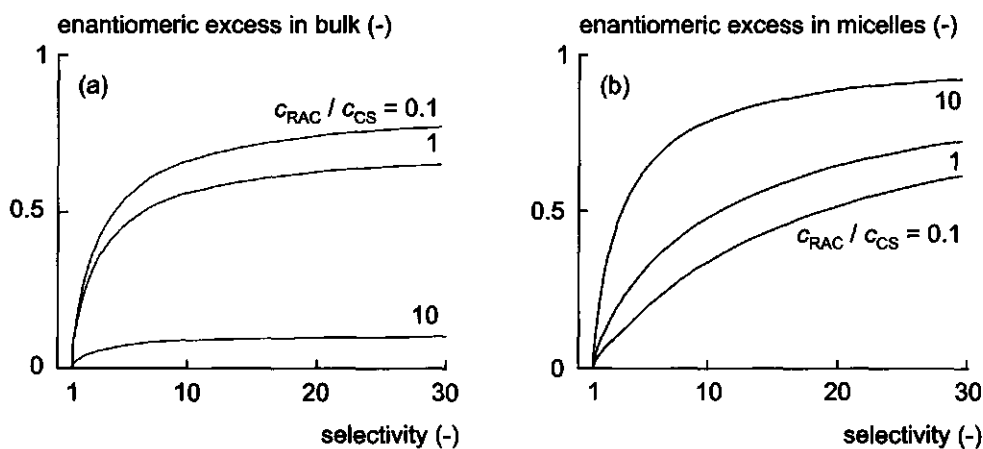


Figure 4. Calculated enantiomer separation in bulk (a) and micelles (b) in a single stage at various racemic mixture and selector concentrations, c_{RAC} and c_{CS} , respectively. The enantiomer complexation can be described by multicomponent Langmuir isotherms.

A cascaded system to fulfill the separation of a racemic mixture

Single stage calculations have shown that a high enantioselectivity alone is not sufficient to acquire both enantiomers in optically pure form (figure 4). Both ee_{CS} and ee_B depend on the ratio of the racemic mixture concentration and the chiral selector concentration. An excess amount of selectors results in an enriched bulk phase. However, the micelles are not enantiomerically enriched due to the surplus of sites (low ee_{CS}). Evidently, a deficiency of selector molecules results in a low ee_B and a high ee_{CS} , due to the competitive nature of the Langmuir complexation.

In order to reach 99% separation of the racemic mixture a multistage separation process is required (figure 5). This system is operated in a counter-current mode, analogous to conventional extraction and distillation processes. Here, the enantioselective micellar phase flows in opposite direction of the bulk phase. In each stage an UF membrane separates the micellar phase from its coexisting aqueous bulk phase.

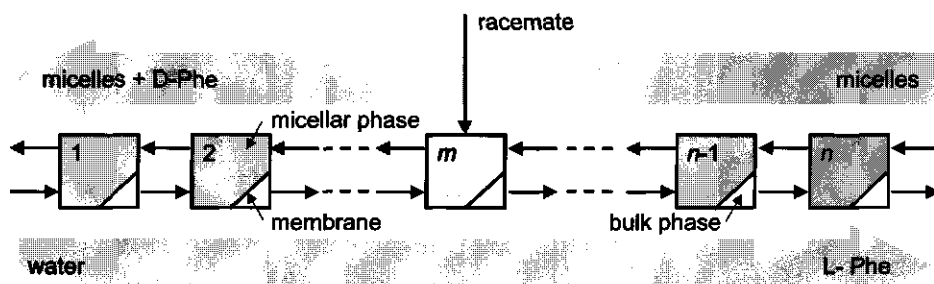


Figure 5. Cascaded system applying the counter-current principle for the 99% separation of racemic mixtures.

Outline of this thesis

In order to design a cascaded system capable of a complete (99⁺%) separation of racemic mixtures into two optically pure compounds, an adequate model is required that describes the separation in this system. The isotherms describing the chelate complexation of D,L-Phe by Cu^{II}-cholesteryl-L-glutamate in nonionic micelles are discussed in chapter 2. Since the interactions between enantiomers, Cu^{II} and enantioselective micelles are pH dependent, this dependency has been studied to optimize both separation and regeneration processes (chapter 3). Kinetic data of these interactions are essential for the process design, *e.g.* to optimize the residence time of the micelles in each stage. This is discussed in chapter 4. Subsequently, the developed separation model is tested for validity using a cascaded system at lab-scale. Moreover, the separation concept and this model are tested at bench-scale using an industrial membrane module (chapter 5). Finally, in chapter 6 the cascaded process is further studied through sensitivity analyses of its separation performance using the dimensionless numbers of the validated model.

References

- (1) FDA's policy statement *Chirality* **1992**, 4, 338.
- (2) Sheldon, R. A. *Chirality: industrial synthesis of optically active compounds*; Marcel Dekker: New York, **1993**.
- (3) Keurentjes, J. T. F.; Nabuurs, L. J. W. M.; Vegter, E. A. *J. Membr. Sci.* **1996**, 113, 351.
- (4) *Chirality in industry I & II: Development in the manufacture and applications of optically active compounds*; Collins, A. N.; Sheldrake, G. N.; Crosby, J., Eds.; John Wiley & Sons: Chichester, **1992 & 1997**.
- (5) Higuchi, A.; Hashimoto, T.; Yonehara, M.; Kubota, N.; Watanabe, K.; Uemiya, S.; Kojima, T.; Hara, M. *J. Membr. Sci.* **1997**, 130, 31.
- (6) Lakshmi, B. B.; Martin, C. R. *Nature* **1997**, 388, 758.
- (7) Aoki, T.; Ohshima, M.; Shinohara, K. I.; Kaneko, T.; Oikawa, E. *Polymer* **1997**, 38, 235.
- (8) Tone, S.; Masawaki, T.; Eguchi, K. *J. Membr. Sci.* **1996**, 118, 31.

- (9) Yoshikawa, M.; Izumi, J. I.; Kitao, T. *Polym. J.* **1997**, *29*, 205.
- (10) Allender, C. J.; Brain, K. R.; Heard, C. M. *Chirality* **1997**, *9*, 233.
- (11) Ersoz, M.; Vural, U. S.; Okdan, A.; Pehlivan, E.; Yildiz, S. *J. Membr. Sci.* **1995**, *104*, 263.
- (12) Shinbo, T.; Yamaguchi, T.; Yanagishita, H.; Sakaki, K.; Kitamoto, D.; Sugiura, M. *J. Membr. Sci.* **1993**, *84*, 241.
- (13) Pickering, P. J.; Chaudhuri, J. B. *J. Membr. Sci.* **1997**, *127*, 115.
- (14) Pickering, P. J.; Chaudhuri, J. B. *Chirality* **1997**, *9*, 261.
- (15) Overdeest, P. E. M.; Van der Padt, A.; Keurentjes, J. T. F.; Van 't Riet, K. In *Surfactant-Based Separations: Science and Technology*; Scamehorn, J. F.; Harwell, J. H., Eds.; ACS Symposium Series 740; American Chemical Society: Washington D.C., **1999**.
- (16) Kellner, K. H.; Blasch, A.; Chmiel, H.; Lammerhofer, M.; Lindner, W. *Chirality* **1997**, *9*, 268.
- (17) Creagh, A. L.; Hasenack, B. B. E.; Van der Padt, A.; Sudhölter, E. J. R.; Van 't Riet, K. *Biotechnol. Bioeng.* **1994**, *44*, 690.
- (18) Lebens, P. J. M.; Keurentjes, J. T. F. *Ind. Eng. Chem. Res.* **1996**, *35*, 3415.
- (19) Scamehorn, J. F.; Christian, S. D.; Ellington, R. T. In *Surfactant-based separation processes*; Scamehorn, J. F.; Harwell, J. H., Eds.; Marcel Dekker: New York, **1989**.

2

COMPLEXATION MODELING

Summary

An increased demand for enantiopure compounds has induced a significant effort in the development of enantiomer separation technologies. The conventional path to obtain homochiral products at a preparative scale is diastereoisomer crystallization. Disadvantages of this separation process are costly scale-up and a high energy requirement. An alternative can be ultrafiltration (UF) of enantioselective micelles, which is an easily scalable process with a low energy requirement. The micelles preferentially form a complex with one of the enantiomers. Only unbound enantiomers can pass the membrane during the UF process.

The work described in this chapter aims at the description of the complexation of phenylalanine (Phe) enantiomers by cholesteryl-L-glutamate anchored in nonionic micelles of nonyl-phenyl polyoxyethylene [E10] ether (NNP10). The description of this model system is used to develop a separation process capable of complete (99⁺%) enantiomer resolution from their racemic mixtures. The influence of membrane rejection and of nonselective complexation on the operational enantioselectivity is investigated. Both statistical analyses of complexation models and UF experiments in absence of chiral selector show that membrane rejection and nonselective complexation are not significant compared to enantioselective complexation. It is concluded that the complexation can be described by straightforward competitive multicomponent Langmuir isotherms. The operational enantioselectivity appears to be constant over a wide concentration range and equals 1.4. Only at extremely low total enantiomer concentrations the enantioselectivity increases to a value of 4.5.

A multistage separation process is required in order to separate a racemic mixture for 99⁺%. Preliminary calculations using the Langmuir model have shown that 60 stages are sufficient to reach a 99⁺% separation of both enantiomers.

This chapter has been published as P.E.M. Overdevest, A. van der Padt, J.T.F. Keurentjes and K. van 't Riet, 'Langmuir isotherms for enantioselective complexation of (D/L)-phenylalanine by cholesteryl-L-glutamate in nonionic micelles' *Colloids and Surfaces A* 2000, 163, 209.

Introduction

Chirotechnology, the applied science of the production of enantiopure compounds, is a fast developing research field and is increasingly applied in pharmaceutical, agrochemical and food industries due to a rise in the demand for enantiomerically pure compounds. The main reasons for an increasing demand are [1]: (i) enantiomers can have different biological activities, e.g. (*S,S*)-ethambutol which is tuberculostatic and the (*R,R*)-enantiomer can cause blindness; (ii) enantiomers can counteract one another's effect, so-called antagonism, as shown by the inhibition of the Japanese beetle pheromone, the (*R,Z*)-isomer, by 1% of the (*S,Z*)-isomer; (iii) the unwanted enantiomer is seen as an impurity as a consequence of registration constraints in certain countries; and (iv) production costs decrease significantly as a result of an increased production capacity.

The most obvious approach to produce optically active components is to use the chiral pool [2]. Since not all optically pure products are available from this pool, enantiomers have to be synthesized from (a) chiral substrates or have to be separated from their equimolar mixture (racemic mixture). The conventional production method, diastereoisomer crystallization, is often a batchwise operation [3] and requires relatively inflexible multistep processing [1], thus inducing low product yields.

Application of membranes for the resolution of racemic mixtures can result in continuous, energy efficient, preparative separation processes. Enantiomer separation using membranes can basically be divided into two types of processes. This classification is based on the location of the chiral selector molecules responsible for chiral discrimination between enantiomers [4], i.e. inside or outside the membrane, respectively. Membranes can be applied as an enantioselective barrier retaining one enantiomer more than the other. Examples thereof are membranes made of chiral polymers [5-7], molecular imprinted membranes [3,8,9], supported liquid membranes [10-12], emulsion liquid membranes [13,14] and membranes containing proteins [15,16]. Alternatively, nonselective membranes can be used to separate two (im)miscible phases of which at least one is chiral. Immiscible phases, like in liquid/liquid extraction, can be used to separate enantiomers [17-19]. However, the performance of conventional extraction equipment is often limited by backmixing and flooding [20]. These limitations are eliminated in hollow-fiber membrane extraction, where nonselective membranes are used to separate both phases [21,22]. If both enantiomers are required the partition of the enantiomers over both phases should not be too far from unity,

since at a high distribution coefficient one of the enantiomers will become extremely diluted which results in loss of valuable product [23]. Alternatively, membranes can be used to separate a miscible enantioselective microheterogeneous phase from an aqueous bulk. An efficient separation process is guaranteed by using molecules or colloidal particles larger than the pore size of the membrane, *e.g.* BSA [24,25] or enantioselective micelles as demonstrated by our group [26]. Micelles have proven their ability to preconcentrate heavy metals and organic compounds from aqueous streams in micelle-enhanced ultrafiltration (MEUF) [27-29]. Ismael and Tondre have successfully applied a metal ion selector in micelles to separate Cu^{II} , Ni^{II} , and Co^{II} ions [30]. Furthermore, micelles are used in micellar electrokinetic capillary chromatography (MEKC) to separate enantiomers on an analytical scale [31-33].

Figure 1 shows our enantioselective micellar system. Anchoring chiral selector molecules in micelles of the nonionic surfactant, nonyl-phenyl polyoxyethylene [E10] ether (NNP10), makes the enantioselective micelles. Chiral selector molecules (cholesteryl-L-glutamate, CLG) can each bind a Cu^{II} ion (not shown) and form chelate complexes, preferentially with one of the two enantiomers (D,L-Phe). Since ionic surfactants are known to interact with amino acids [34] and/or Cu^{II} ions [35] we have used nonionic surfactants. Ultrafiltration (UF) of a solution of enantioselective micelles, Cu^{II} and D,L-Phe results in enantiomer separation as a consequence of:

- enantioselective one-to-one complexation of enantiomers by chiral selectors;
- rejection of micelles by the membrane, and accordingly of the bound enantiomers; and
- permeation of the unbound enantiomers.

The objective of our research is the development of an enantiomer separation process based on micellar UF at a preparative scale. The process design requires a model that describes the complexation of enantiomers by enantioselective micelles. This chapter aims at the elucidation of the mechanism of D,L-Phe complexation by CLG anchored in NNP10 micelles. For this reason, the enantioselective and nonselective complexation and membrane rejection of bulk enantiomers have been studied. Additionally, statistics have been applied to discriminate between different complexation models.

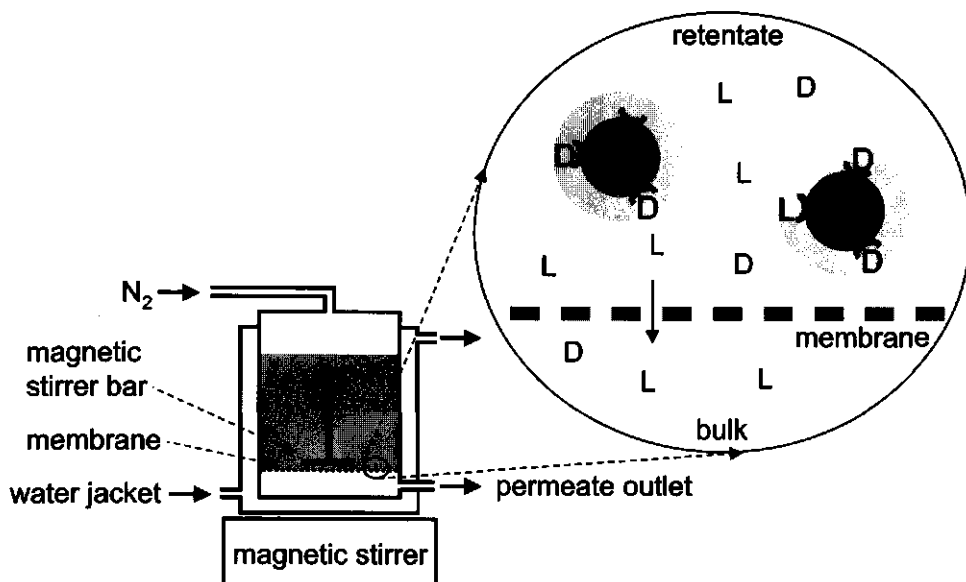


Figure 1. Experimental set-up of the Amicon cell and an impression of the enantiomer separation at the membrane.

Theory

Single and multicomponent complexation isotherm models. Assuming reversible one-to-one complexations of chiral selectors and enantiomers, complexation can be described analogously to Langmuir adsorption isotherms. Considering adsorption equilibrium at equal adsorption and desorption rates, Langmuir has derived the classical equilibrium isotherm for localized nonlinear monolayer adsorption [36]. Originally proposed for single gas adsorption, the isotherm has been adapted for describing solute adsorption by simple replacement of the adsorbate pressure by the solute concentration [37]. The Langmuir isotherm is based on the following assumptions [38]:

- adsorbate molecules are held at a fixed number of localized sites;
- each site can accommodate one single adsorbate molecule;
- adsorption energy is equal for all sites; and
- neighboring adsorbate-adsorbate interactions are absent.

Accordingly, single enantiomer complexation can be described as:

$$q_D = \frac{q_s K_D c_D}{1 + K_D c_D} \quad (\text{mM}) \quad (1)$$

$$q_L = \frac{q_s K_L c_L}{1 + K_L c_L} \quad (\text{mM})$$

where K (mM^{-1}) is the Langmuir affinity constant, c and q (mM) are the equilibrium concentrations of bulk and bound enantiomers, respectively. The indices D and L refer to the D- and L-enantiomers, respectively. The Langmuir saturation constant q_s (mM) is the maximum attainable concentration of bound enantiomer.

In case both enantiomers strive for complexation with the same binding site, the competitive complexation can be described using multicomponent Langmuir isotherms. Several authors have used these isotherms to describe enantiomer complexation [25,39,40]. For the D-enantiomer:

$$q_D = \frac{q_s K_D c_D}{1 + K_D c_D + K_L c_L} \quad (\text{mM}) \quad (2)$$

Besides an isotherm for the D-enantiomer, all isotherm models include an analogous isotherm for the L-enantiomer, as summarized in table 1.

Enantioselectivity. The enantioselectivity $\alpha_{D/L}$ of the micelles containing the selector is defined as the ratio of the bound D and L enantiomer concentrations (q_D / q_L) over the ratio of the bulk concentrations (c_D / c_L) [38]:

$$\alpha_{D/L} = \frac{q_D / q_L}{c_D / c_L} \quad (-) \quad (3)$$

Table 1. An overview of the studied single and multicomponent isotherm models.

Isotherm:	Model
$q_D = \frac{q_s K_D c_D}{1 + K_D c_D}$	(1)
$q_D = \frac{q_s K_D c_D}{1 + K_D c_D + K_L c_L}$	(2)
$q_D = \frac{q_{s,ns} K_{ns} c_D}{1 + K_{ns} (c_D + c_L)}$	(8)
$q_D = \frac{q_s K_D c_D}{1 + K_D c_D} + \frac{q_{s,ns} K_{ns} c_D}{1 + K_{ns} c_D}$	(9)
$q_D = \frac{q_s K_D c_D}{1 + K_D c_D + K_L c_L} + \frac{q_{s,ns} K_{ns} c_D}{1 + K_{ns} (c_D + c_L)}$	(10)

According to multicomponent Langmuir complexation the intrinsic enantioselectivity $\alpha_{D/L,int}$ is written as [38]:

$$\alpha_{D/L,int} = K_D / K_L \quad (-) \quad (4)$$

The bound concentrations can be calculated from the measured bulk concentrations c_D and c_L :

$$q_D = c_{D,tot} - c_D \quad (\text{mM}) \quad (5)$$

$$q_L = c_{L,tot} - c_L \quad (\text{mM}) \quad (6)$$

where the index 'tot' refers to the total enantiomer concentrations at the beginning of an experiment.

The operational enantioselectivity ($\alpha_{D/L,op}$) can be calculated using eqs 3, 5 and 6:

$$\alpha_{D/L,op} = \frac{c_L (c_{D,tot} - c_D)}{c_D (c_{L,tot} - c_L)} \quad (-) \quad (7)$$

By definition, an enantioselectivity larger than one indicates a preference of the enantioselective micelles for the D-enantiomer.

Nonselective enantiomer complexation. In addition to enantioselective complexation, nonselective (ns) complexation of both enantiomers can occur, which leads to a decrease in the operational enantioselectivity. Nonselective complexation can be described as [40]:

$$q_D = \frac{q_{s,ns} K_{ns} c_D}{1 + K_{ns} (c_D + c_L)} \quad (\text{mM}) \quad (8)$$

Assuming nonselective complexation in presence of chiral selector molecules, the single en multicomponent isotherms become, respectively [40]:

$$q_D = \frac{q_s K_D c_D}{1 + K_D c_D} + \frac{q_{s,ns} K_{ns} c_D}{1 + K_{ns} c_D} \quad (\text{mM}) \quad (9)$$

$$q_D = \frac{q_s K_D c_D}{1 + K_D c_D + K_L c_L} + \frac{q_{s,ns} K_{ns} c_D}{1 + K_{ns} (c_D + c_L)} \quad (\text{mM}) \quad (10)$$

where $q_{s,ns}$ (mM) is the maximum enantiomer concentration nonselectively bound by the surfactants and K_{ns} is the affinity constant for nonselective complexation.

Membrane rejection. Besides nonselective complexation, membrane rejection can result in misinterpretation of the measured operational enantioselectivity. In cases where membrane rejection (R) is considered, bulk concentrations in the retentate (c_r) are calculated using eq 11:

$$R = 1 - c_p / c_r \quad (-) \quad (11)$$

where c_p is the measured enantiomer concentration in the permeate. When referred to a model where membrane rejection is assumed, the reference includes 'R', e.g. model 1R.

Materials and Methods

Materials. D-, L-, and DL-Phe, analytical grade $\text{CuCl}_2 \cdot 2\text{H}_2\text{O}$, KCl, and KOH were obtained from Merck (Darmstadt, Germany) and were used without further purification. The surfactant, Serdiox NNP10 (nonyl-phenyl polyoxyethylene [E10] ether), was a gift by Servo Delden b.v. (Delden, The Netherlands). Although the surfactant was most probably a mixture of different NNPs, an average molecular weight of 644 g/mol was assumed (CMC equals 0.047 mM). The chiral selector, cholesteryl-L-glutamate (CLG), was synthesized by the Laboratory of Organic Chemistry of Wageningen University (optical rotation, $[\alpha]_D^{293}$ was -27° at 10.5 g/L chloroform, 3% trifluoroacetic acid). Throughout this study distilled and RO filtered water was used.

Preparing micellar solutions. Batches of 50 mL of solution for ultrafiltration experiments were prepared as follows. CLG, insoluble in water, was dispersed in a concentrated surfactant solution to yield a stable and transparent solution in which the selector was completely dissolved. The selector solubility in the nonionic micelles and the enantioselectivity were found to be optimal using this method. The final solutions were obtained by mixing stock solutions: 5.0 mL 1.0 M KCl, 5.0 mL 3.0 mM CuCl_2 , 2.5 mL 0 - 20 mM D-Phe, 2.5 mL 0 - 20 mM L-Phe and 35 mL of the concentrated CLG/NNP solution. These mixtures were set at pH 11 and stirred overnight. The experimental concentrations and conditions are summarized in table 2. Cu^{II} was added as the chelating agent, being a prerequisite for the enantioselective complexation of Phe by cholesteryl-L-glutamate [26]. KCl was added to ensure a constant ionic strength. To determine the adsorption isotherms of D- and L-Phe the total concentrations of both enantiomers were varied whereas all other solute concentrations remained the same.

Table 2. Solute concentrations and conditions in UF experiments.

Component	Concentration (mM)
NNP10	7.8
LCG	0.3
D-Phe	0 - 1.0
L-Phe	0 - 1.0
CuCl ₂	0.3
KCl	100
Condition	
T	25 °C
pH	11

Analytical methods. Phe enantiomers were analyzed by HPLC using a 4 mm I.D. × 150 mm Crownpak CR(+) chiral crown ether column (Daicel) operated at 5°C. Concentrations were measured by UV absorbance detection at 254 nm (Applied Biosystems). A solution of perchloric acid in water (pH 1.5) was used as the mobile phase (0.8 mL/min). Before use, the mobile phase was filtered through a 0.2 µm membrane filter (Sartopore 300). Between each series of analyses a five-point calibration was used, enabling the estimation of the Phe enantiomer concentration based upon the measured peak area.

Enantioselective complexation experiments. Ultrafiltration experiments were performed in a thermostated Amicon 300-mL cell at 25 °C in at least triplicate (figure 1). The cell was placed on a magnetic stirrer adjusted to 400 rpm to minimize foam production and concentration polarization of micelles. A regenerated cellulose membrane (YM3) with a molecular weight cut off of 3 kDa was used (Amicon Inc., USA). Part of the bulk liquid (7 mL) was forced to permeate through the membrane by applying 3 bar N₂. The first 4 mL were discarded and the following three fractions of 1 mL were collected and analyzed by HPLC.

Measurement of bulk and bound concentrations. Since the permeate concentration remained constant during an ultrafiltration experiment, it could be assumed that the

complexation equilibrium did not shift during the ultrafiltration process. Subsequently, the average permeate concentration is calculated from the three measurements per ultrafiltration experiment. Both the selector and bound concentrations increased proportionally with the decrease in retentate volume (V):

$$q_{D,ini} / q_D = q_{L,ini} / q_L = q_{s,ini} / q_s = V / V_{ini} \quad (-) \quad (12)$$

where the index 'ini' refers to the concentration at the beginning of an ultrafiltration experiment. Since q_s , q_D and q_L had to be multiplied by V/V_{ini} , complexation could still be described using straightforward single and multicomponent isotherms. However, to keep notation simple q_s , q_D and q_L refer to the concentrations at the beginning of an ultrafiltration experiment and not to the actual concentrations during the UF experiment. The bound concentrations were calculated using eqs 5 and 6.

Nonselective complexation and membrane rejection experiments. Nonselective complexation experiments were performed in absence of CLG and took place in an Amicon cell containing 7.8 mM NNP10, 0.3 mM CuCl_2 and 0.1 M KCl (pH 11, 25 °C). To investigate membrane rejection of bulk Phe, an ultrafiltration experiment was carried out in an adapted Amicon cell with a continuous feed. This feed flow was equal to the permeate flow of 0.025 mL/s, guaranteeing a constant cell volume of 200 mL. The feed and initial cell solution contained 0.15 mM D,L-Phe and 0.1 M KCl (pH 11, 25 °C). In addition, the Amicon cell contained 7.8 mM NNP10. Using eq 11 and a mass balance over the set-up, it can be easily shown that:

$$c_p = \left(1 - R e^{-\theta(1-R)}\right) c_f \quad (\text{mM}) \quad (13)$$

where θ is defined as the ratio of time and the residence time of the bulk in the cell and index 'f' refers to the feed concentration.

Statistics

Fitting the isotherm models. To fit model 1 the isotherm was rewritten into an explicit expression of the predicted bulk enantiomer concentration using eq 5:

$$c_{D,\text{pred}} = \frac{-B + \sqrt{B^2 + 4c_{D,\text{tot}}K_D}}{2K_D} \quad (\text{mM}) \quad (14)$$

where $B = K_D(q_s - c_{D,\text{tot}}) + 1$. The same procedure was followed for the L-enantiomer and for model 8. For the models 2, 9 and 10 it was not possible to derive simple explicit expressions for the bulk enantiomer concentrations. Therefore, an iterative procedure was developed to estimate the bulk concentrations $c_{D,\text{pred}}$ and $c_{L,\text{pred}}$ from a dependent set of equations. Using eqs 5 and 6 the following equations could be derived for model 2:

$$c_{D,\text{tot}} - c_{D,\text{pred}} = \frac{q_s K_D c_{D,\text{pred}}}{1 + K_D c_{D,\text{pred}} + K_L c_{L,\text{pred}}} \quad (\text{mM}) \quad (15)$$

$$c_{L,\text{tot}} - c_{L,\text{pred}} = \frac{q_s K_L c_{L,\text{pred}}}{1 + K_D c_{D,\text{pred}} + K_L c_{L,\text{pred}}} \quad (\text{mM}) \quad (16)$$

where the total concentrations $c_{D,\text{tot}}$ and $c_{L,\text{tot}}$ were assumed to be the independent variables. The *RSS* was calculated using the difference between the measured and predicted enantiomer concentrations in the bulk. An algorithm based on the Levenberg-Marquardt method was used to minimize the *RSS*.

Confidence intervals of Langmuir constants. Confidence intervals of predicted Langmuir constants (β_{pred}) were calculated using the estimated (asymptotic) standard error of the parameters (s_β):

$$\beta = \beta_{\text{pred}} \pm s_\beta t_{\alpha/2, \nu} \quad (17)$$

where $t_{\alpha/2, \nu}$ is the upper $\alpha/2$ percent point of the *t*-distribution with $\nu = n - p$ degrees of freedom, n is the number of data, and p is the number of parameters. The diagonal element of the $p \times p$ variance-covariance matrix of the parameters is equal to the square of the corresponding standard error [41]:

$$\text{variance-covariance matrix} = \left(\frac{RSS}{n-p} \right) (J'J)^{-1} \quad (-) \quad (18)$$

where J is the $n \times p$ Jacobian matrix which represents the derivative of the nonlinear functions with respect to the parameters. Note that in case of linear regression ($y = X\beta$) the Jacobian matrix equals X , thus making the estimation of confidence intervals straightforward.

Confidence intervals of enantioselectivity. The intrinsic enantioselectivity was calculated from the estimated Langmuir affinity constants K_D and K_L using eq 4. This equation was expanded as a Taylor series to obtain the standard error of $\alpha_{D/L,int}$ $s_{\alpha_{D/L,int}}$ [42]:

$$\frac{s_{\alpha_{D/L,int}}^2}{\alpha_{D/L,int}^2} \approx \frac{s_{K_D}^2}{K_D^2} + \frac{s_{K_L}^2}{K_L^2} = C_{K_D}^2 + C_{K_L}^2 \quad (-) \quad (19)$$

where $s_{K_D}^2$ and $s_{K_L}^2$ are elements of the variance-covariance matrix (18) and C_{K_D} and C_{K_L} are the relative variances of K_D and K_L , respectively. This Taylor approximation is valid for a relative variance of less than 0.15 [42]. It was obvious that the calculated confidence interval of $\alpha_{D/L,int}$ was symmetric using this approximation. However, error distributions of parameters in nonlinear models are not necessarily symmetric [43-45]. The customary assumptions that the effects of covariance between pairs of parameters can be ignored and that the distributions of parameters are normal can lead to a significant error, up to 2- and 3-fold in the calculated uncertainties [46]. Therefore, a Monte Carlo method was also used to calculate the confidence interval of $\alpha_{D/L,int}$. This procedure contained the calculation of [46]:

- (i) $\alpha_{D/L,int}$, using eq 4 and the estimated K_D and K_L ;
- (ii) a new set of K_D and K_L , using s_{K_D} and s_{K_L} and the normal distribution; and of
- (iii) $\alpha_{D/L,int}$, using eq 4 and the simulated K_D and K_L ;

After repeating step (ii) and (iii) many times (> 2000), the confidence interval was obtained from the ordered list by eliminating the upper and lower 2.5% of the simulations. The confidence interval of the operational enantioselectivity ($\alpha_{D/L,op}$) was obtained by a similar procedure as described above. However, $\alpha_{D/L,op}$ was calculated using the measured bulk enantiomer concentrations and eq 7. New sets of c_D and c_L were simulated using s_D , s_L and the normal distribution.

Criteria for choice of best model. To select the best model, lower (low) models were compared to an extended (ext) model with the use of t -tests on estimated parameters and F -statistics to test the *lack of fit* [47]. The t -test confidence intervals of the estimated parameters

were calculated using eq 17. The variance of the lack of fit and the variance of the extended model were compared as follows:

$$f = \frac{(RSS_{\text{low}} - RSS_{\text{ext}}) / (v_{\text{low}} - v_{\text{ext}})}{RSS_{\text{ext}} / v_{\text{ext}}} \quad (-) \quad (20)$$

If f was smaller than $F_{v_{\text{ext}}}^{v_{\text{low}} - v_{\text{ext}}}(1 - \alpha)$, the lower model was adequate and the additional term was not statistically significant, where $1 - \alpha$ is the confidence level. For nonlinear models the statistical analysis is at best only an approximate, since f and b_{pred} / s_b do not have an exact F - and t -distribution, respectively [47].

Results and Discussion

Single component isotherm models. Single component complexation of D- and L-Phe by enantioselective micelles have been measured (figure 2). The measurements indicate a higher affinity of the micelles for D-Phe than for L-Phe. The bound enantiomer concentrations q are calculated by eqs 5 and 6 and approach the CLG concentration (0.3 mM) at high enantiomer concentrations. The measured permeate concentrations appear to have a heterogeneous error variance (figure 3). Therefore, a weighted least-squares method is used to minimize the residual sum of squares (RSS), since information availability for parameter estimation decreases at larger variances [41]. For D-Phe:

$$RSS = \sum \left(\frac{(c_D - c_{D,\text{pred}})^2}{s_D^2} \right) \quad (-) \quad (21)$$

where s_D^2 and s_L^2 are the estimated variances of the measured D-Phe and L-Phe concentrations, respectively. Estimation of the Langmuir constants by fitting the isotherms of model 1 on the measurements, confirm the expectations (figure 2). The saturation constants are 0.30 ± 0.013 and 0.38 ± 0.078 and the Langmuir affinity constants are 28 ± 0.067 and $3.7 \pm 1.5 \text{ mM}^{-1}$ for D- and L-Phe, respectively (table 3). The 95% confidence intervals are calculated using the variance-covariance matrix and eq 17. The affinity constants suggest an intrinsic enantioselectivity of 7.7 ± 3.1 (table 4). Although, it seems that the two saturation

constants are different, a *t*-test analysis has shown that the overlap is just over 5%. This is in agreement with our expectations that the number of attainable sites is equal for both enantiomers.

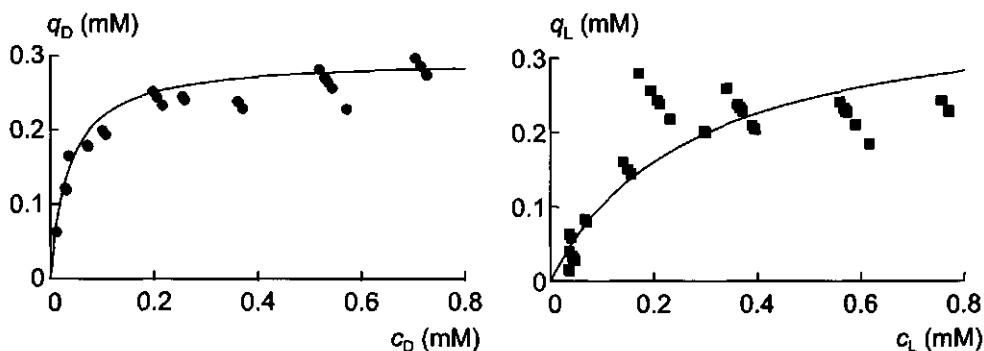


Figure 2. Single component complexation isotherm of D-Phe (●, left) and L-Phe (■, right). The single component data have been used to separately fit the isotherms of model 1 (—).

Nonselective complexation and membrane rejection of unbound enantiomers have been investigated, since these effects increase the apparent affinity and can therefore influence the intrinsic enantioselectivity. Model 9, which adds nonselective complexation to model 1, is fitted on the single component data. In addition, the same is done with models 1R and 9R, where membrane rejection is assumed (eq 11). The four models describing single component complexation of D- and L-Phe will be discussed separately.

Firstly, D-Phe complexation is discussed. In this case, model 9R is the extended model (table 3). Of the estimated parameters of the extended model only q_s and K_D are significant, whereas membrane rejection and nonselective complexation can be neglected. It has to be noted that the nonselective Langmuir saturation constant $q_{s,ns}$ of model 9 is nearly zero but significantly negative. However, a negative binding saturation concentration is not realistic. The 95% confidence interval of R in model 1R demonstrates that membrane rejection does not make it a better model than model 1. In addition, testing the lack of fit shows that all lower models are just as good as the extended model ($f < F$).

Table 3. Single component Langmuir constants and membrane rejection constants.

Model	q_s (mM)	K_D (mM ⁻¹)	K_L (mM ⁻¹)	$q_{s,ns}$ (mM)	K_{ns} (mM ⁻¹)	R (-)	v	RSS	f	$F^{(c)}$
(1)	0.30 ± 0.013	28 ± 0.067					32	1854	1.1	2.9
(1R)	0.34 ± 0.063	25 ± 6.5				-0.10 ± 0.16	31	1801	1.1	3.3
(9)	0.35 ± 0.038	25 ± 0.25		-0.11 ± 0.086	5.1 ± 0.15		30	1676	0.069	4.2
(9R) ^(a)	0.35 ± 0.18	25 ± 8.5		-0.11 ± 0.27	5.0 ± 7.8	0.0058 ± 0.20	29	1672		
(1)	0.38 ± 0.078		3.7 ± 1.5				39	370.3	11	4.1
(1R) ^(b)	1.3 ± 1.2		3.1 ± 1.2			-1.3 ± 2.6	38	285.0		
(9)	1.3 ± 4.2		6.5 ± 4.9	-0.95 ± 4.2	8.0 ± 7.9		37	313.7		
(9R)	3.2 ± 3.8		11 ± 3.1	-2.7 ± 3.8	13 ± 2.1	-0.20 ± 0.16	36	178.6		

Table 4. Langmuir constants of single and multicomponent isotherms with 95% confidence intervals (c.i.).

Model	K_D (mM ⁻¹)	s_{D_1} (mM)	K_L (mM ⁻¹)	s_{K_1} (mM)	$\alpha_{D/L,int}$ (-)	c.i. $\alpha_{D/L,int}^{(d)}$	c.i. $\alpha_{D/L,int}^{(e)}$
(1)	28 ± 0.067	0.033	3.7 ± 1.5	0.75	7.7	-2.2 / + 5.2	± 3.1
(2)	28 ± 1.3	0.64	20 ± 0.76	0.39	1.4	-0.080 / + 0.083	± 0.081

Table 5. Multicomponent Langmuir constants and membrane rejection constants.

Model	q_s (mM)	K_D (mM ⁻¹)	K_L (mM ⁻¹)	$q_{s,ns}$ (mM)	K_{ns} (mM ⁻¹)	R (-)	v	RSS	f	$F^{(c)}$
(2)	0.28 ± 0.0039	28 ± 1.3	20 ± 0.76				215	55725	15	2.6
(2R)	0.33 ± 0.014	22 ± 0.84	16 ± 0.57			-0.058 ± 0.016	214	46354	0.6	3.0
(10)	0.38 ± 0.19	24 ± 2.0	19 ± 0.97	-0.11 ± 0.20	13 ± 8.2		213	54723	40	3.9
(10R) ^(d)	0.29 ± 0.052	22 ± 2.0	15 ± 1.2	0.059 ± 0.073	6.8 ± 7.0	-0.071 ± 0.027	212	46092		

References for tables 3, 4 and 5: ^(a) D-Phe extended model, ^(b) L-Phe extended model, ^(c) $F_{v_{ext}}^{v_{low} - v_{ext}}(0.95)$, ^(d) using s_{K_D} , s_{K_L} and the Monte-Carlo method, ^(e) using eq 19, ^(f) D,L-Phe extended model.

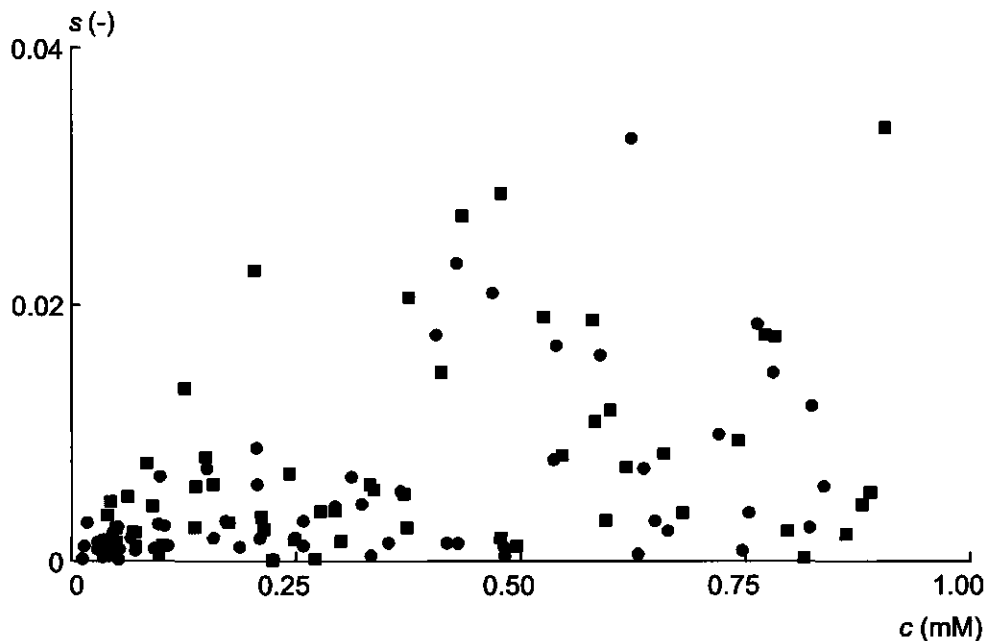


Figure 3. Calculated standard deviation (s) of all measured D-Phe (●) and L-Phe (■) concentrations as a function of the measured permeate concentration (c).

To support the irrelevance of a negative value of $q_{s,ns}$, nonselective complexation of Phe by micelles has been studied in presence Cu^{II} . Since Cu^{II} ions are capable of binding to the hydrophilic head groups of NNP10 [29], it can be hypothesized that Cu^{II} : Phe accumulates in the hydrophilic shell of the micelles. Figure 4 shows the data and the fit of model 8 on these data ($q_{s,ns} = 0.16 \pm 0.069$ mM, $K_{ns} = 1.6 \pm 3.4$ mM⁻¹). From these data it can be concluded that nonselective complexation is significant, which can be attributed to a limited availability of Cu^{II} ions. Hence, the estimated negative $q_{s,ns}$ of model 9 is irrelevant. The value of q_s estimated by fitting model 1 equals the CLG and Cu^{II} concentration. Hence, all Cu^{II} ions form chelates with CLG and Phe. Therefore, it can be assumed that the presence of CLG eliminates the nonselective complexation.

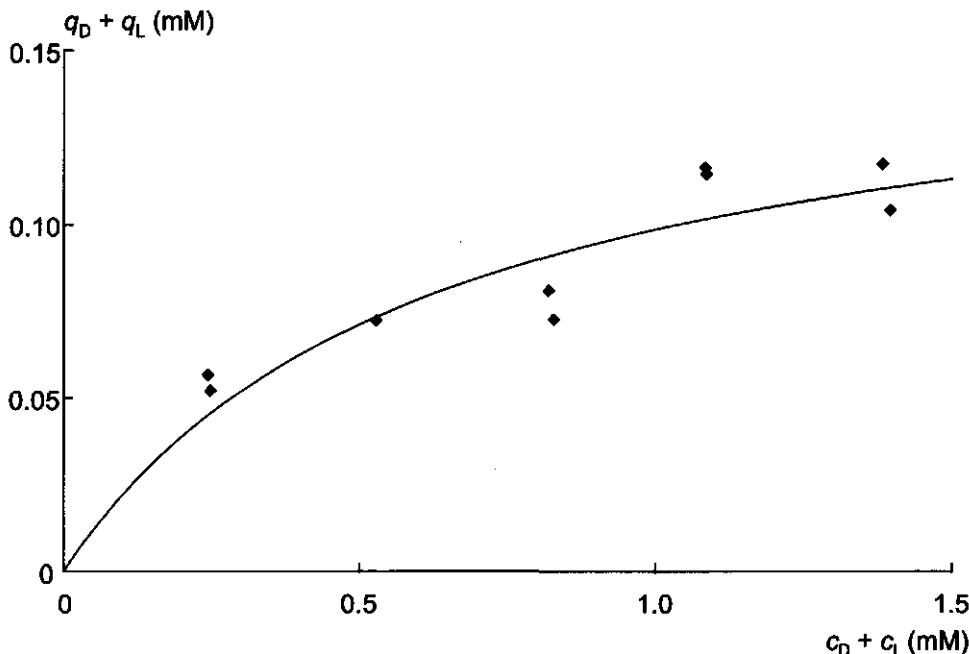


Figure 4. Nonselective enantiomer complexation data (◆) in presence of Cu^{II} ions and absence of CLG molecules. The data have been used to fit model 8 (—).

Secondly, when the single component models are fitted on the L-Phe data, models 9 and 9R turn out to be irrelevant, since both Langmuir saturation constants q_s and $q_{s,ns}$ are equal to zero. Therefore, model 1R is chosen as the extended model. The membrane rejection parameter in this model equals zero, thus model 1 is just as adequate as model 1R. Nonetheless, lack of fit testing shows a significant difference between both models. This is probably caused by the fact that these models are nonlinear. For linear models these tests would never lead to contrary conclusions.

Statistics and independent nonselective complexation experiments point out that model 1 can be applied to describe single component complexation of both D- and L-enantiomers by enantioselective micelles (figure 2).

Multicomponent complexation isotherms of D,L-Phe. As a consequence of the third and fourth assumption of the Langmuir isotherm, the affinity constants of single component isotherms can be used for multicomponent isotherms. Therefore, the multicomponent

isotherms have been measured to check these assumptions (figures 5 and 6). Again, the measurements indicate a higher affinity of the micelles for D-Phe than for L-Phe. At the same total enantiomer concentration, the micelles have bound more D-Phe than L-Phe. A similar weighted least-squares method as eq 21 has been used to minimize RSS :

$$RSS = \sum \left(\frac{(c_D - c_{D,pred})^2}{s_D^2} + \frac{(c_L - c_{L,pred})^2}{s_L^2} \right) \quad (-) \quad (22)$$

The multicomponent models 2, 2R, 10 and 10R have been fitted on all single and multicomponent complexation measurements. To complete the comparison, nonselective complexation is taken into account again, although it has been shown that this effect is insignificant (table 5). Moreover, the 95% confidence intervals of the estimated parameters have been calculated using the variance-covariance matrix and eq 17.

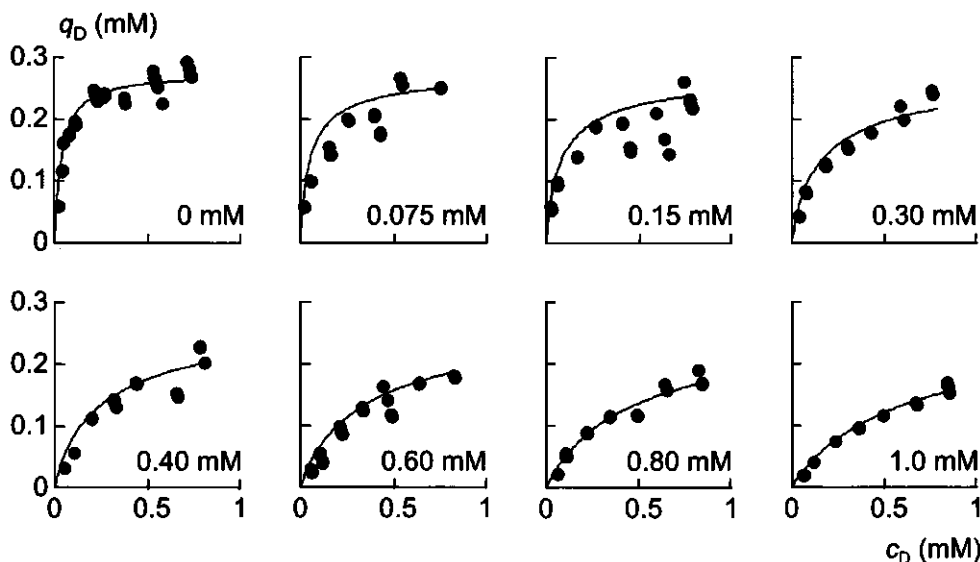


Figure 5. Multicomponent D-Phe complexation isotherms at different $c_{L,tot}$ given in each figure. The data (\bullet) have been used to fit model 2 (—).

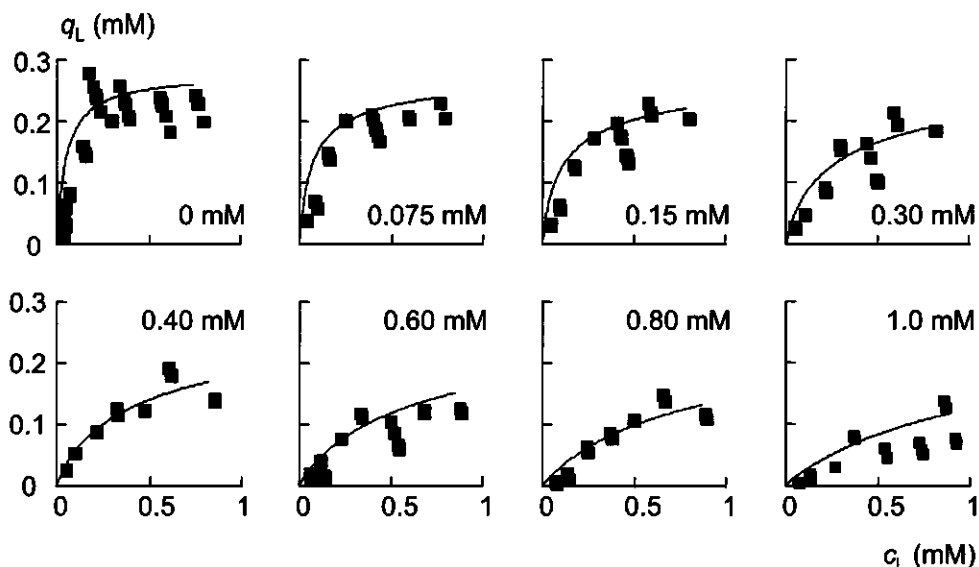


Figure 6. Multicomponent L-Phe complexation isotherms at different $c_{D,tot}$ given in each figure. The data (■) have been used to fit model 2 (—).

The estimated membrane rejection of model 2R and the extended model 10R are significantly smaller than zero. A significant rejection is also demonstrated by the lack of fit of model 2 and 10. Nevertheless, a negative R is not expected with our membrane system at these low concentrations and pressures. The confidence intervals of $q_{s,ns}$ and K_{ns} include zero when fitting model 10 and the extended model. In addition, the lack of fit of model 10 shows that nonselective complexation can be neglected.

To test whether membrane rejection has occurred, a set of independent experiments has been performed in an Amicon cell with a continuous feed. Accordingly, eq 13 has been fitted on the measured permeate concentrations (figure 7). In presence of surfactant the membrane rejection of Phe (R) equals 0.078 ± 0.0064 (-). Hence, negative membrane rejection constants are irrelevant in our system.

Since nonselective complexation is negligible and the Langmuir saturation concentrations of the single and multicomponent complexation isotherms approach the selector and Cu^{II} concentrations (0.3 mM), it can be concluded that over 93% of CLG and Cu^{II} ions participate in enantioselective enantiomer complexation. This supports the assumption that the CLG: Cu^{II} complex can be seen as a localized complexation site. The formation of $\text{Cu}(\text{Phe})_2$ in the

aqueous phase can probably explain the fact that not all Cu^{II} ions participate in the enantioselective complexation by CLG.

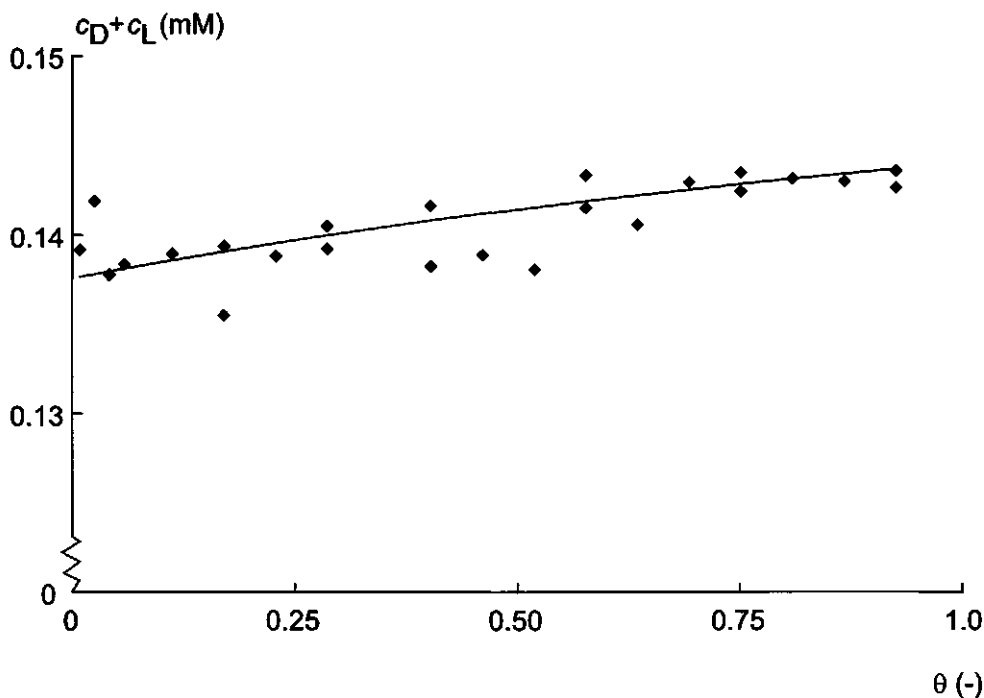


Figure 7. Membrane rejection (R) estimation of Phe in an Amicon cell with a continuous feed. The measured permeate concentrations (\blacklozenge) have been used to fit eq 13 (—).

Parity-plots have been made by plotting the measured permeate concentrations against the corresponding predicted concentrations using model 2 and the corresponding parameters of table 5 (figure 8). From these figures it can be concluded that a straightforward multicomponent Langmuir isotherm is capable of predicting the bulk enantiomer concentrations. Only at extremely low L-enantiomer concentrations ($c_L < 0.035$ mM) predictions are underestimated. However, these low L-Phe concentrations can be regarded not to be part of the relevant concentrations. Comparing the single and multicomponent models, it is remarkable that K_D is the same in both cases and K_L is significantly higher in the multicomponent case. Apparently, some neighbour-neighbour interactions occur in the system. Taking statistics and the parity-plots into consideration the multicomponent

Langmuir model 2 is able to describe the multicomponent complexation data (figures 5 and 6).

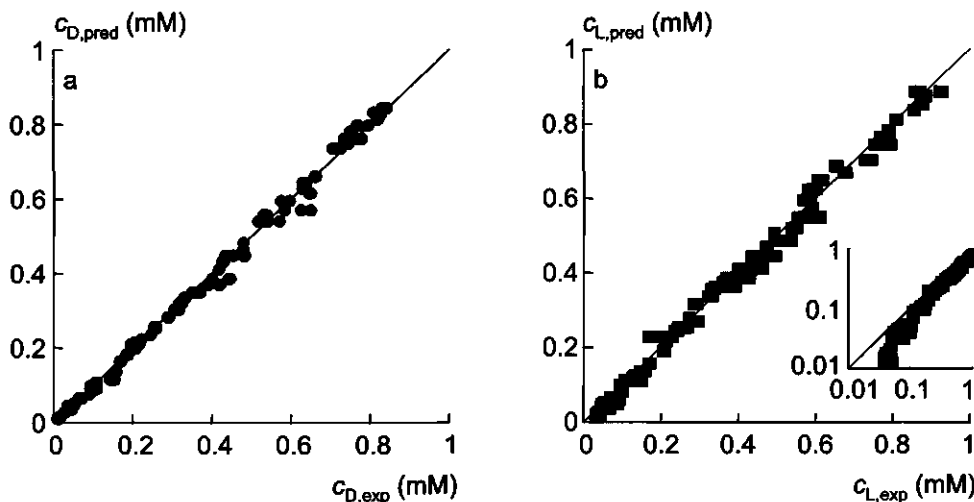


Figure 8. Parity-plots of all measurements (c_{exp}) and predictions (c_{pred}) for D-Phe (a, left) and L-Phe (b, right). At extremely low L-Phe concentrations predictions are underestimated (see insert with logarithmic scale).

Intrinsic and operational enantioselectivity. Based on the single component model 1 and eq 4, a substantial intrinsic enantioselectivity of the enantioselective micelles for D-Phe over L-Phe is calculated, $5.5 < \alpha_{D/L,int} = 7.7 < 13$ (table 4). The asymmetry of the confidence interval is caused by the nonlinearity of eq 4 and a value of C_{K_L} greater than 0.15. Subsequently, the use of the Monte-Carlo method is compulsory. However, by fitting the multicomponent model 2 the calculated enantioselectivity equals $1.3 < \alpha_{D/L,int} = 1.4 < 1.5$. In order to study the difference in $\alpha_{D/L,int}$ based on the single and multicomponent models, the operational enantioselectivity ($\alpha_{D/L,op}$) is calculated for each ultrafiltration experiment using eq 7 (figure 9). The confidence intervals of $\alpha_{D/L,op}$ are calculated using the Monte Carlo method. For simplicity the error bars are replaced by a grey rectangle at higher enantiomer concentrations. At $c_{D,tot} + c_{L,tot} > 0.5$ mM the operational enantioselectivities equal the intrinsic enantioselectivity as predicted by model 2. However, the measured operational enantioselectivity increase significantly to 4.5 at decreasing $c_{D,tot} + c_{L,tot}$, which cannot be predicted by multicomponent Langmuir isotherms. It appears that $\alpha_{D/L,op}$ will even increase to

7.7, which equals $\alpha_{D/L,int}$ based on single component isotherms. Contrary to the operational enantioselectivity, the complexation of D-Phe and L-Phe are well fitted by model 2 using concentration independent K values, which implies a constant enantioselectivity. Deviations of predicted bulk L-Phe concentrations ($c_L < 0.035$ mM) from the measured ones are responsible for the increase in operational enantioselectivity at decreasing $c_{D,tot} + c_{L,tot}$. These minor deviations have been negligible when fitting the isotherm models. Based on the intrinsic and operational enantioselectivities it is concluded that an enantioselectivity of 1.4 should be used to develop an enantiomer separation process at pH 11.

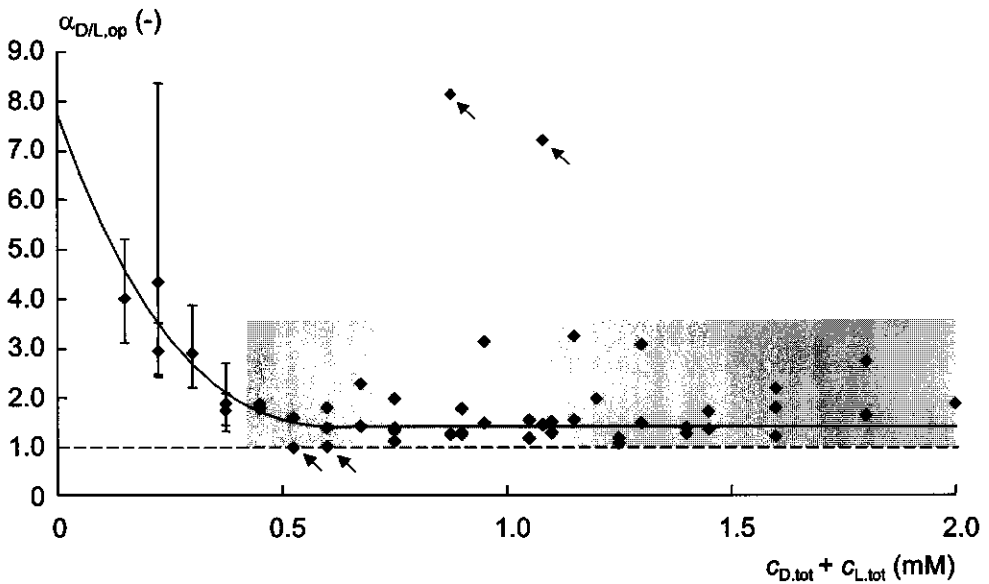


Figure 9. Operational enantioselectivities for all multicomponent UF experiments (◆). The confidence intervals of the data indicated by an arrow include zero.

Concluding Remarks

D,L-Phe enantiomers can be separated using a separation process based on ultrafiltration of nonionic enantioselective micelles containing cholesteryl-L-glutamate. Operational enantioselectivities of 1.4 to 4.5 have been measured. Straightforward multicomponent Langmuir isotherms can be used to describe Phe enantiomer complexation by enantioselective micelles, where $K_D = 28 \text{ mM}^{-1}$ and $K_L = 20 \text{ mM}^{-1}$. The estimated Langmuir saturation concentration q_s is 0.28 mM and equals 93% of CLG and Cu^{II} ion concentrations and guarantees a high efficiency of these molecules. By two independent routes it is shown that extension of the complexation model by membrane rejection and/or nonselective complexation of enantiomers will not lead to a better model. Statistical analysis of the investigated models results in the classical Langmuir isotherms. Secondly, independent experiments show that both effects can be neglected if compared to enantioselective complexation.

In order to separate a racemic mixture for 99⁺% a multistage separation process will be required, since the differences between D- and L-Phe complexation are relatively subtle. The multicomponent isotherm model is a key element in the development of this multistage system. Preliminary calculations have shown that 60 stages are sufficient to reach a 99⁺% separation. In addition, an increase in enantiomer and selector concentration is still needed to obtain a cost effective separation system.

Acknowledgements

Financial support for this work was provided by the Dutch Technology Foundation (grant no. WCH44.3380), Akzo Nobel, and DSM. The authors wish to thank drs. T.J.M. de Bruin and dr. A.T.M. Marcelis for valuable discussions.

References

- (1) Crosby, J. *Tetrahedron* **1991**, *47*, 4789.
- (2) Sheldon, R. A. *Chirotechnology: industrial synthesis of optically active compounds*; Marcel Dekker: New York, **1993**.
- (3) Yoshikawa, M.; Izumi, J. I.; Kitao, T.; Sakamoto, S. *Macromolecules* **1996**, *29*, 8197.
- (4) Davankov, V. A. *Chirality* **1997**, *9*, 99.
- (5) Aoki, T.; Ohshima, M.; Shinohara, K. I.; Kaneko, T.; Oikawa, E. *Polymer* **1997**, *38*, 235.
- (6) Tone, S.; Masawaki, T.; Eguchi, K. *J. Membr. Sci.* **1996**, *118*, 31.
- (7) Masawaki, T.; Sasai, M.; Tone, S. *J. Chem. Eng. Japan* **1992**, *25*, 33.
- (8) Yoshikawa, M.; Izumi, J. I.; Kitao, T. *Polym. J.* **1997**, *29*, 205.
- (9) Allender, C. J.; Brain, K. R.; Heard, C. M. *Chirality* **1997**, *9*, 233.
- (10) Ersoz, M.; Vural, U. S.; Okdan, A.; Pehlivan, E.; Yildiz, S. *J. Membr. Sci.* **1995**, *104*, 263.
- (11) Bryjak, M.; Kozlowski, J.; Wieczorek, P.; Kafarski, P. *J. Membr. Sci.* **1993**, *85*, 221.
- (12) Shinbo, T.; Yamaguchi, T.; Yanagishita, H.; Sakaki, K.; Kitamoto, D.; Sugiura, M. *J. Membr. Sci.* **1993**, *84*, 241.
- (13) Pickering, P. J.; Chaudhuri, J. B. *J. Membr. Sci.* **1997**, *127*, 115.
- (14) Pickering, P. J.; Chaudhuri, J. B. *Chirality* **1997**, *9*, 261.
- (15) Higuchi, A.; Hashimoto, T.; Yonehara, M.; Kubota, N.; Watanabe, K.; Uemiya, S.; Kojima, T.; Hara, M. *J. Membr. Sci.* **1997**, *130*, 31.
- (16) Lakshmi, B. B.; Martin, C. R. *Nature* **1997**, *388*, 758.
- (17) Kellner, K. H.; Blasch, A.; Chmiel, H.; Lammerhofer, M.; Lindner, W. *Chirality* **1997**, *9*, 268.
- (18) Pickering, P. J.; Chaudhuri, J. B. *Chem. Eng. Sci.* **1997**, *52*, 377.
- (19) Takeuchi, T.; Horikawa, R.; Tanimura, T. *Sep. Sci. Technol.* **1990**, *25*, 941.
- (20) Keurentjes, J. T. F.; Voermans, F. J. M. In *Chirality in industry II: Development in the manufacture and applications of optically active compounds*; Collins, A. N.; Sheldrake, G. N.; Crosby, J., Eds.; John Wiley & Sons: Chichester, **1997**.
- (21) Ding, H. B.; Carr, P. W.; Cussler, E. L. *AIChE J.* **1992**, *38*, 1493.
- (22) Pirkle, W. H.; Bowen, W. E. *Tetrahedron: Asymm.* **1994**, *5*, 773.

- (23) Keurentjes, J. T. F.; Nabuurs, L. J. W. M.; Vegter, E. A. *J. Membr. Sci.* **1996**, *113*, 351.
- (24) Poncet, S.; Randon, J.; Rocca, J. L. *Sep. Sci. Technol.* **1997**, *32*, 2029.
- (25) Itoh, T.; Saura, Y.; Tsuda, Y.; Yamada, H. *Chirality* **1997**, *9*, 643.
- (26) Creagh, A. L.; Hasenack, B. B. E.; Van der Padt, A.; Sudhölter, E. J. R.; Van 't Riet, K. *Biotechnol. Bioeng.* **1994**, *44*, 690.
- (27) Scamehorn, J. F.; Christian, S. D.; Ellington, R. T. In *Surfactant-based separation processes*; Scamehorn, J. F.; Harwell, J. H., Eds.; Marcel Dekker: New York, **1989**.
- (28) Hong, J. J.; Yang, S. M.; Lee, C. H. *J. Chem. Eng. Japan* **1994**, *27*, 314.
- (29) Akita, S.; Yang, L.; Takeuchi, H. *J. Membr. Sci.* **1997**, *133*, 189.
- (30) Ismael, M.; Tondre, C. *J. Colloid Interf. Sci.* **1993**, *160*, 252.
- (31) Nishi, H. *J. Chromatogr. A* **1997**, *780*, 243.
- (32) Swartz, M. E.; Mazzeo, J. R.; Grover, E. R.; Brown, P. R. *J. Chromatogr. A* **1996**, *735*, 303.
- (33) Dalton, D. D.; Taylor, D. R.; Waters, D. G. *J. Chromatogr. A* **1995**, *712*, 365.
- (34) Yagi, H.; Uenishi, K.; Kushijima, H. *J. Ferment. Bioeng.* **1993**, *76*, 306.
- (35) Scamehorn, J. F.; Ellington, R. T.; Christian, S. D. *Rec. Adv. Sep. Techniq.* **1996**, *82*, 48.
- (36) Langmuir, I. *J. Am. Chem. Soc.* **1918**, *40*, 1361.
- (37) Guiochon, G.; Shirazi, S. G.; Katti, A. M. *Fundamentals of preparative and nonlinear chromatography*; Academic Press: Boston, **1994**.
- (38) Ruthven, D. M. *Principles of adsorption and adsorption processes*; John Wiley & Sons: New York, **1984**.
- (39) Lim, B. G.; Ching, C. B.; Tan, R. B. H. *Sep. Technol.* **1995**, *5*, 213.
- (40) Charton, F.; Jacobsen, S.; Guiochon, G. *J. Chromatography* **1993**, *630*, 21.
- (41) Myers, R. H. *Classical and modern regression with applications*; PWS-Kent: Boston, **1989**.
- (42) Chatfield, C. *Statistics for technology*; Chapman and Hall: New York, **1983**.
- (43) Van Boekel, M. A. J. S. *J. Food Sci.* **1996**, *61*, 477.
- (44) Press, W. H.; Flannery, B. P.; Teukolsky, S. A.; Vetterling, W. T. *Numerical recipes, the art of scientific computing*; Cambridge: New York, **1986**.
- (45) Straume, M.; Johnson, M. L. *Methods Enzymol.* **1992**, *210*, 117.
- (46) Alper, J. S.; Gelb, R. I. *J. Phys. Chem.* **1990**, *94*, 4747.
- (47) Bates, D. M.; Watts, D. G. *Nonlinear regression analysis and its applications*; John Wiley & Sons: New York, **1988**.

3

COMPLEXATION AND REGENERATION

Summary

Many enantiomer separation systems are studied to meet the increasing demand for enantiopure compounds. One way to obtain pure enantiomers is the application of enantioselective micelles in ultrafiltration systems. We have studied the separation of phenylalanine enantiomers by ultrafiltration of cholesteryl-L-glutamate (CLG) anchored in nonionic micelles. Cu^{II} ions have been used to form 1:1:1 chelate complexes between CLG and a Phe enantiomer, preferably with the D-enantiomer. Since the net charges of enantiomers and CLG are pH dependent, it is expected that the complexation and enantioselectivity are a function of the pH as well. Consequently, it is foreseen that pH will be an important factor in the design of a cascaded separation process that yields 99+% enantiopure products. This chapter aims at the description of the complexation equilibria at various pHs.

Batch and continuous experiments at pH 7, 9 and 11 have shown that the competitive complexation of enantiomers can be described by multicomponent Langmuir isotherms. The enantioselectivity of CLG for D-Phe increases upon a decreasing pH, 1.4, 1.7 and 1.9 for pH 11, 9 and 7, respectively. Since at the reduced pHs the electrostatic interactions diminishes, it is hypothesized that the weak enantioselective interactions will be more pronounced. Accordingly, the saturation concentration and the affinity constants decrease upon decreasing pH, finally resulting in no complexation at pH 6.

To design an economically attractive separation process, regeneration of D-Phe saturated micelles leaving the multistage system is inevitable. Regeneration, *i.e.* recovery of enantioselective micelles for reuse, is possible at $\text{pH} \leq 4$. To keep the salt production to a minimum, the shift in pH between the separation and the regeneration process must be minimized. Therefore, a separation process at pH 7 seems the most attractive.

This chapter has been submitted for publication as P.E.M. Overdeest, T.J.M. de Bruin, E.J.R. Sudhölter, K. van 't Riet, J.T.F. Keurentjes and A. van der Padt, 'Separation of racemic mixtures by ultrafiltration of enantioselective micelles I. Effect of pH on complexation and regeneration'

Introduction

Enantiopure compounds are essential constituents of pharmaceuticals, crop protection agents and food. The fact that in various countries the inactive enantiomer is legally seen as an impurity is another reason for a greatly increased demand for pure enantiomers over the years [1]. This chapter emphasizes a route for the separation of racemic mixtures by filtration of enantioselective micelles using ultrafiltration membranes.

The separation concept is based on Ligand-Modified Micelle-Enhanced UltraFiltration (LM-MEUF) [2]. Enantioselective micelles, aggregates of chiral selector molecules and nonionic surfactants, have the ability to discriminate between D- and L-enantiomers [3]. The chiral selector used in our study, cholesteryl-L-glutamate (CLG), prefers the formation of a chelate complex with a Cu^{II} ion and a D-Phe enantiomer over the formation of a chelate complex with a Cu^{II} ion and a L-Phe enantiomer [4]. The pores of the ultrafiltration membrane are small enough to reject the micelles and are large enough to allow permeation of unbound enantiomers. Therefore, after mixing enantioselective micelles with a racemic mixture, ultrafiltration results in a D-Phe enriched retentate and an L-Phe enriched permeate.

At pH 11 we have measured an enantioselectivity of 1.4 for this system [4]. This enantioselectivity implies that a multistage process will be needed to obtain products with a 99+% enantiopurity (figure 1). The effect of the pH on the performance of the enantioselective micelles is essential to minimize the number of stages necessary for 99+% separation. At pH 11 both the selector and the enantiomers are negatively charged and form a neutral chelate complex by Cu^{II} ion binding [5]. Since the charge of selectors and enantiomers depends on the pH ($pI_{\text{CLG}} \approx pI_{\text{Phe}} = 5.5$), it is hypothesized that the chelate complex formation and enantioselectivity will depend on pH as well [6,7]. Brookes and Pettit have measured a maximum enantioselectivity at pH 6 for chelate complexes containing a Cu^{II} ion, a L-amino acid, and a D- or a L-histidine enantiomer [5].

The high affinity of CLG for D-Phe at pH 11 ($K_{\text{D}} = 28 \text{ mM}^{-1}$) [4] suggests that decomplexation will result in highly diluted solutions and consequently in a product loss. It is expected that a decrease in pH can be used to regenerate the saturated micelles that leave the multistage separation process. To reduce salt built-up after multiple separation/regeneration cycles, the associated pH shift must be minimized. Additionally, it is desirable to run the separation process under mild conditions, *i.e.* neutral pH and room temperature. This chapter

aims at the description of complexation and decomplexation at various pH values, which will be used for the development of a separation system under milder conditions than at pH 11.

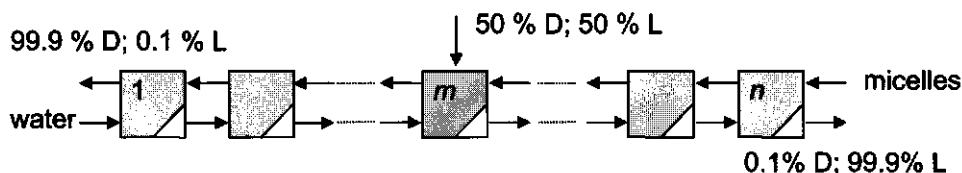


Figure 1. A multistage ultrafiltration system for the separation of enantiomers.

Multicomponent Langmuir complexation isotherms

In our previous work [4], it is concluded that multicomponent Langmuir isotherms (eq 1) can describe the unbound and bound enantiomer concentrations (c and q , respectively):

$$q_e = \frac{q_s K_e c_e}{1 + K_D c_D + K_L c_L} \quad (\text{mM}) \quad (1)$$

where e represents the D- or the L-enantiomer and q_s is the saturation complexation concentration (mM). The ratio of the Langmuir affinity constants, K_D and K_L (mM^{-1}), is equal to the intrinsic enantioselectivity, $\alpha_{D/L, \text{int}}$. Consequently, an enantioselectivity larger than one indicates a complexation preference for the D enantiomer.

Materials and Methods

Materials. The nonionic surfactant, nonyl-phenyl polyoxyethylene [E10] ether (NNP10), was a gift by Servo Delden b.v. (Delden, The Netherlands). Since the surfactant was most probably a mixture of different NNPs, an average molecular weight of 644 g/mol was assumed. Nonionic micelles were used to prevent unfavorable nonselective charge-charge interactions between enantiomers by micelles. The chiral selector, cholesteryl-L-glutamate (CLG), was synthesized by the Laboratory of Organic Chemistry [8] by esterification of L-glutamate and β -cholesterol. To minimize the loss of chiral selector by permeation, it

contained a large hydrophobic anchor (cholesterol) to make it water insoluble. Therefore, it was expected that the cholesterol group was completely absorbed by the hydrophobic core of the nonionic micelles. Throughout this study double distilled water was used. All other components were obtained from Merck (Darmstadt, Germany) and were used without further purification.

Preparation of micellar solutions. The chiral selector was dispersed in the liquid surfactant, followed by the addition of water (5% of final volume) to yield a highly concentrated surfactant solution. This strongly enhanced the solubilization process of CLG in the nonionic micelles. After 24 hours equilibration, water and stock solutions of Phe, CuCl_2 and KCl were added. The final solutions contained 7.8 mM NNP10, 0.3 mM CLG, 0.3 mM CuCl_2 , and 0.1 M KCl, respectively. Throughout the experiments different total enantiomer concentrations $c_{e,\text{tot}}$ were used (0.01 mM – 1.25 mM). After the pH was set using concentrated HCl and KOH solutions, the solutions were equilibrated for another 24 hours.

Three micelle-enhanced ultrafiltration systems. The membranes used in the ultrafiltration systems were regenerated cellulose ultrafiltration membranes with a molecular weight cut off of 3 kDa (YM3, Millipore) and hollow fiber modules (Centrysystem 300 HG, Secon, Germany) with a molecular weight cut off of 10 kDa. The membrane rejection of NNP10 micelles was high for both membranes (99+%). Since membrane rejection of unbound enantiomers can be neglected [4], it can be assumed that the permeate concentrations are equal to the bulk enantiomer concentrations in the retentate. Furthermore, since nonselective complexation by micelles can be neglected [4], the bound enantiomer concentration can be calculated by simple mass balances: $q_e = c_{e,\text{tot}} - c_e$. Measurement of the permeate concentrations c_e was performed by HPLC as described before [4]. Three types of ultrafiltration systems were used:

Dead-end ultrafiltration system. Equilibrium experiments were conducted in a stirred cell (8400 series, Amicon) (figure 2). During these dead-end ultrafiltration experiments the volume decreased. Accordingly, the bound and the unbound selector concentrations increased proportionally. If mentioned, the bound concentrations q_e will refer to the concentrations at the start of the ultrafiltration. Since rejection of unbound enantiomers is negligible [4], it was expected that the equilibrium would not shift. Before ultrafiltration, a micellar solution was placed in the cell and the experiment started by applying 3 bar N_2 . Consequently, part of the

bulk liquid (7 mL) was forced to permeate through the membrane. Only the last three 1 mL samples were analyzed.

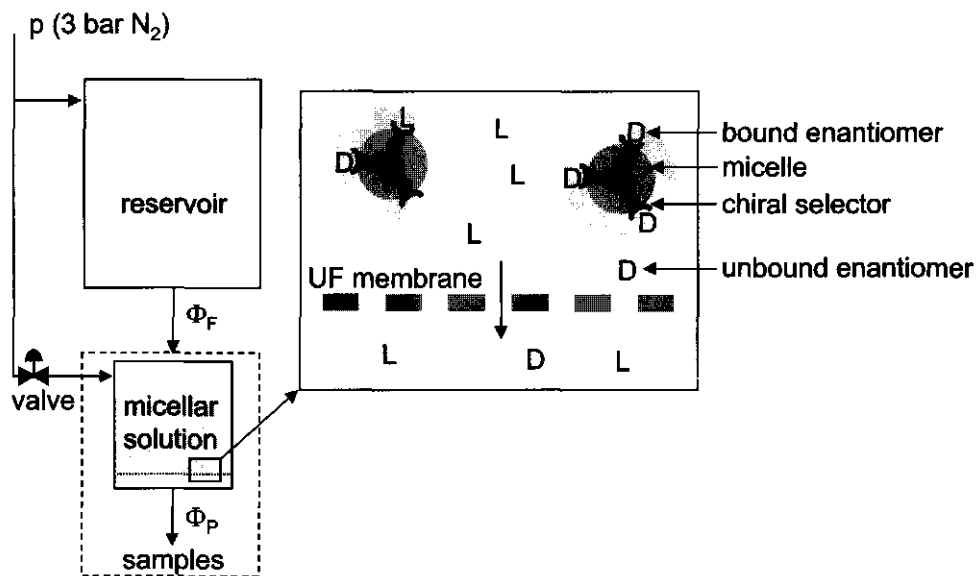


Figure 2. Enantiomer separation in a dead-end UF system (dashed box) with continuous feed.

Dead-end ultrafiltration system with continuous feed. A stirred cell with a continuous feed was used to perform wash-in and wash-out experiments [9]. This way, multiple equilibrium data points of enantiomer complexation by enantioselective micelles could be measured in a single experimental run [10] (figure 2). This set-up resembled a single stage chromatography column consisting of 1 theoretical transfer unit only, however, contrary to chromatography, a step function input was used instead of a pulse. The ultrafiltration experiment started by applying 3 bar N₂ at both the reservoir and the stirred cell. Immediately after this, the valve was closed resulting in equal feed and permeate flows, $\Phi_F = \Phi_P (= 2.8 \cdot 10^{-5} \text{ L/s})$. Consequently, the cell volume remained constant. Since the residence time $\tau (= V / \Phi_F)$ was 2 hours and the mixing time was in the order of seconds, it could be assumed that the stirred cell was ideally mixed. Throughout this study we used a dimensionless time $\theta (= t / \tau)$. The samples were collected in a fraction collector and analyzed by HPLC.

Cross-flow ultrafiltration system. Regeneration of the micelles was studied at various pHs by measurement of the unbound enantiomer concentration in time using a cross-flow ultrafiltration system. The micellar solution was pumped (Watson Marlow, 505S) through a hollow fiber module, where the transmembrane pressure was set at 1.5 bar. The sample volume was kept to a minimum (0.5 mL), to maintain a constant selector concentration. The (de)complexation was followed by sampling the permeate every 0.25 hours.

Influence of pH on complexation. In order to interpret the influence of the pH on the complexation of D- and L-Phe by the enantioselective micelles, the performance of the micellar system was studied at pH 5 – 12. The specific optical rotation $[\alpha]_D^{293}$ of the chiral selector is -34° at 10.5 g/L chloroform (3% trifluoroacetic acid) [8]. A series of eight 50 mL micellar solutions were prepared, in which the racemic mixture concentrations were 0.15 mM ($c_{e,tot} = 0.075$ mM). These equilibrium experiments were performed in a dead-end UF system (figure 2).

Complexation isotherms. Since the complexation model is known from the experiments at pH 11 [4], it could be expected that we could make use of experimental design. A D-optimal design is one that maximizes the determinant of Fisher's information matrix $X'X$, where X is the design matrix for the linear model $y = X\beta$. Consequently, this procedure leads to the minimization of the volume of the confidence ellipsoid of the estimated regression parameters β . Since the Langmuir isotherm model is a nonlinear model, the design matrix depends on the regression parameters. Hence, in nonlinear cases experimental design is an unsuitable tool. However, experiments at high enantiomer concentrations result in a good estimate of the saturation concentration q_s . Experiments performed at relatively low concentrations result in good estimates of the affinity constants. Keep in mind that the slope at the origin of the complexation isotherm equals $q_s \cdot K_e$. To measure the complexation isotherms at pH 7 and 9, two series of 50 mL micellar solutions were filtrated by a dead-end UF system (figure 2), at various racemic mixture concentrations ($c_{e,tot} = 0.01$ mM – 1.25 mM). The Langmuir isotherms were fitted on the measured permeate concentrations.

A newly synthesized batch of chiral selector was used ($[\alpha]_D^{293} = -27^\circ$, conditions as before). Based on optical rotation measurements we expected the selector to be more enantioselective than the one we used in the previously discussed experiments, since the optical rotations of cholesteryl-D-glutamate and cholesteryl-DL-glutamate are -38° and -33° , respectively [11].

Langmuir affinity constants. A dead-end ultrafiltration cell with a continuous feed was used to obtain better estimates of the affinity constants (figure 2). Three 200 mL micellar solutions were prepared as described previously, however, no enantiomers were added. The feed solution contained 0.15 mM D,L-Phe ($c_{e,feed} = 0.075$ mM) and 0.1 M KCl. Both the micellar solution and the feeding solution were set at the same pH (6, 7 or 9).

Regeneration of enantioselective micelles. The regeneration of saturated micelles was studied by measurement of the decomplexation at pH 2, 3, and 4. For this purpose, three 200 mL micellar solutions were prepared with 0.15 mM D,L-Phe and set at pH 7. After 24 hours equilibration the solutions were set at pH 2, 3, and 4, respectively. After another 24 hours the solutions were placed in a dead-end ultrafiltration cell with a continuous feed (figure 2). Subsequently, the equilibrated micellar solutions were fed with 0.1 M KCl of the same pH. This way, the wash-out of enantiomers could be studied in a single stage, the first step in the regeneration process.

The second step of the regeneration process is to reset the pH of the enantioselective micelles by increasing the pH to the value of the separation process, in order to reuse the micelles. Four 200 mL micellar solutions were prepared with 0.15 mM D,L-Phe. The solutions were set at pH 7 and equilibrated for 24 hours. Afterwards, the solutions were filtrated in a cross-flow ultrafiltration system. The experiments started by setting the solutions at pH 3. To study the decomplexation rate, the first experiment was kept to pH 3. While running the other three experiments, the pH was changed to a value of 7 after a regeneration time t_{reg} of 2, 6, and 10 hours, respectively, so that the reusability of the enantioselective micelles could be studied.

Fitting procedure. The models were fitted on the corresponding data points by minimization of the Residual Sum of Squares (*RSS*). The *RSS* was based on the difference between the measured c_e and predicted $c_{e,pred}$ permeate concentrations:

$$RSS = \sum (c_D - c_{D,pred})^2 + \sum (c_L - c_{L,pred})^2 \quad (2)$$

where the *RSS* was minimized by a Levenberg-Marquardt method. Additionally, the fitting procedure yielded the Jacobian matrix which was used to calculate the 95% confidence intervals of the estimated parameters. A more detailed explanation of the fitting procedure and the Monte Carlo simulations used to estimate the parameter confidence intervals are given in chapter 2.

Results and Discussion

Influence of pH on complexation. To optimize the selector performance, the complexation has been studied at pH 5 up to 12. Figure 3 clearly shows that no complexation takes place at low and high pH values. At pH 5 and 6, there is less attraction between CLG, Cu^{II} and Phe as a consequence of a lower net negative charge of both selector and enantiomer. At high pH, the high hydroxide ion concentration causes Cu^{II} ions to precipitate as copperhydroxide, making these ions unavailable for the chelate formation between selector and enantiomer. The observed trends indicate that the pH interval of interest lies between pH 7 and 11. This tendency corresponds with the species distribution calculation by Creagh *et al.* [12]. Consequently, we have continued our studies focussing on the complexation isotherms of D- and L-Phe at pH 7 and 9, since the isotherms at pH 11 have previously been measured [4].

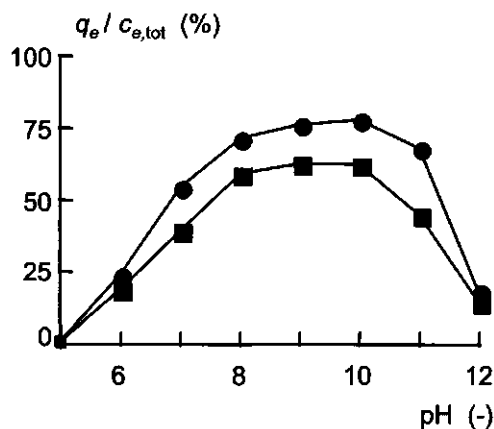


Figure 3. Effect of pH on complexation of D- (●) and L-Phe (■).

Complexation isotherms. The complexation isotherms of D,L-Phe and enantioselective micelles measured by dead-end ultrafiltration experiments at pH 7 and 9 are given in figure 4. Analogous to our study at pH 11, these measurements confirm that multicomponent Langmuir isotherms can be used to describe the Phe enantiomer complexation by CLG in NNP10 micelles. The solid lines in figure 4 show the fitted Langmuir isotherms. The deviations between the measured and predicted concentrations appear to be large. However, the deviation in the fitted permeate concentrations is only minor and approaches the

measurement error. This is illustrated by the dashed line in figure 4 given by $q_{e,\text{pred}} = c_{e,\text{tot}} - c_{e,\text{pred}}$ (mM). The lack of fit is given by $c_e - c_{e,\text{pred}}$ which is equal to the minor distance between c_e and the intersection of the dashed line and the Langmuir isotherm. Hence, a small error in the measured permeate concentration results in a much larger error in the calculated bound concentration. Of course one could argue whether nonselective complexation could explain the residual part of the deviation. However, independent experiments at pH 7 and 9 have shown that nonselective complexation is less than 3% of the selective complexation and could therefore be neglected.

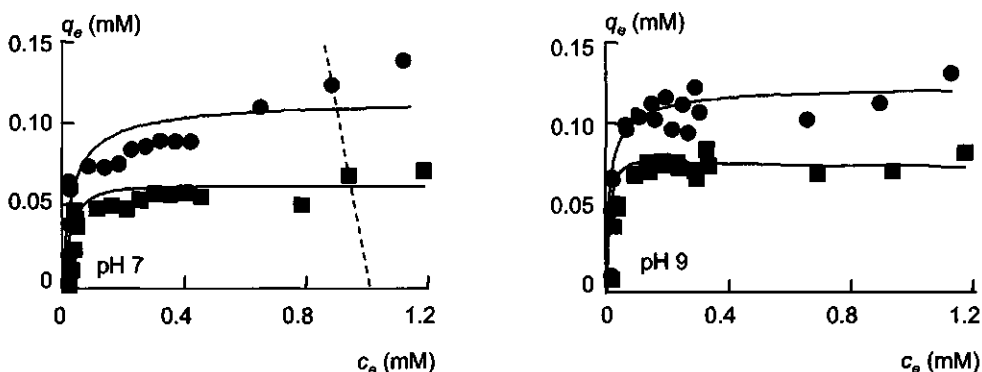


Figure 4. Complexation isotherms at pH 7 (left) and 9 (right), where e represents D- (●) and L-Phe (■).

The estimated Langmuir constants q_s (mM), K_D (mM^{-1}) and K_L (mM^{-1}) using eq 1 are summarized in table 1, the Langmuir parameters at pH 11 have been added from chapter 2. Case 1 represents the estimation of q_s , K_D and K_L at pH 7, 9 and 11, respectively. It shows that the Langmuir saturation concentration q_s increases with pH. Apparently, at pH 7 a large part of the selector molecules are shielded from Cu^{II} complexation due to a deeper location in the micelle caused by a lower net charge of CLG than at pH 11.

Since the negative charges of the enantiomers and the selector molecules increase with an increasing pH between 7 and 11, an increase in the affinity constants could be expected. The confidence intervals of the estimated affinity constants at pH 7 and 9 are large, due to the low number of measurements. As a result, the intrinsic enantioselectivity $\alpha_{\text{D/L,int}}$ calculated as K_D over K_L has such a large confidence interval that no conclusions can be drawn. Notwithstanding, it is expected that the enantioselectivity is significantly larger than 1, since q_D/q_L is larger than 1 for all c_e (figure 4). At pH 11, a significant enantioselectivity could be

calculated from the Langmuir affinity constants, 1.4 ± 0.081 , since many more measurements (218) have been done.

Table 1. Langmuir coefficients and $\alpha_{D/L,int}$ estimated from equilibrium experiments at pH 7, 9 and 11, where $\alpha_{D/L,int}$ is calculated (case 1) or estimated (case 2 and 3).

Case	pH	q_s (mM)	K_D (mM ⁻¹)	K_L (mM ⁻¹)	$\alpha_{D/L,int}$ (-)
1	7	0.17 ± 0.019	24 ± 17	13 ± 9.0	$1.9 \pm 1.9^{(a)}$
	9	0.19 ± 0.012	63 ± 49	37 ± 28	$1.7 \pm 1.9^{(a)}$
	11	0.28 ± 0.0039	28 ± 1.3	20 ± 0.76	$1.4 \pm 0.081^{(a)}$
2	7	0.17 ± 0.019	24 ± 17		1.9 ± 0.40
	9	0.19 ± 0.012	63 ± 49		1.7 ± 0.21
3	7	0.17 ± 0.019		13 ± 9.0	1.9 ± 0.40
	9	0.19 ± 0.012		37 ± 28	1.7 ± 0.21

$$^{(a)} s_{\alpha_{D/L,int}} = \alpha_{D/L,int} ((s_{K_D}/K_D)^2 + (s_{K_L}/K_L)^2)^{1/2}, \text{ where } s \text{ is the standard deviation [4].}$$

To circumvent the large confidence intervals of $\alpha_{D/L,int}$ in case 1, we have substituted K_D by $\alpha_{D/L,int} K_L$ in eq 1 in order to estimate $\alpha_{D/L,int}$, K_L and q_s (case 2). Additionally, we have estimated q_s , K_D and $\alpha_{D/L,int}$ by substitution of K_L by $K_D/\alpha_{D/L,int}$ in eq 1 (case 3). As expected, the estimated values of the parameters are the same in all cases, since the minimum in *RSS* is independent of these substitutions. Contrary to the large confidence intervals of the affinity constants, the enantioselectivities deviate significantly from unity. These measurements have shown that the enantioselectivity decreases upon increasing pH. Since the number of charge interactions increases upon increasing pH, the nonselective electrostatic interactions become more and more pronounced, causing the enantioselectivity to decrease. Optimization must prove if at a lower pH the lower saturation concentration is compensated by the higher enantioselectivity.

Langmuir affinity constants. To estimate the Langmuir affinity constants accurately (*i.e.* smaller estimated standard deviation of the estimated parameters) we have chosen a different experimental approach, dead-end ultrafiltration with a continuous feed. A racemic mixture of phenylalanine is continuously fed to a micellar solution in a dead-end UF system. Figure 5 shows so-called break-through curves of D- and L-Phe at pH 6, 7 and 9, respectively, which

are the permeate concentrations of both enantiomers in time. The dashed lines represent the concentrations in case that no complexation has occurred: $c_e/c_{e,feed} = 1 - e^{-\theta}$. Similar to the batch experiments (figure 3), these measurements easily show that only little complexation has taken place at pH 6 and considerably more at pH 7 and 9.

A mass balance over the micellar solution assuming instantaneous Langmuir complexation leads to unsatisfactory fits (not shown). Therefore, we have assumed that the enantiomer complexation is limited by a complexation reaction rate. For this, the model is extended with a Linear Driving Force model (LDF model), which describes the complexation rate as the product of a driving force $c_e - c_{e,eq}$ (mM), and a reaction rate constant k_e (s^{-1}) [13,14]:

$$\frac{dc_e}{d\theta} = c_{e,feed} - c_e - \tau k_e (c_e - c_{e,eq}) \quad [\text{mM}] \quad (3)$$

where $c_{e,eq}$ (mM) represents the coexisting unbound concentration in equilibrium with the actual bound enantiomer concentration, θ is the dimensionless time, and τ (s) is the residence time of the aqueous bulk in the stirred cell. The equilibrium concentration $c_{e,eq}$ is calculated by the Langmuir isotherms. This chapter focuses on the complexation isotherms, the rate constants will be discussed in chapter 4.

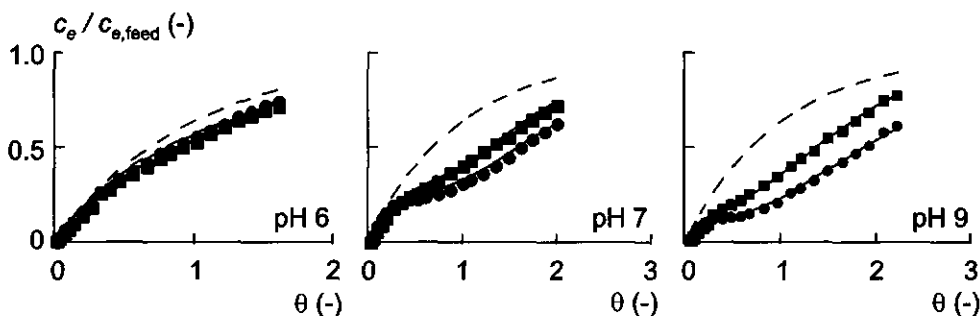


Figure 5. Break-through curves of D- (●) and L-Phe (■) at pH 6, 7 and 9 (from left to right).

The LDF model has been fitted on the measured break-through curves by minimizing the difference between the measured and predicted permeate concentrations (table 2 and solid lines in figure 5). To reduce the number of parameters to be estimated, the previously estimated q_s and $\alpha_{D/L,int}$ values have been used to fit eq 3 on the kinetic data at pH 7 and 9 (table 1). The estimated values for K_L at pH 7, 9 and 11 confirm that the affinity constant

increases upon increasing pH: 8.9, 14, and 20 mM^{-1} , respectively. Although, the enantioselectivity decreases with increasing pH, the calculated values for K_D ($= \alpha_{D/L,int} K_L$) still increase upon increasing pH: 17, 24, and 28 mM^{-1} , respectively.

Table 2. Dead-end ultrafiltration experiments with a continuous feed of D,L-Phe.

pH	q_s (mM)	$\alpha_{D/L,int}$ (-)	K_L (mM^{-1})	K_D (mM^{-1}) ^(b)
6	0.037 ± 0.022	0.67 ± 0.15	20 ± 28	13 (-15; +16)
7	0.17 ^(a)	1.9 ^(a)	8.9 ± 1.3	17 (-3.2; + 3.6)
9	0.19 ^(a)	1.7 ^(a)	14 ± 2.3	24 (-3.7; + 4.0)
11	0.28 ^(a)	1.4 ^(a)	20 ^(a)	28 (-1.6; + 1.7)

^(a) taken from table 1.

^(b) K_D is calculated as $\alpha_{D/L,int} K_L$, the 95% confidence intervals of K_D are calculated by Monte Carlo simulations and are given between parentheses [4].

Regeneration of enantioselective micelles. To reuse the micelles leaving the separation system (stage 1 in figure 1), the bound enantiomers must be dissociated from the micelles. We have considered three options: (i) an increase in temperature, (ii) dilution, and (iii) a decrease in pH. Since affinity usually decreases with temperature, it could be expected that temperature could induce decomplexation. However, ultrafiltration experiments at temperatures above the cloud-point of NNP10 (57°C) have shown negligible decomplexation. Although not applicable for decomplexation, cloud-point extraction could be considered for enantiomer separation instead of using ultrafiltration membranes [15,16]. Secondly, decomplexation by dilution is not an option either, since the high affinity constant would result in highly diluted systems. According to the equilibrium Langmuir model an unbound D-Phe concentration of 0.004 mM is required in order to remove 90% of the bound D-Phe enantiomers.

To prevent these highly diluted solutions we have studied the decomplexation of enantiomers by the third option: a decrease in pH. At pH 2, 3, and 4, the positive charge induces charge repulsion between selector molecules, enantiomers and Cu^{II} . Therefore, ultrafiltration experiments have been performed in a dead-end UF system with a continuous water feed of the same pH (figure 2).

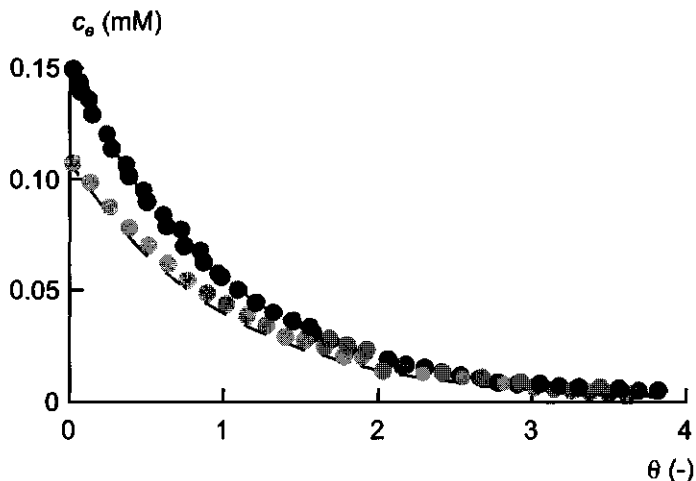


Figure 6. Wash-out curves of D-Phe at pH 2 (●), 3 (●), and 4 (○).

Figure 6 shows that at pH 2 and 3 all enantiomers are dissociated from the micelles, since the initial permeate concentration, c_D , is equal to the total enantiomer concentration, $c_{D,tot}$ (0.15 mM). After 24 hours at pH 4, only 70% of the bound D-Phe molecules have been dissociated. At pH 3, the reusability of the enantioselective micelles has been studied in more detail.

At pH 3 the complete decomplexation has taken 10 hours (figure 7a). Unfortunately, after 10 hours at pH 3 the micellar solution has lost 35 % of its complexation capacity (figure 7b). It has been expected that the unbound concentrations return to the initial unbound concentrations indicated by the horizontal dashed lines when the pH is reset to 7 at $t = t_{reg}$. Therefore, we have studied shorter regeneration times at pH 3. For t_{reg} is 6 hours the reusability is better than for t_{reg} is 10 hours (figure 7c). Still, the micelles have lost 20 % of their complexation capacity. After two hours at pH 3 only 60% of the bound enantiomers have been dissociated (figure 7d). However, the micelles retain nearly all their complexation capacity. It is concluded that hydrolysis of CLG could not have been responsible for the decreased effectiveness, since glutamic acid could not be found in the permeate. These regeneration experiments have shown that only partial dissociation should be allowed at pH 3 to keep the enantioselective micelles effective. Moreover, pH 4 could be further optimized in a multistage system to minimize the dilution.

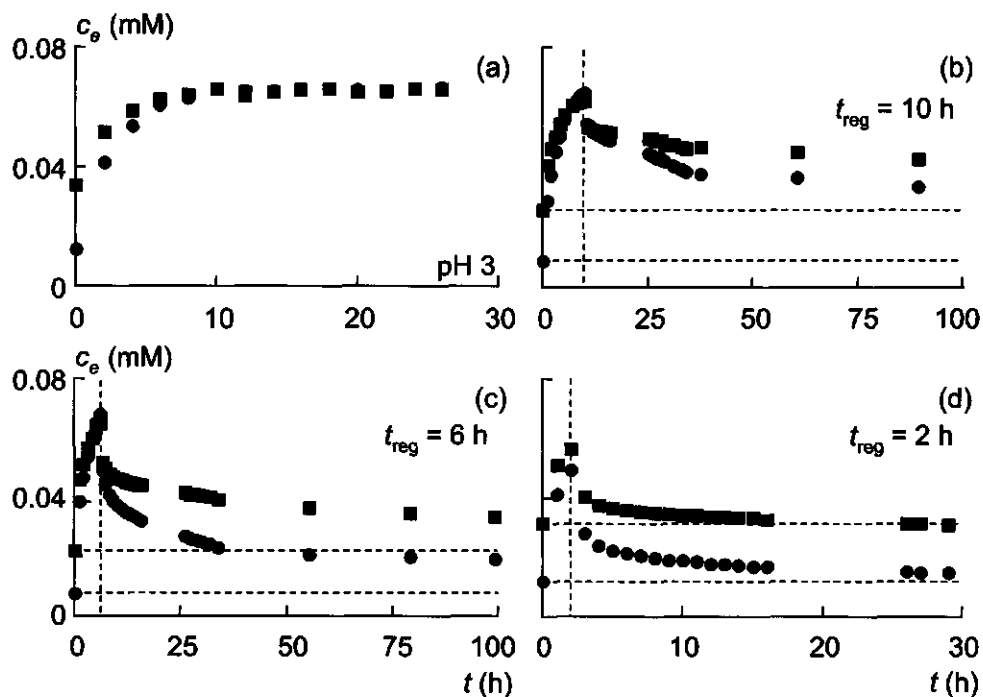


Figure 7. Decomplexation at pH 3 (a) and subsequent complexation at pH 7 at different regeneration times, $t_{reg} = 10, 6,$ and 2 hours (b, c, and d, respectively), see vertical dashed lines.

Conclusions

The separation of Phe enantiomers by cholesteryl-L-glutamate (CLG) anchored in micelles of the nonionic surfactant NNP10 is strongly effected by pH. The complexation of D,L-Phe by these enantioselective micelles can be described by straightforward multicomponent Langmuir isotherms. For pH 7, 9 and 11 the Langmuir constants have been estimated by fitting the isotherms on ultrafiltration data. The intrinsic enantioselectivity $\alpha_{D/L,int}$ decreases with increasing pH: 1.9, 1.7, and 1.4 for pH 7, 9, and 11, respectively. An increase in pH results in more charge interactions, which are unfavorable for enantioselective complexation. Evidently, as a result of these charge interactions, the Langmuir affinity constants increase with pH, K_L is 8.9, 14, and 20 mM^{-1} for pH 7, 9, and 11, respectively. Moreover, an

increasing pH results in an increasing maximum binding concentration, 57, 63 and 93% of the CLG concentration, respectively.

Decomplexation of enantiomers is mandatory to reuse the enantioselective micelles and to obtain the bound enantiomer, in our study D-Phe. However, regeneration of saturated micelles at $\text{pH} \geq 7$ results in highly diluted solutions, due to the high Langmuir affinity constants. A decrease in pH results in charge repulsion between CLG, Cu^{II} , and Phe, and consequently in decomplexation. Unfortunately, a $\text{pH} \leq 3$ results in inactivation of CLG. At pH 4 only 70% of the bound enantiomers have been dissociated in a single stage. A multistage system could be used to complete the decomplexation.

For $\alpha_{\text{D/L,int}} = 1.9$ a multistage system is still needed for 99% separation of enantiomers. For further optimization, the effect of the pH on the separation performance, the costs of the chiral selector and the number of stages should be taken into account.

Nomenclature

q, c	bound and unbound concentration, respectively	[mM]
$q_{e,\text{pred}}, c_{e,\text{pred}}$	estimated bound and unbound concentration, respectively	[mM]
q_s	saturation concentration	[mM]
K	affinity constant	[mM ⁻¹]
$\alpha_{\text{D/L,int}}$	intrinsic enantioselectivity ($= K_{\text{D}} / K_{\text{L}}$)	[-]
$[\alpha]_{\text{D}}^{293}$	optical rotation at 293 K, using sodium emission spectrum (589 nm).	[°]
k	reaction rate constant	[s ⁻¹]
pI	isoelectric point	[-]
s	standard deviation of parameter	
t, τ	time and residence time, respectively	[s]
$\Phi_{\text{P}}, \Phi_{\text{F}}$	permeate and feed flow rate, respectively	[L/s]
V	volume	[L]
θ	time	[-]

The subscripts D, L, e, F, P, eq, tot and reg refer to the D-enantiomer, the L-enantiomer, the D- or the L-enantiomer, the feed, the permeate, the equilibrium state the total concentration and regeneration, respectively.

References

- (1) *Chirality in industry I & II: Development in the manufacture and applications of optically active compounds*; Collins, A. N.; Sheldrake, G. N.; Crosby, J., Eds.; John Wiley & Sons: Chichester, 1992 & 1997.
- (2) Klepac, J.; Simmons, D. L.; Taylor, R. W.; Scamehorn, J. F.; Christian, S. D. *Sep. Sci. Technol.* **1991**, *26*, 165.
- (3) Overdeest, P. E. M.; Van der Padt, A.; Keurentjes, J. T. F.; Van 't Riet, K. In *Surfactant-Based Separations: Science and Technology*; Scamehorn, J. F.; Harwell, J. H., Eds.; ACS Symposium Series 740; American Chemical Society: Washington D.C., 1999.
- (4) Overdeest, P. E. M.; Van der Padt, A.; Keurentjes, J. T. F.; Van 't Riet, K. *Colloids and Surfaces A* **2000**, *163*, 209.
- (5) Brookes, G.; Pettit, L. D. *J. Chem. Soc. Dalton Trans.* **1977**, 1918.
- (6) Reiller, P.; Lemordant, D.; Hafiane, A.; Moulin, C.; Beaucaire, C. *J. Colloid Interf. Sci.* **1996**, *177*, 519.
- (7) Galaverna, G.; Corradini, R.; Munari, E. d.; Dossena, A.; Marchelli, R. *J. Chromatogr. A* **1993**, *657*, 43.
- (8) De Bruin, T. J. M.; Marcelis, A. T. M.; Zuilhof, H.; Rodenburg, L.M.; Niederländer, H.A.G.; Koudijs, A.; Overdeest, P. E. M.; Van der Padt, A.; Sudhölter, E. J. R. *Chirality* – accepted.
- (9) Blatt, W. F.; Robinson, S. M. *Anal. Biochem.* **1968**, *26*, 151.
- (10) Ahmadi, S.; Batchelor, B.; Koseoglu, S. S. *J. Membr. Sci.* **1994**, *89*, 257.
- (11) De Bruin, T.J.M. *Ph.D. Thesis*, Wageningen University, Wageningen, 2000.
- (12) Creagh, A. L.; Hasenack, B. B. E.; Van der Padt, A.; Sudhölter, E. J. R.; Van 't Riet, K. *Biotechnol. Bioeng.* **1994**, *44*, 690.
- (13) Guiochon, G.; Shirazi, S. G.; Katti, A. M. *Fundamentals of preparative and nonlinear chromatography*; Academic Press: Boston, 1994.
- (14) Li, Z.; Yang, R. T. *AIChE J.* **1999**, *45*, 196.
- (15) Lebens, P. J. M.; Keurentjes, J. T. F. *Ind. Eng. Chem. Res.* **1996**, *35*, 3415.
- (16) Tani, H.; Kamidate, T.; Watanabe, H. *J. Chromatogr. A* **1997**, *780*, 229.

4

COMPLEXATION KINETICS

Summary

Application of enantioselective micelles in ultrafiltration systems can be an alternative route to meet the increasing demand for enantiopure products. Previously, we have studied the separation of D,L-phenylalanine (D,L-Phe) by cholesteryl-L-glutamate anchored in nonionic micelles (intrinsic enantioselectivity $\alpha_{D/L,int} = 1.9$). A cascaded system is needed to complete the separation, since a single stage is insufficient to obtain 99+% optically pure products. It is shown that complexation and decomplexation processes are not instantaneous, hence elucidation of the complexation kinetics is inevitable to design a multistage system.

Linear driving force (LDF) models describe both the complexation and decomplexation rates of enantiomers. It can be concluded that the complexation rates of D- and L-Phe, $(32 \pm 11) \cdot 10^{-5} \text{ s}^{-1}$ and $(28 \pm 14) \cdot 10^{-5} \text{ s}^{-1}$, respectively, are not limited by enantiomer diffusion in the hydrophilic shell of the micelles. Consequently, the formation and rearrangement of the chelate complexes must be rate limiting. In addition, decomplexation of both enantiomers is even slower, in the order of 10^{-6} s^{-1} . Fortunately, ultrafiltration experiments have indicated that a rapid exchange of bound L-Phe by unbound D-Phe improves the decomplexation of L-Phe, $(360 \pm 250) \cdot 10^{-5} \text{ mM}^{-1} \text{ s}^{-1}$. This exchange process can be described by a second order LDF model.

This chapter has been submitted for publication as P.E.M. Overdeest, M.A.I. Schutyser, T.J.M. de Bruin, K. van 't Riet, J.T.F. Keurentjes and A. van der Padt, 'Separation of racemic mixtures by ultrafiltration of enantioselective micelles II: (de)complexation kinetics'

Introduction

Different biological activities of enantiomers make enantiopure compounds essential constituents of pharmaceuticals, crop protection agents and food. Therefore, numerous methods are studied to obtain these enantiopure products on a preparative scale [1]. We emphasize a route for the separation of racemic mixtures using membranes, potentially leading to continuous and preparative separation processes requiring a low energy input. Ultrafiltration membranes are used to retain enantioselective micelles from an aqueous bulk phase containing the unbound enantiomers, representing a so-called ligand-modified micelle-enhanced ultrafiltration process [2] (figure 1). The enantioselective micelles are composed of a chiral co-surfactant (chiral selector) cholesteryl-L-glutamate, CLG, anchored in micelles of the nonionic surfactant nonyl-phenyl polyoxyethylene [E10] ether [3]. For an efficient separation process, it is prerequisite that the chiral selector is insoluble in water, since solubility in the aqueous bulk phase leads to a loss of selector through the membrane. Nonionic micelles are used to prevent nonselective ion-ion interactions between surfactant and enantiomers. Since a single stage is insufficient, the separation requires a multistage system (cascade) to reach an optical purity of 99% for the desired enantiomer(s).

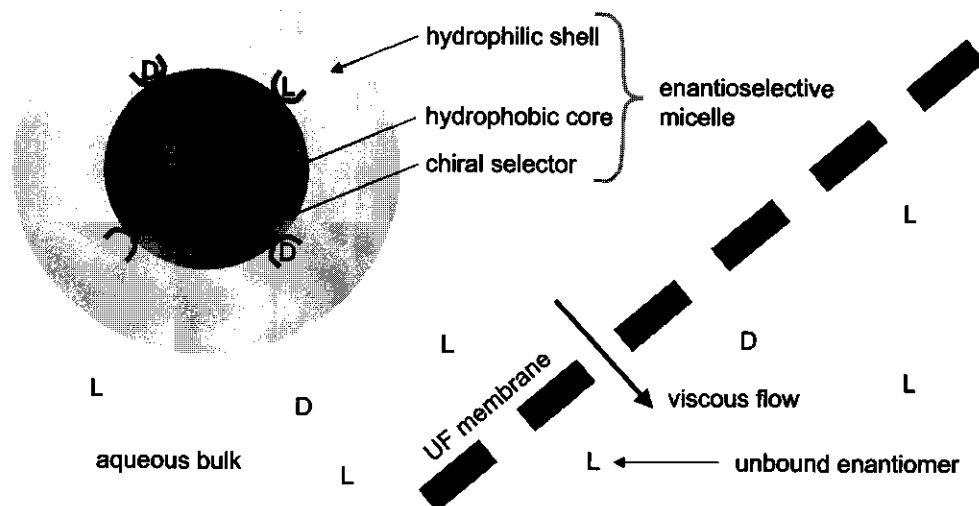


Figure 1. Enantiomer separation by ultrafiltration of enantioselective micelles containing chiral selector molecules. Micelles are rejected by the ultrafiltration (UF) membrane, where unbound enantiomers can pass the membrane. D and L represent the two enantiomers.

The complexation is based on 1:1:1 chelate complexes of selector, Cu^{II} and an enantiomer, where the heterologous complex (CLG:Cu:D-Phe) is more stable than the homologous complex (CLG:Cu:L-Phe) [4]. The complexation equilibria of D,L-Phe by CLG can be described by multicomponent Langmuir isotherms at pH 7, 9 and 11, where $\alpha_{\text{D/L,int}}$ is 1.9, 1.7, and 1.4, respectively [3,5]. Dead-end ultrafiltration with a continuous feed indicates that Phe enantiomer complexation by CLG is not instantaneous [5]. This chapter aims at the description of the (de)complexation kinetics of D,L-Phe by the enantioselective micelles. The (de)complexation rates put restrictions on the residence times of the solutions in each ultrafiltration stage. Long residence times are unfavorable as they lead to larger systems.

Theory

Modeling system kinetics. Complexation in a dead-end ultrafiltration system with a continuous feed can be described by the following mass balance of the unbound enantiomers [6,7]:

$$\frac{dc_e}{d\theta} = c_{F,e} - c_e - \frac{dq_e}{d\theta} \quad (\text{mM}) \quad (1)$$

where e accounts for the D- or the L-enantiomer, c and q (mM) are the unbound and bound enantiomer concentrations, respectively, $c_{F,e}$ (mM) is the enantiomer feed concentration and θ is the dimensionless time and equals the time t (s) over the residence time of the aqueous bulk phase in the stirred cell τ (s). The volume V (L) remains constant, since the feed and permeate flow are equal, Φ_F (L s^{-1}) and Φ_P (L s^{-1}), respectively (figure 2). The influence of the micellar volume on the unbound enantiomer concentration can be neglected since the micelle concentration is only 0.5% w/w. The unbound enantiomer concentration in the cell equals the measured enantiomer concentration in the permeate, since membrane rejection of unbound enantiomers can be neglected [3].

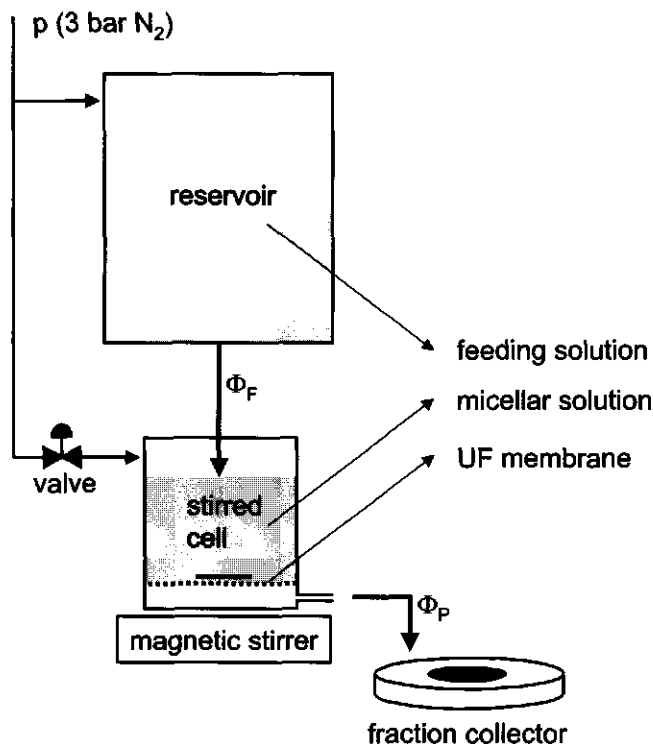
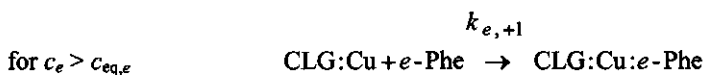


Figure 2. Experimental set-up of dead-end ultrafiltration with continuous feed.

To describe the (de)complexation kinetics, we distinguish 3 processes: (i) complexation of enantiomers by chiral selectors, (ii) decomplexation of enantiomers and chiral selectors, and (iii) exchange of enantiomers. A linear driving force (LDF) model is used to describe these processes [8,9]. This simple model is based on a rate constant k (s^{-1}), and a driving force based on a concentration gradient.

Complexation kinetics. For the complexation three processes can be distinguished: (i) enantiomer diffusion through the hydrophilic shell of the nonionic micelle, (ii) complexation of the enantiomer at an empty site, $CLG:Cu$, to form the chelate complex, $CLG:Cu:Phe$, and (iii) rearrangement of this chelate complex. These processes are lumped in a single complexation equation:



where $k_{e,+1}$ (s^{-1}) is the complexation rate constant. Keep in mind that also decomplexation occurs, as will be given below. The driving force of the complexation reaction is described by the difference between the actual unbound concentration in the bulk c_e (mM) and the equilibrium unbound concentration $c_{eq,e}$ (mM) corresponding to the Langmuir isotherms [3] and the coexisting bound concentration q_e (mM):

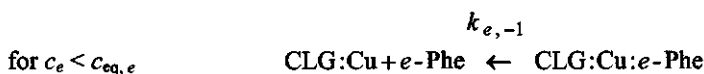
$$c_{eq,e} = \frac{q_e}{K_e (q_s - q_D - q_L)} \quad [\text{mM}] \quad (2e)$$

where K_e (mM^{-1}) is the affinity constant for e -Phe, and q_s (mM) is the Langmuir saturation concentration. Equation 2e is a generic equation for both enantiomers, e.g. equation 2D corresponds with the isotherm for D-Phe. In addition to the mass balance of the unbound enantiomers (eq 1), the mass balance of the bound e -Phe enantiomer is:

$$\text{for } c_e > c_{eq,e} \quad \left. \frac{dq_e}{d\theta} \right|_{\text{complexation}} = \tau k_{e,+1} (c_e - c_{eq,e}) \quad [\text{mM}] \quad (3e)$$

In case both enantiomers have equal complexation rate constants, it can be assumed that diffusion is rate limiting, since this is a nonselective process. On the other hand, being enantioselective processes, complex formation and rearrangement are assumed to be rate limiting if both constants are different.

Decomplexation kinetics. The decomplexation reaction includes the same three processes as the complexation reaction, although in opposite direction:



where $k_{e,-1}$ (s^{-1}) is the decomplexation rate constant of e -Phe. The driving force of the decomplexation reaction is described by the difference between the actual bound concentration in the bulk q_e (mM) and the equilibrium bound concentration $q_{eq,e}$ (mM)

corresponding to the Langmuir isotherms [3] and the coexisting unbound concentration, c_e (mM):

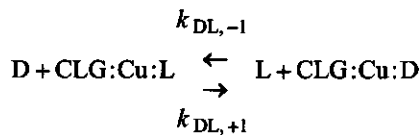
$$q_{eq,e} = K_e c_e (q_s - q_D - q_L) \quad [\text{mM}] \quad (4e)$$

The mass balance of bound *e*-Phe is:

$$\text{for } c_e < c_{eq,e} \quad \left. \frac{dq_e}{d\theta} \right|_{\text{decomplexation}} = -\tau k_{e,-1} (q_e - q_{eq,e}) \quad [\text{mM}] \quad (5e)$$

The dimensionless ratio of the complexation and decomplexation rate constants, $k_{e,+1} / k_{e,-1}$, is not equal to the corresponding affinity constant K_e (mM^{-1}), due to the lumped character of the reaction rate constants. Note that, $c_e < c_{eq,e}$ corresponds with $q_e > q_{eq,e}$ for all concentrations.

Exchange kinetics. Exchange describes an equimolar reaction where a compound is transferred from one phase to another under simultaneous transfer of another compound in opposite direction [10,11]. Applied to our system this exchange reaction is described as:



The rate of this reaction is given by the exchange rate constants $k_{DL,+1}$ ($\text{mM}^{-1} \text{s}^{-1}$) and $k_{DL,-1}$ ($\text{mM}^{-1} \text{s}^{-1}$). A second order LDF-term is used to account for enantiomer exchange [10], where one term represents the driving force of the unbound enantiomers, and the other term represents the driving force of the bound enantiomers. If $c_D > c_{eq,D}$ and $q_L > q_{eq,L}$ (c_D, q_L) exchange of bound D-Phe by unbound L-Phe can be described by:

$$\left. \frac{dq_D}{d\theta} \right|_{\text{exchange}(c_D, q_L)} = \tau k_{DL,+1} (c_D - c_{eq,D}) (q_L - q_{eq,L}) \quad [\text{mM}] \quad (6)$$

$$\left. \frac{dq_L}{d\theta} \right|_{\text{exchange}(c_D, q_L)} = -\tau k_{DL,+1} (c_D - c_{eq,D}) (q_L - q_{eq,L}) \quad [\text{mM}] \quad (7)$$

In case $c_L > c_{eq,L}$ and $q_D > q_{eq,D}$ (c_L, q_D), similar sets of mass balances are used for exchange of bound D-Phe by unbound L-Phe, including $k_{DL,-1}$ ($\text{mM}^{-1} \text{s}^{-1}$), and will be referred to as eqs 8 and 9. The equilibrium concentrations are calculated by eqs 2e and 4e. Obviously, the exchange expression is omitted in case the two LDF-terms have opposite signs.

Materials and Methods

Materials. The nonionic surfactant, nonyl-phenyl polyoxyethylene [E10] ether (NNP10), was a gift by Servo Delden b.v. (Delden, The Netherlands). An average molecular weight of 644 g/mol was assumed. The chiral selector, cholesteryl-L-glutamate (CLG), was synthesized by the Laboratory of Organic Chemistry ($[\alpha]_D^{293} = -27^\circ$ at 10.5 g/L chloroform, 3% trifluoroacetic acid) [12]. Double distilled water was used throughout this study. All other components were obtained from Merck (Darmstadt, Germany) and were used without further purification. The ultrafiltration experiments were performed using a regenerated cellulose membrane of 3 kDa MWCO (YM3, Millipore).

Solution preparation. Batches of 200 mL micellar solution were prepared as follows. The selector was dispersed in the liquid surfactant, followed by addition of 6 mL of water to yield a highly concentrated solution. The solution was stirred for 20 h, during which the selector completely dissolved. Stock solutions of D,L-Phe, CuCl_2 and KCl were added, so that the final concentrations were 7.8 mM NNP10 (0.5% w/w), 0.3 mM CLG, 0.3 mM CuCl_2 , 0.15 mM D,L-Phe and 0.1 M KCl. Equimolar concentrations of selector and Cu^{II} result in the optimal performance of this system [4]. Based on the type of experiment the micellar solution and the feed solution contained 0.15 mM D-, L-, or D,L-Phe or no enantiomers at all (table 1). In addition, the feed solution contained 0.1 M KCl to maintain a constant ionic strength during the experiment. The batches and the feed solutions were set at pH 7 and were equilibrated for another 20 h.

Table 1. The type of experiment is appointed by the initial state of the UF system.

Type of exp.	micellar solution	feed solution
Wash-in		0.15 mM D,L-Phe
Wash-out	0.15 mM D,L-Phe	
Wash-in/out	0.15 mM of one enantiomer	0.15 mM of other enantiomer

Continuous ultrafiltration experiments. A stirred cell (Amicon 8400 series, Millipore) with a continuous feed was used to perform wash-in, wash-out, and wash-in/out experiments [6,7] by ultrafiltration of a micellar solution (figure 2). Both the reservoir and the cell were pressurized at 3 bar by N_2 . Immediately after the system reached 3 bar the pressure valve was closed and the experiment started. The feed flow Φ_F was equal to the permeate flow Φ_P ($2.8 \cdot 10^{-5}$ L/s), so that the volume V remained constant (200 mL). It could be assumed that the solution in the cell was ideally mixed, since the residence time, $\tau = 7.2 \cdot 10^3$ s, was much longer than the mixing time, which was in the order of seconds. Note that, this system resembled a chromatography set-up containing 1 theoretical transfer unit, however, we applied a step function input instead of a pulse.

The permeate was collected in a fraction collector and samples were analyzed by HPLC as described before [3], which enabled us to measure the break-through curves of both the D- and the L-enantiomer. Three experimental procedures were followed to study the complexation, the decomplexation and the exchange of enantiomers by the enantioselective micelles. These procedures will be referred to as wash-in, wash-out and wash-in/out experiments, respectively (table 1).

Fitting procedure. The measured permeate concentrations c_D and c_L were used to fit the kinetic model (eqs 1 – 9). An algorithm based on the Levenberg-Marquardt method was used to minimize the Residual Sum of Squares (RSS):

$$RSS = \sum (c_D - c_{D,pred})^2 + \sum (c_L - c_{L,pred})^2 \quad (10)$$

where $c_{D,pred}$ and $c_{L,pred}$ are the predicted permeate concentrations of D- and L-Phe, respectively, by the Langmuir isotherms [3,5]. Additionally, the algorithm yielded the Jacobian matrix which was used to calculate the 95% confidence intervals of the estimated

parameters. In order to reduce the number of parameters we fixed the saturation concentration q_s , the affinity constant for L-Phe K_L , and the intrinsic enantioselectivity $\alpha_{D/L,int}$. These parameters have been estimated before by dead-end ultrafiltration experiments: 0.17 ± 0.019 mM, 8.9 ± 1.3 mM⁻¹, and 1.9 ± 0.4 , respectively [5].

Results and Discussion

To collect the rate constants three types of experiments were done to study the complexation, decomplexation, and exchange kinetics of D,L-Phe by the enantioselective micelles.

Complexation kinetics. Figure 3a shows the break-through curves of D- and L-Phe measured during wash-in. The dotted line in this figure represents the permeate concentration in case no complexation takes place, $c_e = c_{F,e} (1 - e^{-\theta})$. It can clearly be seen that enantioselective complexation takes place to the advantage of D-Phe. The measured concentrations have been used to fit eqs 1, 2e and 3e (solid lines) by minimizing the difference between the measured and predicted permeate concentrations (eq 10). The estimated complexation rate constants, $k_{D,+1}$ and $k_{L,+1}$, are $(32 \pm 11) \cdot 10^{-5} \text{ s}^{-1}$ and $(28 \pm 14) \cdot 10^{-5} \text{ s}^{-1}$, respectively (table 2). Although exchange could have occurred, addition of the exchange model (eqs 6 and 7) yields the same values for $k_{D,+1}$ and $k_{L,+1}$ (as shown by *t*-tests) and an insignificant exchange parameter, $k_{DL,+1}$ is $(22 \pm 84) \cdot 10^{-5} \text{ mM}^{-1} \text{ s}^{-1}$. Apparently, under these conditions the bound L-Phe concentration was so low that exchange could not be distinguished from complexation. As we will show later, exchange of bound D-Phe by unbound L-Phe (c_L, q_D) is not expected at all.

Since the complexation rate constants, $k_{D,+1}$ and $k_{L,+1}$, are not significantly different, it appears that a nonselective process is rate limiting. Since the chiral selector has a relatively small hydrophilic head group (L-Glu) as compared to the hydrophilic head group of the surfactant (10 ethylene oxide groups), it is hypothesized that equal rate constants could be the result of diffusion limitation of Phe through the hydrophilic shell of the micelle. To check this hypothesis we have calculated the apparent diffusion constant $D_{e,app}$ (m² s⁻¹) of the enantiomers in the hydrophilic shell using the complexation rate constants $k_{D,+1}$ and $k_{L,+1}$:

$$D_{e,app} = \delta k_{e,+1} / A \quad [\text{m}^2 \text{ s}^{-1}] \quad (11)$$

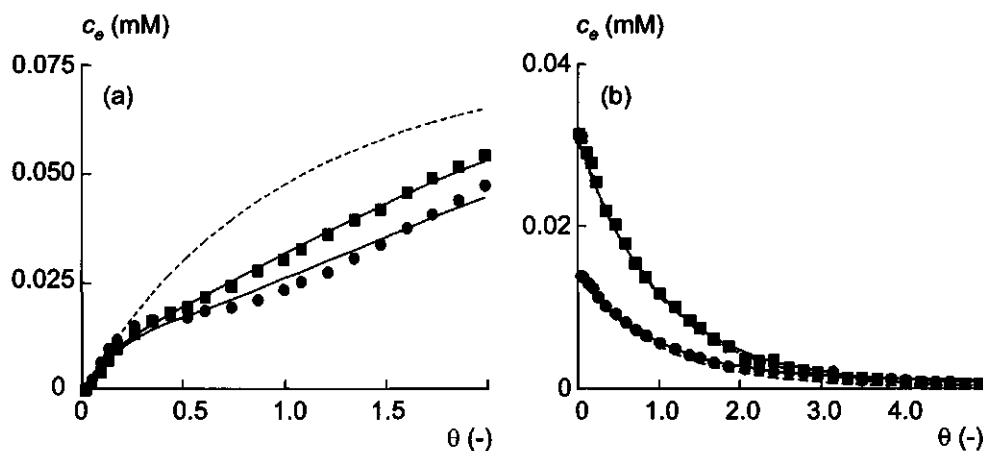


Figure 3. Break-through curves of D- (●) and L-Phe (■) in wash-in (a) and wash-out (b) experiments, with fit (—) and in case no affinity takes place (---).

Table 2. Three types of experiments have been performed to study the complexation kinetics. Exchange rate constant $k_{DL,-1}$ is left out, since it is zero in all cases. *t*-Test analyses show that each estimated rate constant is the same for each type of wash experiment, except for $k_{L,+1}$, which could be explained by the experimental conditions.

type of wash experiment	$k_{D,+1} \cdot 10^5$ (s^{-1})	$k_{D,-1} \cdot 10^5$ (s^{-1})	$k_{L,+1} \cdot 10^5$ (s^{-1})	$k_{L,-1} \cdot 10^5$ (s^{-1})	$k_{DL,+1} \cdot 10^5$ ($mM^{-1} \cdot s^{-1}$)
in	32 ± 11		28 ± 14		22 ± 84
out		0.23 ± 0.09		0.18 ± 0.12	
in/out (c_D, q_L)	51 ± 23			0.86 ± 0.64	360 ± 250
in/out (c_L, q_D)		0.24 ± 0.07	0.42 ± 0.09		
obtained set	32 ± 11	0.23 ± 0.09	28 ± 14	0.18 ± 0.12	360 ± 250

where δ (m) is the diffusion length. The specific area A (m^{-1}) of the micelle is calculated as $3\varepsilon/r$, where the micellar volume fraction ε is 0.005, assuming equal densities of micelles and water. The micelle radius r (m) has been obtained by measurement of the micelle diffusion constant in the aqueous phase using a light scattering technique (ALV3000 digital autocorrelator, $\lambda = 488$ nm, measured angle is 90°). According to the Stokes-Einstein relation, the micellar diffusion constant equals $kT/6\pi\eta r$ [13], where k (JK^{-1}) is the Boltzmann constant, T (K) is the temperature and η ($Ns m^{-2}$) is the viscosity of the bulk

phase. The light scattering measurements have resulted in a hydrodynamic micelle radius of approximately 10 nm, hence we have assumed a diffusion length of 5 nm. Consequently, diffusion constants of $1.3 \cdot 10^{-18}$ and $1.1 \cdot 10^{-18} \text{ m}^2 \text{ s}^{-1}$ are calculated for D- and L-Phe, respectively (eq 11). Even a viscosity correction of 100 for the oily-like polyoxyethylene layer can not explain the deviation from diffusion constants of aqueous solutes in water, which are in the order of $10^{-9} \text{ m}^2 \text{ s}^{-1}$ [14]. It is concluded that chelate formation or rearrangement of the complex in the micelle must be rate limiting.

Decomplexation kinetics. Figure 3b shows the wash-out of D,L-Phe. The measured permeate concentrations approach the concentrations in case no decomplexation occurs, $c_e = c_{F,e} e^{-t}$ (dotted lines). This figure indicates that the decomplexation rate constant is small if compared to the inverse of the residence time ($7.2 \cdot 10^3 \text{ s}$). Indeed, fitting eqs 1, 4e and 5e results in values of only $(0.23 \pm 0.09) \cdot 10^{-5} \text{ s}^{-1}$ and $(0.18 \pm 0.12) \cdot 10^{-5} \text{ s}^{-1}$ for $k_{D,-1}$ and $k_{L,-1}$, respectively (solid lines).

A possible explanation for the slow decomplexation could be that after complexation the neutral CLG:Cu:Phe complex rearranges and relocates to the center of the micelle, due to the hydrophobicity of Phe. Consequently, disassociation requires relocation and rearrangement of the complex, which are probably the rate limiting factors in this system. Therefore, it can be hypothesized that decomplexation of one enantiomer under simultaneous complexation of the other enantiomer (exchange) is faster than just decomplexation of the one enantiomer, since relocation and rearrangement of the complex can then be partly omitted.

Exchange kinetics. Wash-in/out experiments have been performed with two different initial states: D-Phe enantiomers have been fed to micelles equilibrated with L-Phe (figure 4a: c_D , q_L) and visa versa (figure 4b: c_L , q_D). Figure 4a clearly shows that L-Phe decomplexation is induced by feeding the micellar phase with D-Phe. Fitting the kinetic model (eq 1, 2D, 3D 4L, 5L, 6 and 7) on these measured concentrations has yielded the D-Phe complexation rate constant, the L-Phe decomplexation rate constant, and the exchange rate constant, $k_{DL,+1}$ (table 2). The estimated value for the D-Phe complexation rate constant, $(51 \pm 32) \cdot 10^{-5} \text{ s}^{-1}$, is equal to the corresponding value in the wash-in experiment. The estimated L-Phe decomplexation rate constant, $(0.86 \pm 0.64) \cdot 10^{-5} \text{ s}^{-1}$, equals the one estimated in the wash-out experiment. The additional L-Phe decomplexation is described by the exchange rate constant $k_{DL,+1}$ of $(360 \pm 250) \cdot 10^{-5} \text{ mM}^{-1} \text{ s}^{-1}$.

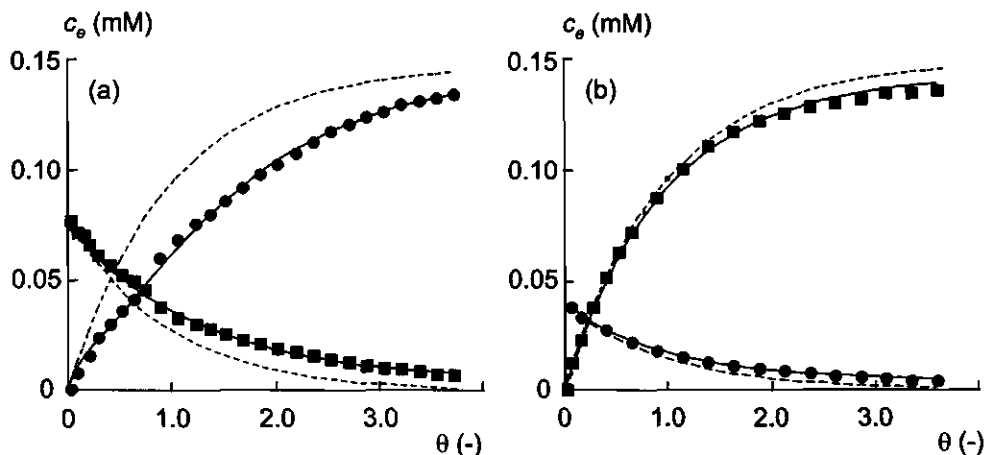


Figure 4. Break-through curves of D- (●) and L-Phe (■) in wash-in/out experiments (a: D-Phe in feed, b: L-Phe in feed), with fit (—) and in case no affinity takes place (- - -).

Figure 4b shows that the D-enantiomer decomplexation rate is not significantly higher than the one estimated in the wash-out experiment (figure 3b). Indeed, fitting the kinetic model (eqs 1, 2L, 3L, 4D, 5D, 8 and 9) has confirmed that $k_{DL,-1}$ is zero. Therefore, we have used eqs 1, 2L, 3L, 4D and 5D to estimate the D-Phe decomplexation rate constant, $k_{D,-1}$ and the L-Phe complexation rate constant, $k_{L,+1}$, as $(0.24 \pm 0.07) \cdot 10^{-5} \text{ s}^{-1}$ and $(0.42 \pm 0.09) \cdot 10^{-5} \text{ s}^{-1}$, respectively (table 2). The fact that the D-Phe decomplexation rate constant is the same in both this exchange experiment and in the wash-out experiment strengthens the assumption that D-Phe decomplexation is independent of the presence of L-Phe.

Finally, one set of kinetic parameters is obtained to describe all kinetic experiments (table 2). For exchange ($k_{DL,+1}$) we have used data of the wash-in/out experiments, while the other parameters originate from wash-in and wash-out experiments (table 1). Figure 5 shows a parity plot of all measured and predicted data using eqs 1, 2e, 3e, 4e, 5e, 6 and 7, and the obtained parameter set given in table 2. It can be concluded that this model adequately describes all the experiments.

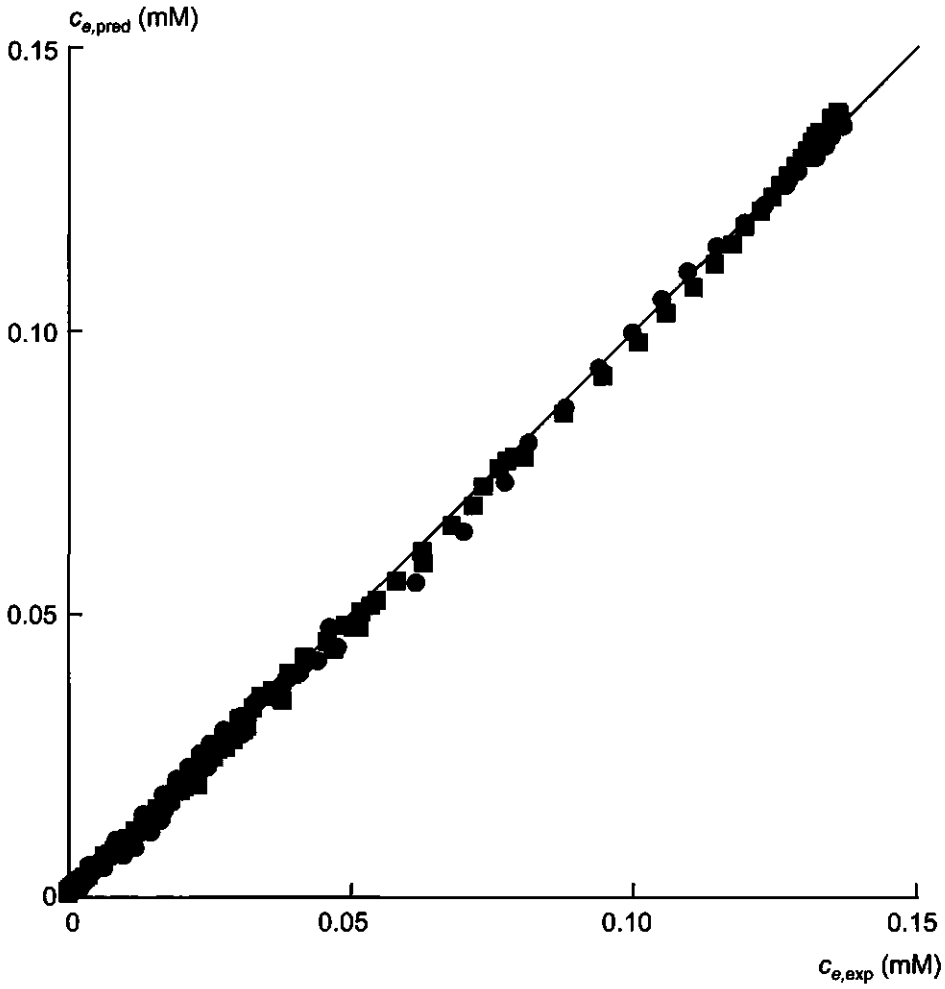


Figure 5. Parity-plot of all measured (exp) kinetic data against the predicted (pred) concentrations based on the LDF-model and the obtained parameter set (table 2).

Conclusions

A model is presented that describes the (de)complexation kinetics of D,L-Phe enantiomers by enantioselective micelles, composed of cholesteryl-L-glutamate (CLG) in micelles of the nonionic surfactant NNP10. The model based on the Linear Driving Force concept was extended by second order enantiomer exchange. These kinetic data are essential to design a multistage system.

Continuous ultrafiltration experiments have shown that the complexation rate constants of D- and L-Phe are $(32 \pm 11) \cdot 10^{-5} \text{ s}^{-1}$ and $(28 \pm 14) \cdot 10^{-5} \text{ s}^{-1}$, respectively. Since the complexation rate constants for the D- and L-enantiomer are equal, it can be concluded that the complexation rate is not limited by chiral recognition during chelate formation. Most likely, rearrangement and relocation (caused by hydrophobicity of Phe) of the chelate complex is rate limiting. Hence, decomplexation should be slow. Indeed, this is the case: $k_{D,-1}$ is $(0.23 \pm 0.09) \cdot 10^{-5} \text{ s}^{-1}$ and $k_{L,-1}$ is $(0.18 \pm 0.12) \cdot 10^{-5} \text{ s}^{-1}$. Fortunately, exchange of the enantiomers is significantly faster, $k_{DL,+1}$ is $(360 \pm 250) \cdot 10^{-5} \text{ mM}^{-1} \text{ s}^{-1}$.

To ensure an efficient use of the enantioselective micelles, it is expected that each stage should be in equilibrium, since the enantioselectivity is not kinetically controlled. Therefore, the residence time per stage τ should be at least $1.1 \cdot 10^4 \text{ s}$ to reach complexation equilibrium, assuming $\tau > 3 / k_{e,+1}$.

Acknowledgements

The authors gratefully acknowledge financial support from the Dutch Technology Foundation (grant no. WCH44.3380), Akzo Nobel, and DSM. The authors wish to thank R. Fokkink for his support with the light scattering measurements.

Nomenclature

A	specific area of the micelle (= $3 \varepsilon / r$)	(m^{-1})
c_e	unbound enantiomer concentration	(mM)

$D_{e,app}$	apparent diffusion coefficient of enantiomers	$(m^2 s^{-1})$
K_e	affinity constant	(mM^{-1})
$k_{e,\pm 1}$	(de)complexation reaction rate constant	(s^{-1})
$k_{DL,\pm 1}$	exchange reaction rate constant	$(mM^{-1} s^{-1})$
q_e	bound enantiomer concentration	(mM)
q_s	saturation concentration	(mM)
t	time	(s)
V	volume	(L)
$\alpha_{D/L,int}$	intrinsic enantioselectivity ($= K_D / K_L$)	$(-)$
$[\alpha]_D^{293}$	optical rotation at 293 K, using sodium emission spectrum (589 nm).	$(^\circ)$
δ	diffusion length	(m)
ε	micellar volume fraction	$(-)$
Φ_P, Φ_F	permeate and feed flow rate, respectively	$(L s^{-1})$
τ	residence time per stage	(s)
θ	dimensionless time ($= t / \tau$)	$(-)$

The subscripts D, L, e, F, P, eq, and tot refer to the D-enantiomer, the L-enantiomer, the D- or the L-enantiomer, the feed, the permeate, the equilibrium state and the total concentration, respectively.

References

- (1) *Chirality in industry I & II: Development in the manufacture and applications of optically active compounds*; Collins, A. N.; Sheldrake, G. N.; Crosby, J., Eds.; John Wiley & Sons: Chichester, 1992 & 1997.
- (2) Fillipi, B. R.; Scamehorn, J. F.; Taylor, R. W.; Christian, S. D. *Sep. Sci. Technol.* **1997**, 32, 2401.
- (3) Overdevest, P. E. M.; Van der Padt, A.; Keurentjes, J. T. F.; Van 't Riet, K. *Colloids and Surfaces A*, **2000**, 163, 209.
- (4) Creagh, A. L.; Hasenack, B. B. E.; Van der Padt, A.; Sudhölter, E. J. R.; Van 't Riet, K. *Biotechnol. Bioeng.* **1994**, 44, 690.
- (5) Overdevest, P.E.M.; De Bruin, T.J.M.; Sudhölter, E.J.R.; Keurentjes, J.T.F.; Van 't Riet, K.; Van der Padt, A. chapter 3.
- (6) Blatt, W. F.; Robinson, S. M. *Anal. Biochem.* **1968**, 26, 151.

- (7) Ahmadi, S.; Batchelor, B.; Koseoglu, S. S. *J. Membr. Sci.* **1994**, *89*, 257.
- (8) Guiochon, G.; Shirazi, S. G.; Katti, A. M. *Fundamentals of preparative and nonlinear chromatography*; Academic Press: Boston, 1994.
- (9) Li, Z.; Yang, R. T. *AIChE J.* **1999**, *45*, 196.
- (10) Rynders, R. M.; Rao, M. B.; Sircar, S. *AIChE J.* **1997**, *43*, 2456.
- (11) Wahlgren, M.; Elofsson, U. *J. Colloid Interf. Sci.* **1997**, *188*, 121.
- (12) De Bruin, T. J. M.; Marcelis, A. T. M.; Zuilhof, H.; Rodenburg, L.M.; Niederländer, H.A.G.; Koudijs, A.; Overdeest, P. E. M.; Van der Padt, A.; Sudhölter, E. J. R. *Chirality* – accepted.
- (13) Evans, D. F.; Wennerström, H. *The colloidal domain*; VCH Publisher: New York, **1994**.
- (14) Atkins, P. W. *Physical chemistry*; Oxford University Press: Oxford, **1987**.

5

MODEL VALIDATION

Summary

The increasing demand for optically pure compounds (enantiomers) stimulates the development of new enantiomer separation processes at industrial scale. We study the separation of enantiomers by ultrafiltration of enantioselective micelles in a cascaded system, since one single stage can only result in 99+% separations of both enantiomers at extremely high enantioselectivities of around 10^4 . The previously described complexation model [1] has been validated by two set-ups: a cascade of 5 lab scale ultrafiltration units and a bench scale system. Thus, this separation concept has proven its suitability for enantiomer separation. In addition, the bench scale experiments have demonstrated that the micellar separation system can be operated at larger scale using industrial type of membrane modules.

Model calculations show that the separation is not greatly improved at enantioselectivities (= ratio of affinity constants) above 10. Moreover, these calculations have made clear that the affinity of the enantioselective micelles for the substrate (enantiomers) plays a crucial role in the performance of the separation process. This will be discussed in detail in chapter 6.

This chapter has been submitted for publication as part of P.E.M. Overdeest, M.H.J. Hoenders, K. van 't Riet, J.T.F. Keurentjes and A. van der Padt, 'Enantiomer separation in a cascaded micellar ultrafiltration system: enantioselectivity, Langmuir affinity, and productivity'.

Introduction

Since the biological activity of enantiomers can be different, the purity of these chiral compounds in pharmaceuticals, agrochemicals and food additives is of crucial importance. Where one enantiomer has the desired activity, the mirror image of this compound can provoke negative side effects. Consequently, the development of new methods for the production of these optically pure compounds is stimulated by the industry.

A new separation technique, based on micelle-enhanced ultrafiltration (MEUF) [2,3], makes use of membranes in order to accomplish the separation of racemic mixtures (*i.e.* an equimolar mixture of the two enantiomers). Membrane separations are attractive and cost-efficient, due to the possibility of continuous operation, a low energy requirement, and ease of scale-up. The developed system contains nonionic micelles in which chiral selector molecules are anchored [4]. Starting with a racemic mixture, the selector preferentially binds one of the two enantiomers. During ultrafiltration, the micelles are retained including the bound enantiomers, while unbound enantiomers pass the membrane.

Equilibrium and kinetic models have been developed to describe the complexation of D,L-phenylalanine (D,L-Phe) enantiomers by cholesteryl-L-glutamate in nonionic micelles [5,6], which is our model system. Design calculations show that extremely high enantioselectivities, of around 10^4 , are required to satisfy the separation constraint in one single stage. However, above an enantioselectivity of 10, the separation hardly improves (Fig. 1). This chapter describes a multistage system that results in the separation of both enantiomers (Fig. 2). If only one enantiomer is required at high purity, the other enantiomer can be re-introduced in the separation system after racemization. Then, the required number of stages will be less than in case both enantiomers are wanted. This chapter aims at the development of a model describing the separation in a multistage system, using the previously fitted complexation model [1]. Cascaded ultrafiltration experiments have been conducted at both laboratory and bench scale to validate the separation model. The lab scale system has consisted of a series of 5 ultrafiltration (UF) units, the bench scale system of only one single UF unit containing an industrial type of membrane module. In the bench scale system the feed concentration is controlled to simulate the condition in each UF stage of the multistage system.

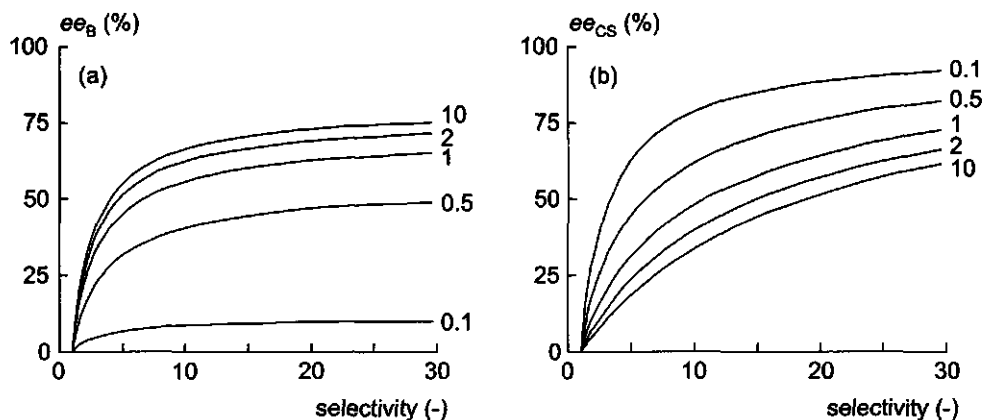


Figure 1. Enantiomer separation in one single stage for several ratios of selector and racemic mixture concentrations (value is shown at the right side of each curve), (a) the *ee* in the bulk phase, $ee_B = |c_D - c_L| / (c_D + c_L)$, and (b) the *ee* of enantiomers on the chiral selectors, $ee_{CS} = |q_D - q_L| / (q_D + q_L)$.

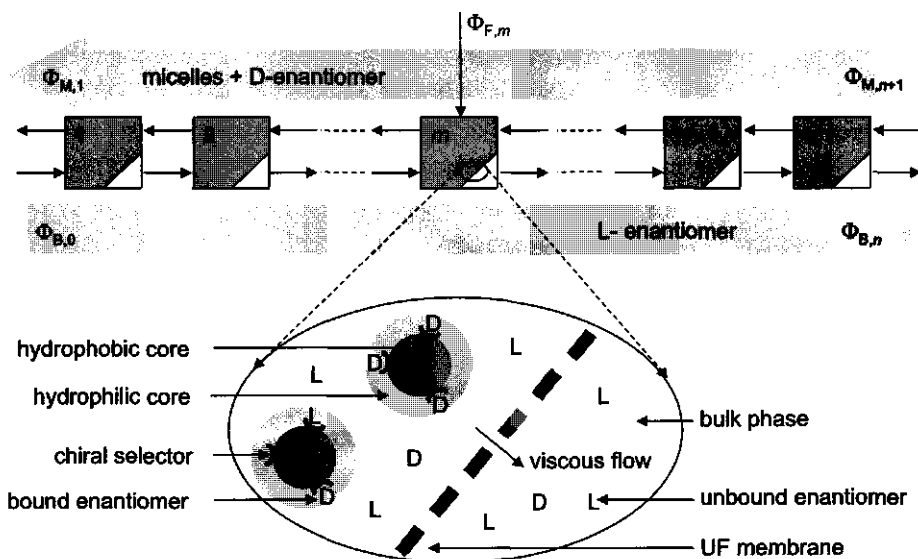


Figure 2. A cascaded counter-current MEUF system for the separation of racemic mixtures. Water enters stage 1, a racemic mixture (equimolar solution of both enantiomers) enters stage *m*, and 'empty' micelles enter the system in stage *n*. Under optimal conditions, the retentate of stage 1 is enriched with the D-enantiomer, where the permeate of stage *n* is enriched with the L-enantiomer.

Theory

Modeling the cascaded ultrafiltration system. Previously, we have fitted the multicomponent Langmuir isotherms [1] and the (de)complexation kinetics [6]. These models are used to describe the enantiomer separation in a cascaded MEUF system of n stages (Fig. 2). For each stage, the mass balances are combined with the multicomponent isotherms. To avoid correlation between system parameters and input variables and to facilitate the scale-up of the separation system, dimensionless numbers are introduced (Fig. 3, appendix I):

$$I_i \frac{d(\sigma_{e,i} + \beta Q_i \theta_{e,i})}{d\theta} = \phi_{M,i} \sigma_{e,i+1} + \phi_{M,i} \beta Q_i (\theta_{e,i+1} - \theta_{e,i}) - \sigma_{e,i} + \phi_{F,i} + \phi_{B,i} \sigma_{e,i-1} \quad (-) \quad (1)$$

where $\sigma_{e,i}$ represents the dilution factor of enantiomer e (D or L) in the system, equal to the unbound enantiomer concentration in stage i $c_{e,i}$ (mM) over the enantiomer feed concentration $c_{F,e}$ (mM). The number β is a measure for the selector requirement: the selector concentration $q_{s,F}$ entering the cascade over $c_{F,e}$. The mass flows through the system are characterized by their stage cut ϕ : the flow fraction of the sum of flows leaving (or entering) a stage. Both I_i and Q_i are functions of these stage cuts (see Appendix I).

At equilibrium, the bound enantiomer concentration $\theta_{e,i}$ is described by the Langmuir isotherms. Introducing the presented dimensionless parameters, these isotherms become:

$$\theta_{D,i} = \frac{\alpha_{D/L,int} \sigma_{D,i}}{1/\kappa_L + \alpha_{D/L,int} \sigma_{D,i} + \sigma_{L,i}} \quad (-)$$

$$\theta_{L,i} = \frac{\sigma_{L,i}}{1/\kappa_L + \alpha_{D/L,int} \sigma_{D,i} + \sigma_{L,i}} \quad (-) \quad (2)$$

where κ_L is the dimensionless affinity number for the L-enantiomer, equal to the affinity for this enantiomer K_L (mM⁻¹) times $c_{F,e}$.

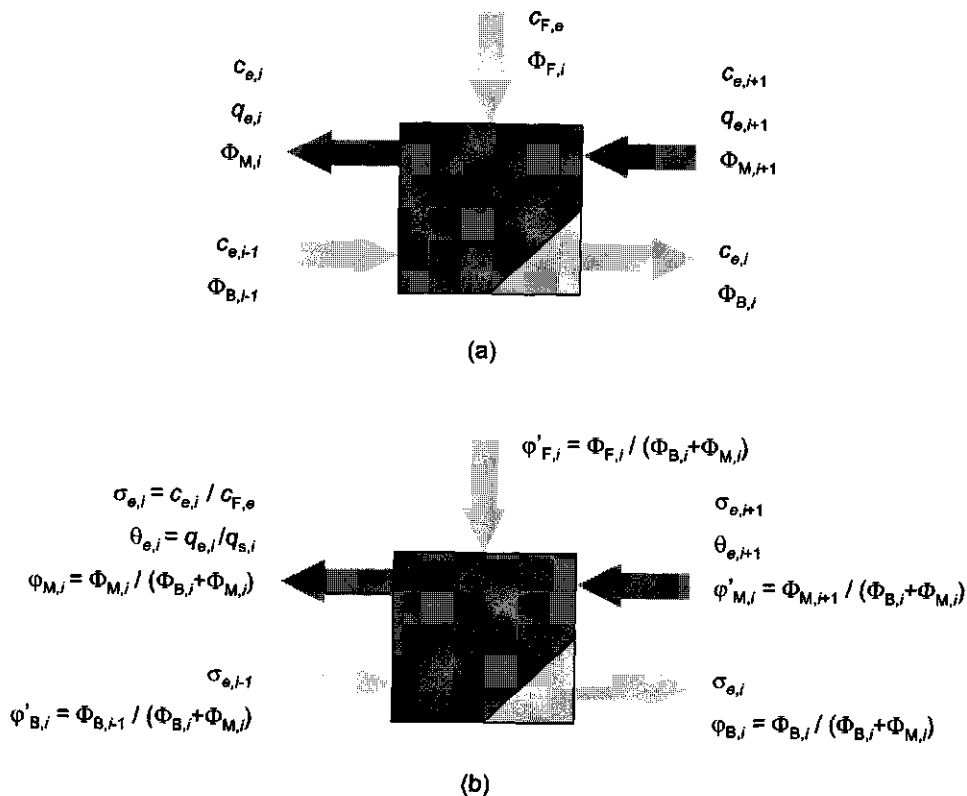


Figure 3. One single stage from the cascaded system, (a) the dimensional variables, and (b) the dimensionless numbers (note, $\Phi_{F,i \neq m} = 0$, and $\varphi_{M,i} = 1 - \varphi_{B,i}$).

The intrinsic enantioselectivity $\alpha_{D/L,int}$ equals K_D over K_L . In case the residence time in the system is long enough to assume equilibrium [σ], the separation can be modeled using eqs 1 and 2; note that, $d\theta_{e,i} / d\theta = (d\theta_{e,i} / d\sigma_{e,i}) \cdot (d\sigma_{e,i} / d\theta)$. Otherwise, the complexation kinetics can be described by a linear driving force model (appendix II).

Optimization criterion and separation constraint. To optimize the separation process, both product yield and purity should be maximized using a minimal number of stages. In order to do so, a yield and purity constraint must be defined. For this cascaded system, we aim at a high purity of both the micellar phase leaving stage 1 and the bulk phase leaving stage n .

Therefore, the sum of the enantiomeric excess in both phases, $ee_{\text{sum}} = ee_{M,1} + ee_{B,n}$ (%), should at least be equal to a chosen set-point:

$$\frac{ee_{\text{sum}}}{100\%} = \frac{|q_{D,1} - q_{L,1} + c_{D,1} - c_{L,1}|}{q_{D,1} + q_{L,1} + c_{D,1} + c_{L,1}} + \frac{|c_{D,n} - c_{L,n}|}{c_{D,n} + c_{L,n}} \quad (-) \quad (3)$$

A set-point of 199% secures a high purity of both enantiomers ($\geq 99\%$). Self-evidently, a high purity of both enantiomers leads to a high recovery of both enantiomers.

Extraction factor. The extraction factor $\Lambda_{e,i}$ describes the ratio of the number of molecules of a certain species that leave separation stage i in the two opposite directions [7] (Fig. 3):

$$\Lambda_{e,i} = P_{e,i} \frac{1 - \varphi_{B,i}}{\varphi_{B,i}} = \left(\frac{c_{e,i} + q_{e,i}}{c_{e,i}} \right) \frac{1 - \varphi_{B,i}}{\varphi_{B,i}} \quad (-) \quad (4)$$

where $P_{e,i}$ is the partition factor of an enantiomer in micellar and bulk phase, given by the Langmuir isotherms. Both $P_{e,i}$ and $\Lambda_{e,i}$ are useful tools in the development of the cascaded system, since it provides insight how the separation can be improved. By controlling the stage cuts $\varphi_{B,i}$, the extraction factors of the two enantiomers can be set oppositely from one, so that the D-enantiomers move effectively with the micellar phase ($\Lambda_{D,i} > 1$) and the L-enantiomers move in opposite direction with the bulk phase ($\Lambda_{L,i} < 1$). Consequently, all $\varphi_{B,i}$ must be larger than 0.5.

Materials and Methods

Materials. We used nonionic micelles to prevent unfavorable nonselective ion-ion interactions between enantiomers and micelles. The nonionic surfactant, nonyl-phenyl polyoxyethylene [E10] ether (NNP 10), was a gift by Servo Delden b.v. (Delden, The Netherlands). The NNP 10 batch was a mixture of different NNPs, therefore, an average molecular weight of 644 g/mol was assumed. The chiral selector, cholesteryl-L-glutamate (CLG), was synthesized by the Department of Organic Chemistry [4]. The optical rotation of the chiral selector $[\alpha]_D^{293}$ was -27° at 10.5 g/L chloroform (3% trifluoroacetic acid). The

chiral selector contained a large hydrophobic anchor (cholesterol) to secure their solubility in the micelle. Throughout this study double distilled water was used. All other components came from Merck (Darmstadt, Germany) and were used without further purification.

Preparation of micellar solutions. The micellar solutions were prepared as described previously [1]. The final solutions were set at pH 7 and contained 7.8 mM NNP10, 0.3 mM CLG, 0.3 mM CuCl_2 , and 0.1 M KCl. To generalize terminology the selector concentration refers to the Langmuir saturation concentration q_s .

Micelle-enhanced ultrafiltration in cascaded systems. Two types of experiments were conducted to validate the developed model for the separation of enantiomers in a cascaded system. First, a cascaded system was used containing 5 stages. Second, one single stage bench scale system was used to simulate the separation in a cascaded system of 60 stages. Measurements of the enantiomer concentrations were performed by HPLC as described before [5].

Cascaded system. Similar to the cascaded system shown in Fig. 2, a five stage system was operated in a counter-current mode ($n = 5$). Each stage consisted of a stirred vessel with 0.5 L micellar solution and a hollow-fiber membrane module. A peristaltic pump (Watson Marlow 505S with 5 pump heads) was used to simultaneously pump the micellar solution through 5 independent hollow-fiber cross-flow systems (Bio-Nephross Allegro dialyzers by Cobe Nephross BV) at $4.2 \cdot 10^{-4}$ L/s. A second peristaltic pump with a multitube cassette (Watson Marlow 205U) pumped the permeate from membrane module i to micellar solution $i + 1$ at $\Phi_{B,0 \leq i < m} = 8.11 \cdot 10^{-6}$ L/s and $\Phi_{B,m \leq i \leq n} = 8.72 \cdot 10^{-6}$ L/s, so that $\varphi_{B,1 < i < m} = 0.700$ and $\varphi_{B,m \leq i \leq n} = 0.715$. The bulk phase that entered stage 1 contained 0.1 M KCl at pH 7. A second Watson Marlow 205U pumped the micellar solution from stage i to stage $i - 1$ at $\Phi_{M,i} = 3.47 \cdot 10^{-6}$ L/s ($\varphi_{M,i} = 1 - \varphi_{B,i}$). The micellar solution that entered the system in stage 5 was the same as was initially present in each stage. The racemic mixture fed to stage 4 ($m = 4$) at $6.08 \cdot 10^{-7}$ L/s ($\varphi_{F,m} = 0.05$) contained 6 mM of D,L-Phe. The residence time in the membrane module (order of minutes) can be neglected if compared to the residence time in each stage (12 h). Therefore, we could regard both flask and module as one single stage.

Samples were taken daily from both the permeate and micellar phase of each stage. It could be assumed that both nonselective enantiomer complexation by the nonionic surfactants and

membrane rejection of unbound enantiomers can be neglected [5]. Therefore, in each stage the bound enantiomer concentration $q_{e,i}$ (mM) could be calculated by subtracting the measured enantiomer concentration in the bulk phase $c_{e,i}$ (mM) from the one in the micellar phase. The enantiomer concentration in the micellar phase was measured after diluting the 0.2 mL samples with 0.1 mL 2 M hydrochloric acid to provoke decomplexation. The cascade experiment ran for 10 days at 4 °C to avoid bacterial growth in the system. Plate counting of the micellar flow leaving stage 1 showed indeed that no micro-organisms were present.

Bench scale system. Fig. 4 depicts the cross-flow system used for the bench scale ultrafiltration experiments (Amalfilter b.v., Alkmaar, The Netherlands). The micellar solution was circulated at 0.125 L/s from a 10 L vessel through a spiral wound membrane module with a 1 m² cellulose membrane (Hoechst UF-C-10, 10 kDa MWCO) using a diaphragm pump (Wanner Engineering Inc., model D-10/G-10). The transmembrane pressure was set at 2.0 bar realizing a permeate flow of $5.56 \cdot 10^{-3}$ L/s, which resulted in a residence time of the permeate in the module under 5 minutes.

The equilibrium separation model (appendix I, $\alpha_{D/L,int} = 1.9$, $\beta = 1$, $\kappa_L = 2.5$, so that $c_{F,e} = 0.28$ mM) was used to calculate the $c_{D,i}$ and $c_{L,i}$ profiles of Phe in a cascade of 60 stages resulting in an ee_{sum} of 199%. The stage number of the single stage bench scale system in this cascaded system was simulated by controlling the feed concentrations of both enantiomers entering the bench scale system $c_{F,e}$. The feed concentrations of the bench scale system were calculated using the equilibrium separation model, so that at steady state the unbound concentrations in the cascaded system will equal the unbound concentration in the bench scale system in time:

$$c_{F,e} = c_e + \tau \frac{dc_e}{dt} \left(1 + \frac{dq_e}{dc_e} \right) \quad (\text{mM}) \quad (5)$$

where c_e and dc_e/dt are derived from the calculated concentration profiles in the cascade, dq_e/dc_e is obtained from the Langmuir isotherms, and τ is the residence time of the bulk phase in the bench scale system, which was set at 10 h. The equilibrium model (eq 5) would still result in a good approximation, comparing the residence time with the complexation kinetics [6].

The concentration profiles could not be simulated by one single experiment within a time span of a few days, due to the discontinuity at the feeding stage of the cascade ($m = 35$).

Therefore, two experiments were conducted, one simulating stage 1 to stage 35, the other started in stage 60 and stopped in stage 35.

After pump calibration, $c_{F,e}$ was related to the speed of pumps 1 and 3 (Fig. 4). Water was added to the bench scale system to compensate the total flow for a constant residence time (pump 2).

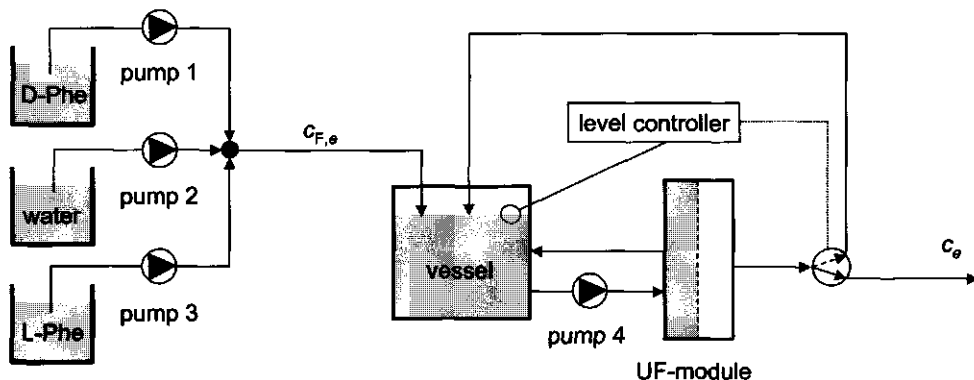


Figure 4. Bench scale cross-flow system. Pumps 1, 2, and 3 were PC controlled using Keithley's Testpoint software and I/O-card DDA-08/16 (Cleveland, Ohio, US). The vessel volume was kept at 10 L by an electronic level-controlled valve at the permeate side of the module.

Results and Discussion

Ultrafiltration experiments with a cascaded system. A run with a five-staged ultrafiltration system has been conducted in order to validate the separation model (eqs 1 and 2). Figs. 5a and 5b show the unbound and bound enantiomer concentrations leaving the cascade from stage 1 and 5, respectively. The preference of CLG for D-Phe causes $q_{D,1}$ to exceed $q_{L,1}$ (Fig. 5a). Consequently, the bulk phase is enriched with L-Phe (Fig. 5b). The deviation between the measured and predicted unbound concentrations in stage 5 can be explained by just a 4% off-set in the bulk phase flow. In spite of this minor deviation the separation is well predicted, $ee_{B,5}$ (Fig. 5c). Measuring and predicting an $ee_{CS,1}$ of 41% in a cascade of 5 stages (Fig. 5c), calculations for one single stage have shown that under the same conditions an $ee_{CS,1}$ of only

27% is expected. Of course, $ee_{B,n}$ (4%) is not strongly influenced by the number of stages, since the feed stage is only one stage away from the outlet.

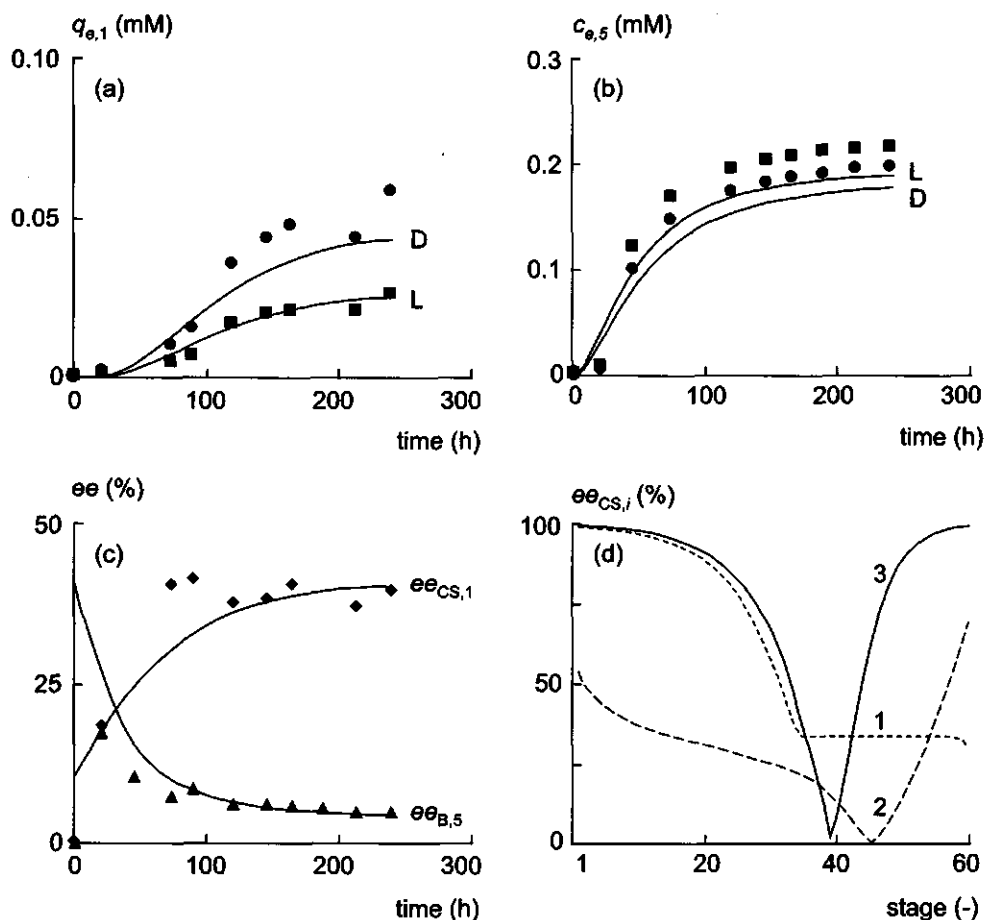


Figure 5. Ultrafiltration experiments in a cascade of 5 stages ($c_{F,e} = 3$ mM), (a) bound concentrations of D- (●) and L-Phe (■) in stage 1, (b) unbound concentrations in stage 5, (c) excess of (un)bound enantiomers, ee_B (▲) and ee_{CS} (◆), respectively, and (d) ee_{CS} in a cascade of 60 stages under similar experimental conditions (dotted line 1), after process optimization (dashed line 2) and after additional medium optimization (solid line 3). The solid lines in figure a, b, and c are equilibrium model predictions.

Cascade optimization. Despite the separation enhancement of the cascade as compared to one single stage, these measurements easily show that 5 stages are still not sufficient to satisfy the constraint of $ee_{\text{sum}} > 199$ (Eq. 3). Dotted line 1 shows that the current experimental conditions can never lead to two optically pure products using any number of stages, where $\varphi_{B,1 < i < m} = 0.700$ and $\varphi_{B,m \leq i \leq n} = 0.715$. In this case most enantiomers leave the system from stage n , due to the relatively high bulk phase flow. Only a small amount leaves the system from stage 1, of course, with a high purity. Therefore, the bulk phase flow fractions of the total flow leaving each stage, $\varphi_{B,i} = \Phi_{B,i} / (\Phi_{B,i} + \Phi_{M,i})$, have been optimized in order to improve the separation. At the optimized set of $\varphi_{B,i}$, the relative transport of bound enantiomers increases, so that the separation improves at stage 60 and decreases at stage 1 (dashed line 2, $\varphi_{B,1 < i < m} = 0.560$ and $\varphi_{B,m \leq i \leq n} = 0.575$). This shows that at a racemic mixture feed concentration of 6 mM optimization of the stage cuts alone is not enough to reach 99% separation of both enantiomers. Medium engineering is inevitable to reduce the affinity of the chiral selector for the L-enantiomer from 8.9 to 0.83 mM⁻¹ and increase the Langmuir saturation concentration (read chiral selector concentration) from 0.17 to 3 mM to keep $c_{F,e}$ at 3 mM and still achieve that $ee_{\text{sum}} > 199\%$ (solid line 3). In dimensionless terms this implies that κ_L is reduced from 27 to 2.5 and β is increased from 0.057 to 1. An improved separation can also be achieved by diluting the system to $c_{F,e} = 0.28$ mM and $q_{s,n+1} = 0.28$ mM, keeping K_L at 8.9 mM⁻¹. All the above calculations have been performed using the experimentally determined $\alpha_{D/L,\text{int}} = 1.9$ [1]. The effect of the enantioselectivity on the separation performance will be discussed in the next chapter.

Extraction factors. The effect of κ_L on the separation performance of the cascade is shown by the extraction factors in Fig. 6. At high values for κ_L nonlinear complexation behavior becomes apparent having a negative effect on the separation (Fig. 6a). In this case, both enantiomers are transported in the same direction with the micellar phase. Reducing κ_L (read K_L) cause the separation to become ineffective, $\Lambda_{L,i} = \Lambda_{D,i}$ (Eq. 4). Fig. 6b shows $\Lambda_{e,i}$ at the optimized κ_L of 2.5, which implies a $c_{F,e}$ of 0.28 mM, since the affinity of CLG for L-Phe is 8.9 mM⁻¹. The next session discusses the validation of the separation model using a cascade approximation under these experimental conditions. The relations between the process and medium parameters and their effect on the ee_{sum} are further discussed in chapter 6 using the defined dimensionless numbers.

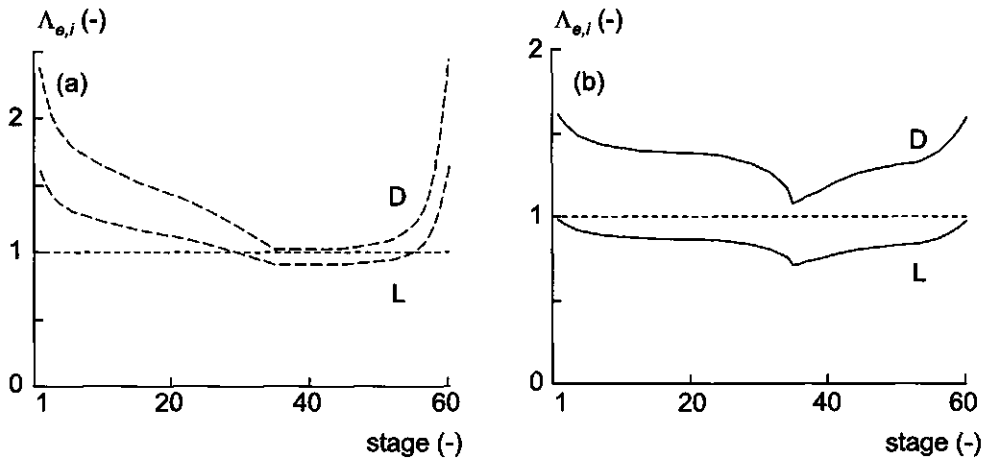


Figure 6. Extraction factors ($\Lambda_{e,i}$) in the 60 stage cascade corresponding to lines 2 (a, dashed lines, $\kappa_L = 27$) and 3 (b, solid lines, $\kappa_L = 2.5$) of Fig. 5d. The horizontal dotted line indicates $\Lambda_{e,i} = 1$. For an effective separation process, it should be pointed that $\Lambda_{L,i} < 1 < \Lambda_{D,i}$.

Cascade approximation by one single stage and a calculated feed concentration strategy.

To validate the model for 60 stages is hardly possible using the previously discussed lab scale cascade set-up. Hence, we have simulated a cascade of 60 stages by one single stage ultrafiltration system and controlling the feed concentrations of both enantiomers $c_{F,e}$ (mM). The location of the single stage bench scale system in the cascade can be approximated by a place to time transformation of the concentration profiles in the cascade. Therefore, the feed concentrations are chosen so that the expected unbound concentrations in the bench scale system are equal to the calculated concentration profiles in the cascade corresponding to the solid line in Fig. 5d.

Fig. 7 shows the measured unbound concentrations of D- and L-Phe of the two independent experiments. The solid lines represent the expected concentrations using the kinetic model, including both the Langmuir isotherms and the linear driving force model [6]. The minor difference between both model predictions is explained by the relatively long residence time, if compared to the complexation kinetics. Since the measurement error is in the order of 0.002 mM, it is shown that both models describe the measurements well.

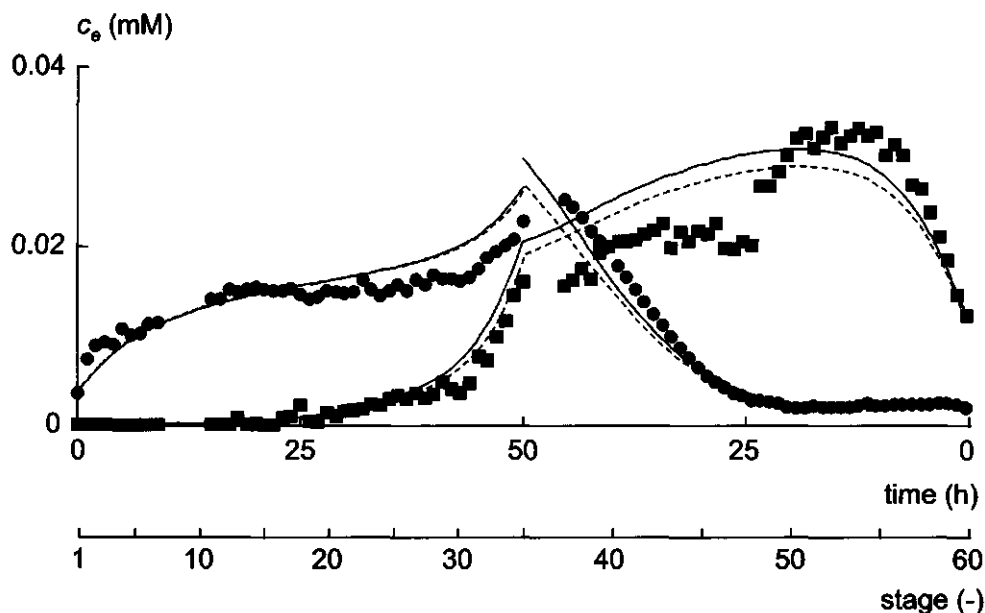


Figure 7. Ultrafiltration experiments in a bench scale system simulating the separation of D- (●) and L-Phe (■) in a cascade of 60 stages. The kinetic model predictions (solid lines) are not connected in stage 35, since the feed concentrations and unbound concentrations have been calculated with different models, the equilibrium and kinetic model, respectively. The equilibrium model predictions are presented by the dotted lines. The deviation between model and measured data from stage 35 to 45 could not be explained.

Conclusions

Validation experiments prove the suitability of the previously estimated Langmuir isotherms to describe the separation of Phe enantiomers by our enantioselective micelles in cascaded ultrafiltration systems. Using the experimentally determined $\alpha_{D/L,int}$ of 1.9, model calculations show that 60 stages are sufficient to separate both enantiomers at 99% purity. However, the enantiomer feed concentration of the cascade is in that case still very low, *i.e.* tenths of mM. The validated Langmuir equilibrium model can be used to maximize the enantiomer feed concentration and minimize the number of stages while satisfying the purity constraint of 99%. This is discussed in the next chapter.

Acknowledgements

Financial support for this work was provided by the Dutch Technology Foundation (grant no. WCH44.3380), Akzo Nobel, and DSM.

Nomenclature

$c_{e,i}$	unbound concentration in stage i	(mM)
$c_{F,e}$	enantiomer feed concentration (50% of racemic mixture)	(mM)
The enantiomer feed concentration $c_{F,e}$ is half of the racemic mixture feed concentration.		
ee	enantiomeric excess	(%)
K_e	affinity constant	(mM ⁻¹)
$k_{e,\pm 1}$	(de)complexation reaction rate constant	(s ⁻¹)
$k_{DL,\pm 1}$	exchange reaction rate constant	(mM ⁻¹ s ⁻¹)
$q_{e,i}$	bound enantiomer concentration in stage i	(mM)
$q_{s,i}$	selector concentration in stage i	(mM)
$q_{s,F}$	selector concentration in $\Phi_{M,n+1}$	(mM)
t	time	(s)
V_i	volume of micellar phase in stage i	(L)
$[\alpha]_D^{293}$	optical rotation at 293 K, using sodium emission spectrum (589 nm).	(°)
$\Phi_{M,i}$	flow of micellar phase leaving stage i	(L/s)
$\Phi_{B,i}$	flow of bulk phase leaving stage i	(L/s)
$\Phi_{F,i}$	flow of feed entering stage i	(L/s)
τ	residence time per stage	(s)

Dimensionless numbers

$\alpha_{D/L,int}$	intrinsic enantioselectivity	K_D / K_L
β	relative selector concentration	$q_{s,F} / c_{F,e}$
$\varphi'_{M,i}$	stage cut of micellar phase entering stage i	$\Phi_{M,i+1} / (\Phi_{B,i} + \Phi_{M,i})$
$\varphi_{M,i}$	stage cut of micellar phase leaving stage i	$\Phi_{M,i} / (\Phi_{B,i} + \Phi_{M,i})$
$\varphi'_{B,i}$	stage cut of bulk phase entering stage i	$\Phi_{B,i-1} / (\Phi_{B,i} + \Phi_{M,i})$
$\varphi_{B,i}$	stage cut of bulk phase leaving stage i	$\Phi_{B,i} / (\Phi_{B,i} + \Phi_{M,i})$

$\Phi'_{F,m}$	stage cut of feed entering stage m ($\Phi'_{F,i=m} = 0$)	$\Phi_{F,m} / (\Phi_{B,m} + \Phi_{M,m})$
I_i	reciprocal of relative sum of flows into stage i ($\Phi_{B,1} + \Phi_{M,1}$) / ($\Phi_{B,i} + \Phi_{M,i}$)	$(\Phi_{B,1} + \Phi_{M,1}) / (\Phi_{B,i} + \Phi_{M,i})$
κ_e	relative affinity	$K_e C_{F,e}$
$\Lambda_{e,i}$	extraction factor in stage i	$P_{e,i} (1 - \Phi_{B,i}) / \Phi_{B,i}$
$P_{e,i}$	partition factor in stage i	$(q_{e,i} + c_{e,i}) / c_{e,i}$
Q_i	relative Langmuir saturation concentration in stage i	$q_{s,i} / q_{s,F}$
r_e	(de)complexation and exchange kinetics	
$\sigma_{e,i}$	dilution factor in stage i	$c_{e,i} / C_{F,e}$
$\theta_{e,i}$	bound fraction in stage i	$q_{e,i} / q_{s,i}$
θ	relative time	$t \Phi_{T,1} / V_1$

An apostrophe indicates a stage cuts of a flow entering a stage. Subscripts: M, micellar phase; B, bulk phase; e , D- or L-enantiomer; i , stage number; m , feeding stage number; n , number of stages.

References

- (1) Overdevest, P.E.M.; de Bruin, T.J.M.; Sudhölter, E.J.R.; Keurentjes, J.T.F.; van 't Riet, K.; van der Padt, A. chapter 3.
- (2) Scamehorn, J. F.; Christian, S. D.; Ellington, R. T. In *Surfactant-based separation processes*; Scamehorn, J. F.; Harwell, J. H., Eds.; Marcel Dekker: New York, 1989.
- (3) Overdevest, P. E. M.; Van der Padt, A.; Keurentjes, J. T. F.; Van 't Riet, K. In *Surfactant-Based Separations: Science and Technology*; Scamehorn, J. F.; Harwell, J. H., Eds.; ACS Symposium Series 740; American Chemical Society: Washington D.C., 1999.
- (4) De Bruin, T. J. M.; Marcelis, A. T. M.; Zuilhof, H.; Rodenburg, L.M.; Niederländer, H.A.G.; Koudijs, A.; Overdevest, P. E. M.; Van der Padt, A.; Sudhölter, E. J. R. *Chirality* - accepted.
- (5) Overdevest, P. E. M.; Van der Padt, A.; Keurentjes, J. T. F.; Van 't Riet, K. *Colloids and Surfaces A* 1999, 163, 209.
- (6) Overdevest, P. E. M.; Schutyser, M. A. I.; de Bruin, T. J. M.; Keurentjes, J. T. F.; Van 't Riet, K.; Van der Padt, A. chapter 4.
- (7) Alders, L. *Liquid-liquid extraction*; Elsevier: Amsterdam, 1959.

Appendix I

The separation in a cascade of ultrafiltration stages is modeled by n mass balances to describe the total enantiomer concentration $c_{e,i} + q_{e,i}$ (mM) of each enantiomer e in the micellar phase of each stage i (Fig. 3):

$$V_i \left(\frac{dc_{e,i}}{dt} + \frac{dq_{e,i}}{dt} \right) = \Phi_{M,i+1} (c_{e,i+1} + q_{e,i+1}) - \Phi_{M,i} (c_{e,i} + q_{e,i}) + \quad (\text{mol/s})$$

$$+ \Phi_{F,i} c_F + \Phi_{B,i-1} c_{e,i-1} - \Phi_{B,i} c_{e,i}$$

where $c_{e,i}$ and $q_{e,i}$ are the unbound and bound enantiomer concentrations, respectively, V (L) is the volume of the micellar phase, and Φ (L s^{-1}) represents the various mass flows through the system. Normalizing both the unbound concentration as $\sigma_{e,i} = c_{e,i} / c_{F,e}$ and the bound concentration as $\theta_{e,i} = q_{e,i} / q_{s,i}$ yields:

$$V_i \left(\frac{d\sigma_{e,i}}{dt} + \beta Q_i \frac{d\theta_{e,i}}{dt} \right) = \Phi_{M,i+1} (\sigma_{e,i+1} + \beta Q_{i+1} \theta_{e,i+1}) - \Phi_{M,i} (\sigma_{e,i} + \beta Q_i \theta_{e,i}) + \quad (\text{L/s})$$

$$+ \Phi_{F,i} + \Phi_{B,i-1} \sigma_{e,i-1} - \Phi_{B,i} \sigma_{e,i}$$

where β is the ratio of $c_{F,e}$ and the selector concentration entering the cascade in stage n , $q_{s,F}$ (mM), and Q_i is the ratio of $q_{s,F}$ and the selector concentration in stage i , $q_{s,i}$ (mM). Since $\Phi_{M,i+1} Q_{i+1} = \Phi_{M,i} Q_i$, the former equation can be rewritten as:

$$V_i \left\{ \frac{d\sigma_{e,i}}{dt} + \beta Q_i \frac{d\theta_{e,i}}{dt} \right\} = \Phi_{M,i+1} \sigma_{e,i+1} + \Phi_{M,i} \beta Q_i (\theta_{e,i+1} - \theta_{e,i}) + \quad (\text{L/s})$$

$$- (\Phi_{M,i} + \Phi_{B,i}) \sigma_{e,i} + \Phi_{F,i} + \Phi_{B,i-1} \sigma_{e,i-1}$$

Introducing the dimensionless stage cuts φ yields Eq. 1:

$$I_i \left\{ \frac{d\sigma_{e,i}}{d\theta} + \beta Q_i \frac{d\theta_{e,i}}{d\theta} \right\} = \varphi'_{M,i} \sigma_{e,i+1} + \varphi_{M,i} \beta Q_i (\theta_{e,i+1} - \theta_{e,i}) + (-) \quad (1)$$

$$-\sigma_{e,i} + \varphi'_{F,i} + \varphi_{B,i} \sigma_{e,i-1}$$

where the apostrophe indicates the stage cut of a flow entering a stage, and I_i is the ratio of the sum of flows into stage 1 and the sum of flows into stage i .

Appendix II

The complexation kinetics have been thoroughly investigated in the previous chapter. According to the kinetic complexation model, the bound enantiomer concentration in stage i $q_{e,i}$ (mM) can not be directly calculated using the Langmuir isotherms and the unbound concentrations in stage i $c_{e,i}$ (mM). Therefore, mass balances for both unbound and bound enantiomers must be distinguished. Following a similar approach as in appendix I, these mass balances are:

$$I_i \frac{d\sigma_{e,i}}{d\theta} = \varphi'_{B,i} \sigma_{e,i-1} - \sigma_{e,i} + \varphi'_{M,i} \sigma_{e,i+1} + \varphi_{F,i} - r_e$$

$$I_i \frac{d\theta_{e,i}}{d\theta} = \varphi_{M,i} (\theta_{e,i+1} - \theta_{e,i}) + \frac{r_e}{\beta Q_i}$$

where r_e is the kinetic term representing the complexation, decomplexation, or exchange process. For complexation ($\sigma_{e,i} > \sigma_{eq,e,i}$):

$$r_e = k_{e,+1} \tau_i (\sigma_{e,i} - \sigma_{eq,e,i})$$

For decomplexation ($\theta_{e,i} > \theta_{eq,e,i}$):

$$r_e = -k_{e,-1} \tau_i \beta Q_i (\theta_{e,i} - \theta_{eq,e,i})$$

And for exchange ($\sigma_{D,i} > \sigma_{eq,D,i} \wedge \theta_{L,i} > \theta_{eq,L,i}$):

$$\begin{aligned}
 r_D &= k_{D,+1} \tau_i (\sigma_{D,i} - \sigma_{eq,D,i}) + \\
 &\quad + k_{DL,+1} \tau_i \beta Q_i c_F (\sigma_{D,i} - \sigma_{eq,D,i}) (\theta_{L,i} - \theta_{eq,L,i}) \\
 r_L &= -k_{L,-1} \tau_i \beta Q_i (\theta_{L,i} - \theta_{eq,L,i}) + \\
 &\quad - k_{DL,+1} \tau_i \beta Q_i c_F (\sigma_{D,i} - \sigma_{eq,D,i}) (\theta_{L,i} - \theta_{eq,L,i})
 \end{aligned}$$

The Langmuir isotherms are used to calculate the unbound and bound enantiomer concentrations in stage i ($c_{eq,e,i}$ and $\theta_{eq,e,i}$) in equilibrium with the actual bound and unbound enantiomer concentrations, respectively [6].

6

CONCLUDING REMARKS

Introduction

This thesis presents a cascaded enantiomer separation process that is based on the ultrafiltration of enantioselective micelles containing chiral selector molecules (Fig. 1). As a model system, we have studied the separation of D,L-phenylalanine (D,L-Phe) enantiomers by cholesteryl-L-glutamate (CLG) in nonionic micelles [1,2]. The stability difference between two chelate complexes results in chiral separation at a molecular level, where the stability of CLG:Cu^{II}:D-Phe exceeds the one of CLG:Cu^{II}:L-Phe. Further, an ultrafiltration (UF) membrane causes the micelles to be separated from the unbound enantiomers, *i.e.* separation on process scale. Since one single UF stage is inadequate to achieve 99% separation of both enantiomers, the separation has been studied in a cascaded system [3].

Chapters 2 and 3 describe the development of a two component Langmuir model that is capable of predicting the competitive complexation at various pH. Both independent experiments and statistics show that membrane rejection of unbound enantiomers and nonselective complexation can be neglected if compared to the enantioselective complexation by CLG [4]. It is shown that complexation only occurs at pH 7 and higher [5]. Regeneration of D-Phe saturated micelles can be improved by a pH reduction. In order to minimize salt production the pH shift should be minimal.

Section 'Chiral selector engineering' is written by T.J.M. de Bruin and P.E.M. Overdeest as a result of the collaboration within the STW project (WCH44.3380).

Sections 'Nonionic surfactants' and 'pH of the medium' have been published as part of P.E.M. Overdeest and A. van der Padt, 'Optically pure compounds from ultrafiltration' *CHEMTECH* 1999, 29, no. 12, 17.

Sections 'Affinity of microheterogeneous media for the substrate', 'Process engineering' and 'From dimensionless numbers back to system dimensions' have been submitted for publication as part of P.E.M. Overdeest, M.H.J. Hoenders, K. van 't Riet, J.T.F. Keurentjes and A. van der Padt, 'Enantiomer separation in a cascaded micellar-enhanced ultrafiltration system: enantioselectivity, Langmuir affinity, and productivity'.

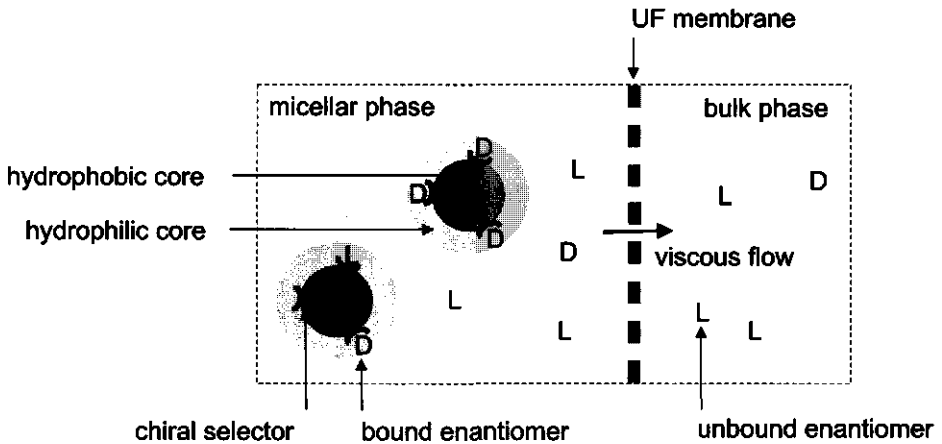


Figure 1. Ultrafiltration (UF) of micelles for the separation of enantiomer. The separation is the result of enantioselective partition between bulk and micellar phase. Separation of bulk and micellar phase by a UF membrane is based on size exclusion.

The equilibrium experiments have indicated that the complexation of enantiomers by the enantioselective micelles is not instantaneous [6]. Chapter 4 discusses the Linear Driving Force model that describes both the complexation and decomplexation rates of enantiomers.

Finally, the developed model is validated by cascaded ultrafiltration experiments at both lab and bench scale [7].

The scope of this chapter is to indicate how the performance of cascaded UF systems or any cascaded counter-current nonlinear complexation system can be optimized. Therefore, we have analyzed the equilibrium model and selected the dimensionless numbers effecting the separation by the cascade. Medium parameters ($\alpha_{D/L,int}$, β , and κ_L) describing the intrinsic properties of the enantioselective microheterogeneous medium are distinguished from process parameters (n and φ) that can be used to control the process at macroscopic scale:

- $\alpha_{D/L,int}$ D-enantiomer affinity constant / L-enantiomer affinity constant
- β selector feed concentration / enantiomer feed concentration
- κ_L L-enantiomer affinity constant \cdot enantiomer feed concentration
- n number of stages
- φ flow in or out a stage / sum of flows in or out a stage

These dimensionless numbers facilitate the elimination of correlation between system parameters and input variables. The stage cuts (φ) have been optimized for a given set of

medium parameters to minimize n under the constraint that the ee_{sum} ($= ee_{M,1} + ee_{B,n}$) exceeds the required enantiomeric excess [7]. Depending on the undesirability of an impurity this could be 199% or even 199.9%. In this chapter, the feeding stage (m) is chosen to be $n/2$ for all calculations. Furthermore, the implications of the optimized numbers will be discussed for both the model system and the competitive nonlinear complexation processes in general.

Engineering aspects effecting the performance of the separation system

Two groups at the Wageningen University closely cooperate in the development of this chiral resolution system. On a molecular level the interactions within the ternary complexes are studied at the Laboratory of Organic Chemistry. At the Food and Bioprocess Engineering Group the separation process is studied at laboratory scale and bench scale. Here, we present an overview of the most important engineering aspects that influence the performance of the separation system.

Chiral selector engineering

At the Laboratory of Organic Chemistry several routes have been followed to elucidate the molecular interactions between the selector and the enantiomers, in order to optimize the chiral selector molecules [8]. In this study derivatives of glutamic acid are used, esterified at its γ -position with a large hydrophobic anchor, *e.g.* cholesterol. The operational enantioselectivities $\alpha_{D/L,op} = q_D c_L / c_D q_L$ of stereoisomers of cholesteryl-glutamate for the separation of DL-Phe are presented in Table 1. High enantioselectivities have been measured for cholesteryl-L-glutamate (CLG). Cholesteryl-D-glutamate (CDG) is synthesized to study the enantioselective site of the chiral selector. If chiral recognition takes place exclusively at the amino acid head group, it is expected that the enantioselectivity of CDG is equal to the reciprocal value of CLG. However, a significantly lower operational enantioselectivity for CDG of 0.45 is found, this is far from 1 over 8.2. This strongly suggests that apart from the glutamate head group also the chiral hydrophobic anchor (cholesterol) contributes to the chiral recognition process. This is supported by the fact that if cholesteryl-DL-glutamate is used, the enantioselectivity still significantly deviates from unity.

Table 1. Operational enantioselectivities ($\alpha_{D/L,op}$) for D,L-Phe of some chiral selectors (0.30 mM) dissolved in micelles of the nonionic surfactant nonyl-phenyl polyoxyethylene [E10] ether, NNP10 (7.8 mM) at pH 9 and 25 °C. The concentrations of D,L-Phe, Cu^{II} , and KCl are 0.15 mM, 0.30 mM, and 0.1 M, respectively.

chiral selector	$\alpha_{D/L,op}$
cholesteryl-L-glutamate	8.2 ± 1.8
cholesteryl-D-glutamate	0.45 ± 0.07
cholesteryl-DL-glutamate	1.6 ± 0.2

Modification in the substrate. The chiral microheterogeneous medium was tested for 12 different amino acids, which were used as test compounds [8]. Table 2 shows only part of the tested amino acids. The experiments have shown that the enantioselectivity is related to the π value of an amino acid. Hydrophobic amino acids (high π value) dissolve nonselectively in the micelle, whereas hydrophilic amino acids (low π value) prefer the aqueous bulk. A modification of the amino acid is required, if the hydrophobicity differs from the indicated range. For example, tyrosine that cannot be separated with this system, has been converted into *O*-methyl-tyrosine, which yields $\alpha_{D/L,op} = 7.2$. The amino acids which have a hydrophobicity within the above-mentioned range can be separated very well: in case of phenylglycine (PheGly) up to $\alpha_{D/L,op} = 14$. This wide range of measured enantioselectivities might point to different types of coordination for different amino acids and hence different amino acid-amino acid interactions. This suggests that the geometry around Cu^{II} in such complexes is highly dependent on the type and size of the substrate.

Table 2. Operational enantioselectivities ($\alpha_{D/L,op}$) of cholesteryl-L-glutamate for some amino acids. See Table 1 for the concentrations and conditions.

substrate	$\alpha_{D/L,op}$ (-)	$\pi^{(a)}$ (-)
phenylglycine	14.5 ± 2.5	1.22
phenylalanine	8.2 ± 1.8	1.63
homophenylalanine	-	2.04
<i>O</i> -methyl-tyrosine	7.2 ± 1.6	1.87

^(a) $\pi = \log P_{OW}(\text{amino acid}) - \log P_{OW}(\text{glycine})$, where P_{OW} is the partition coefficient of the enantiomer in octanol and water.

Quantum mechanical techniques. Therefore, the geometric structure was investigated using computational techniques. Since the parameters for Cu^{II} in molecular mechanics (MM) are not sufficiently accurate, the complex was computed quantum mechanically (QM) [9,10] with the use of density functional theory (B3LYP) [11,12]. However, due to long computation times (several months on a Cray C916 / 12104), the diastereomeric complex had to be simplified to bis-glycinato- $\text{Cu}^{\text{II}} \cdot n \text{H}_2\text{O}$ ($n = 0 - 4$). From these computational studies it is concluded that: (i) such complexes are only well described if large basis sets are used [6-311+G(d,p)] [13]; (ii) hydrogen bond formation strongly influences the final geometry; (iii) a *trans* complex is always more stable than the corresponding *cis* complex; and (iv) no single set of electrostatic potential charges (from methods such as CHELPG and Merz-Kollman) can be derived for the description of either *cis* or *trans* Cu^{II} -bis-amino acids complexes, thereby hampering the parameterization for molecular mechanics. The electrostatic potential charges are used to calculate Coulomb interactions in molecular mechanics. To perform meaningful calculations on large Cu^{II} amino acids complexes QM/MM calculations most probably offer the best solution [14].

Isothermal titration calorimetry. Furthermore, the formation of the diastereomeric complexes has been investigated by Isothermal Titration Calorimetry (ITC) [15]. Thermodynamic data of the complexation reaction can be straightforwardly determined with this technique: the affinity constant K , the change in enthalpy ΔH , in entropy ΔS and in Gibbs free energy ΔG . From Table 3 it follows that the data ($\alpha_{\text{D/L,int}} = K_{\text{D}} / K_{\text{L}}$) are in agreement with the ultrafiltration: the D-enantiomer forms the most stable diastereomeric complex for Phe and PheGly. The difference in magnitude in enantioselectivity between ITC and ultrafiltration measurements could be explained by the fact that only the rapid complexation between substrate and selector is measured with ITC, whereas the exchange of one enantiomer for the other (which forms the most stable diastereomeric complex) is not [6]. From the ITC experiments it can be concluded that the reaction is endothermic ($\Delta H > 0$), and is driven by entropy ($\Delta S > 0$). This can be interpreted as the release of water molecules from the $\text{CLG}:\text{Cu}^{\text{II}}$ complex if the substrate is bound.

Table 3. Isothermal Titration Calorimetry (ITC) at pH 7 and 25 °C. The concentrations of CLG, NNP 10, titrant, Cu^{II}, and NaOAc are 1.5 mM, 7.8 mM, 25 mM, 1.5 mM, and 0.1 M, respectively.

titrant	<i>n</i>	<i>K</i> (mol ⁻¹)	ΔH (kJ mol ⁻¹)	ΔG (kJ mol ⁻¹)	ΔS (J mol ⁻¹ K ⁻¹)	$\alpha_{D/L,int}$
D-Phe	0.900	9437	16.85	-22.67	132.6	1.17
L-Phe	0.922	8033	17.43	-22.28	133.2	
D-PheGly	0.897	3640	18.81	-20.31	131.3	1.26
L-PheGly	0.963	2900	19.27	-19.75	131.0	

Medium engineering

Nonionic surfactants. Besides the chiral selector the micelles contain achiral nonionic surfactants. Use of a nonionic surfactant prevents undesired electrostatic interactions between ionic surfactants and other charged species in the medium: chiral selectors, enantiomers, and Cu^{II} ions. In addition, to minimize the leakage of surfactant molecules through the ultrafiltration membrane, the critical micelle concentration (CMC) of the surfactant should be extremely low. For a given hydrophobic tail group, the CMC of a nonionic surfactant is substantially lower than for an ionic surfactant [16]. Of course, the CMC can be even eliminated by polymerizing the hydrofobic tails of the surfactants in the micelle [17,18].

To study the influence of the nonionic surfactants on the performance of the chiral selector molecules, we have tested two series of commercially available surfactants: Tween and Brij (see appendix). At first, we did not expect any effect of the surfactant on $\alpha_{D/L,op}$, because we did not believe that it had a significant role in the formation of ternary complexes. Some preliminary experiments with a Tween surfactant, however, have indicated otherwise. Therefore we have started a more thorough study. The experimental results with the Tween and Brij surfactants are shown in Figs. 2a and 2b, respectively. These figures clearly show that the operational enantioselectivity is higher when shorter surfactant chains are used. Of course, there is a restriction, since at very short chain lengths no micelles are formed. The

experiments with Tween 60 and 80 show that even unsaturated C-bonds improve the enantioselectivity (Fig. 2a).

The formed 1:1:1 complexes of CLG, Cu^{II} , and D,L-Phe are diastereomeric complexes, thus having different physical properties and different geometries. It can be hypothesized that the difference in stability (enantioselectivity) of these complexes is enhanced by the ordered microstructure of the medium in which these complexes are dissolved, *i.e.* the achiral micelles. Possibly, the enantioselective interactions decrease upon an increase in micellar size due to steric effects which are more pronounced in larger micelles. Note, the micellar size is directly related to its aggregation number which decreases upon shorter chain lengths. At 25 °C the aggregation number of Brij 56 and 58 micelles are 80 and 200, respectively.

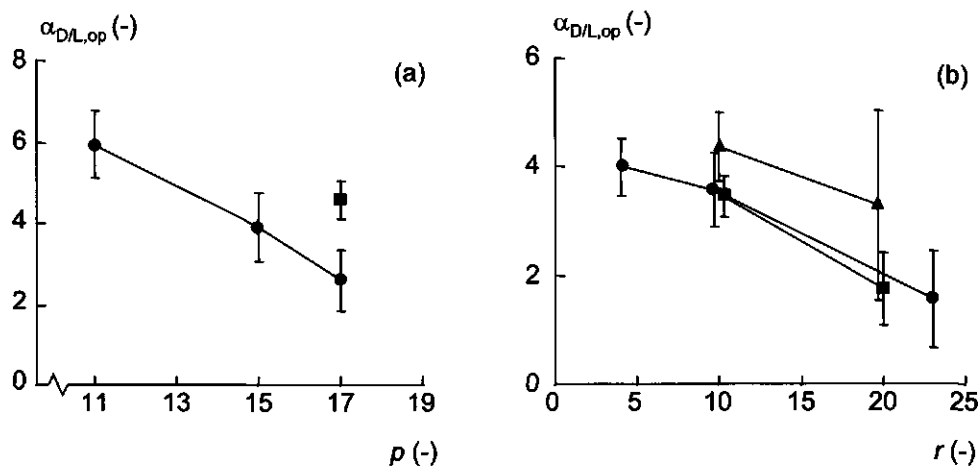


Figure 2. Operational enantioselectivity $\alpha_{D/L,op}$ of CLG (0.30 mM) for various nonionic surfactants: (a) $C_{12}E_8$ (●); Tween80 (■) and (b) $C_{12}E_8$ (●); $C_{16}E_8$ (▲); and $C_{18}E_8$ (■). The concentrations of D,L-Phe, Cu^{II} , surfactant, and KCl were 0.15 mM, 0.30 mM, 7.8 mM, and 0.1 M, respectively (pH 11). Equilibrated solutions were ultrafiltered using a stirred cell (Amicon, 8400 series) to separate the unbound enantiomers from the micelles and the bound enantiomers (25 °C).

pH of the medium. The pH of the microheterogeneous medium plays a significant role in the performance of the enantioselective micelles. Since the charge of both the enantiomers and the chiral selector is pH dependent, it is obvious that the formation of the ternary complexes is pH dependent as well. For this, we have studied the complexation of enantiomers by enantioselective micelles at pH 11 down to 6 [5]. From the results it is concluded, that the

enantioselectivity increases upon decreasing pH. However, the affinity decreases upon decreasing pH, ending in no complexation at pH 6.

To regenerate the saturated micelles leaving the cascade, we have tested decomplexation of bound enantiomers. Ultrafiltration experiments have shown that dilution and an increased temperature do not lead to a considerable decomplexation. However, a decrease in pH causes repulsion between selector and enantiomer, due to their positive charges, leading to the desired decomplexation [5]. In order to keep the salt production to a minimum, after multiple separation cycles, the difference between complexation and decomplexation pH should be minimized.

Enantioselectivity. The enantioselectivity $\alpha_{D/L}$ quantifies the preference of the chiral selector for one of the two enantiomers, and is defined as $(q_D/c_D) / (q_L/c_L)$, where q and c are the bound and unbound concentration, respectively, of the D- and L-enantiomers [19]. For Langmuir isotherms, $\alpha_{D/L}$ equals the ratio of the two coexisting affinity constants, $K_D / K_L (= \alpha_{D/L,int})$. Single stage calculations have shown that an increase of $\alpha_{D/L,int}$ from the experimentally measured value of 1.9 to a value of 5 implies a dramatic increase in separation [7]. Moreover, this increase in separation is only minor if $\alpha_{D/L,int}$ is further increased above 5. Selector engineering by both quantum mechanical calculations [13,14] and minor modifications in either the chiral selector or the racemic substrate [8] should accelerate the development of selector molecules having an enantioselectivity of at least 5.

Ultrafiltration experiments at pH 7 up to 11 with cholesteryl-L-glutamate and D,L-Phe have shown that the affinity is based on ionic interactions which predominate the enantioselective interactions [5]. So, the enantioselectivity of the system can be improved by reducing the ionic interactions, possibly by increasing the salt concentration. Ultrafiltration experiments with various nonionic surfactants have shown that the enantioselectivity of CLG is dependent of the type of achiral surfactant [3]. It is therefore expected, that the ordered microstructure of the microheterogeneous media can be exploited to maximize the difference in stability of the two possible diastereomeric complexes: CLG:Cu^{II}:D-Phe and CLG:Cu^{II}:L-Phe. Later in this chapter the separation improvement will be quantified by a reduction in the number of stages required to achieve $ee_{sum} = 199\%$.

Selector concentration. The productivity of the separation system depends on the selector concentration in the cascade. If properly operated, the higher the selector concentration, the

more enantiomers can be separated in a certain time span. Of course, the enantiomer concentration is limited by its solubility in the microheterogeneous medium and by solubility of the microheterogeneous medium itself. Various microheterogeneous media have been reviewed at their capacity to anchor sufficient selector molecules to separate enantiomers at their solubility concentration.

Preliminary optimization calculations show that the selector feed concentration $q_{s,F}$ should be around half of the racemic mixture feed concentration. Since β is proportional to the selector costs being the determining factor of the total system costs, it is imperative to include β in the final system optimization. For all subsequent calculations β has been set to 1. For an optimal ee_{sum} , this corresponds to an average requirement of 3 chiral selector molecules per enantiomer entering the cascade. As will be shown in the next section, the selector per enantiomer requirement decreases upon enantioselectivity.

For our model system, $\beta = 1$ implies that the selector concentration should be 40 mM to separate a Phe racemic mixture at its solubility concentration of 80 mM in water at 25°C. Assuming that each selector molecule requires 2 nm² to bind an enantiomer A_{CS} (nm²) [20], the selector feed concentration $q_{s,F}$ (mM) can be calculated as:

$$q_{s,F} = \frac{10^4 \varepsilon}{d_p A_{CS}} \quad (\text{mM}) \quad (1)$$

where ε (-) is de volume fraction of the media particles in the solution, and d_p (nm) is the particle diameter, assuming spherical media. Table 4 shows d_p of various microheterogeneous media from literature that can be used to absorb or covalently bind chiral selector molecules. Subsequently, using Eq. 1 and common ε from literature the attainable $q_{s,F}$ can be calculated for various microheterogeneous media. This short review is at best only an approximation, since micelles are likely to be polydisperse in mass and oblate in shape [21,22].

For conventional vesicles and micelles, it can be concluded that the desired selector concentration of 40 mM can not be achieved in the concentration range where micelles and vesicles are thermodynamically stable. Viscosity measurements of aqueous solutions of nonyl-phenyl polyoxyethylene [E10] ether have shown that at volume fractions above 0.02 the micelles increase in size, so that the specific area decreases. This phenomenon can be overcome using polymerized micelles, where the unsaturated carbons of the hydrophobic tail groups have been polymerized [30]. This eliminates the critical micelle concentration and

makes them independent of self-assembly, characteristic to conventional micelles. Consequently, these particles can be concentrated to a volume fraction of 0.08, sufficient to locate 40 mM of chiral selectors, number 3 of Table 4. To generalize this concept, it is assumed that each selector is effectively used, contrary to the experimental data of chapter 3 for our model system.

Table 4. Various microheterogeneous media to anchor chiral selector molecules.

no.		d_p (nm)	ref.	ε (-)	$q_{s,F}$ (mM)
1.	vesicle	150	[23,24]	0.02	1
2.	micelles	10 - 20	[25,6]	0.02	10
3.	polymerized micelles	10	[26,27]	0.08	40
4.	dendrimers	3 - 10	[28,29]	0.024 - 0.08	40

A second alternative is the use of dendrimers, which have a well defined size and structure (number 4). In general, common properties of dendrimers are the high number of functional groups on the surface, excellent solubility, guest molecule encapsulation, and very low solution viscosity [31]. Fréchet reports a solubility of $1.15 \cdot 10^3$ g/L for a 5 generation dendrimer (MW of 11 kDa) in tetrahydrofuran as compared to its linear analogue, 25 g/L [31]. These physical properties make dendrimers an attractive microheterogeneous medium to separate enantiomers in the cascaded ultrafiltration system. Either, the dendrimer is chemically modified to become enantioselective [28,29], or chiral selector molecules are encapsulated in its internal cavity [32]. The molecular weight of dendrimers, 1 up to 30 kDa [31], facilitates the separation of bound and unbound enantiomers by ultrafiltration membranes.

Affinity of microheterogeneous media for the substrate. To study the effect of κ_L on the separation performance of the cascaded system, ee_{sum} has been calculated as a function of this dimensionless affinity number (Fig. 4a). These calculations show that there is a window where ee_{sum} complies with the optimization constraint. Below this κ_L window the enantiomer concentrations of the micellar phase $c_{e,i} + q_{e,i}$ and the bulk phase $c_{e,i}$ become similar, caused by decreasing affinity, $q_{e,i} \rightarrow 0$. Therefore, the extraction factors [33] of both enantiomers ($\Lambda_{e,i}$) become equal:

$$\lim_{K_L \downarrow 0} \Lambda_{e,i} = \lim_{K_L \downarrow 0} \left(\frac{c_{e,i} + q_{e,i}}{c_{e,i}} \right) \frac{1 - \varphi_{B,i}}{\varphi_{B,i}} = \frac{1 - \varphi_{B,i}}{\varphi_{B,i}} \quad (-) \quad (2)$$

To explain the diminishing separation above the κ_L window, the total concentrations $q_{e,i} + c_{e,i}$ have been calculated for the cascade of 60 stages of Fig. 4a at maximum ee_{sum} where $\kappa_L = 2.5$ (Fig. 4b). From these characteristic concentration profiles, it can be concluded that in the outer stages of the cascade the enantiomer concentrations are lower than in the center stages of the cascade. For linear extraction processes the partition factor is a constant. The complexation behavior of the enantioselective micelles, however, is described by nonlinear Langmuir isotherms causing the partition factor $P_{e,i} = (q_{e,i} + c_{e,i}) / c_{e,i}$ to decrease upon increasing concentration. In other words, at both ends of the cascade, the micelles bind to many enantiomers, including the low-affinity substrate, in our case the L-enantiomer. Consequently, the extraction factor profiles are V-shaped, note that $\varphi_{B,i}$ are constants at both sides of the feeding stage (Fig. 3).

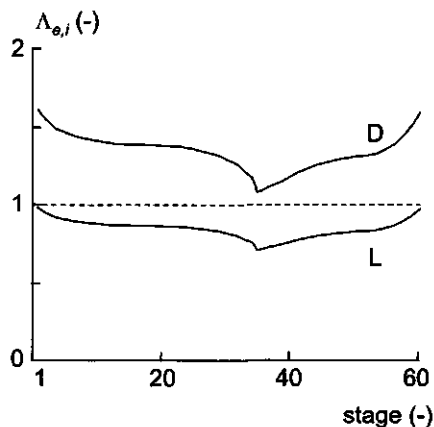


Figure 3. Extraction factors ($\Lambda_{e,i}$) in a 60 stage cascade where $\kappa_L = 2.5$. The horizontal dotted line indicates $\Lambda_{e,i} = 1$. For an effective separation process, it should be pointed that $\Lambda_{L,i} < 1 < \Lambda_{D,i}$.

Calculations show that the differences between $P_{D,i}$ and $P_{L,i}$ increase with κ_L . Above the κ_L window the nonlinearity of $P_{e,i}$ increases to the extent where it is impossible to correct all $P_{e,i}$ by a constant $\varphi_{B,i}$ to get all $\Lambda_{e,i}$ at opposite sides from one [7]. In agreement to our findings Morbidelli *et al.* have shown that complete separation occurs only in certain regions of flow

ratios, studying both feed concentration and substrate affinity independently in simulated moving bed units [34,35].

The existence of a κ_L window implies that a reduction in affinity improves the productivity of the cascaded system, since the racemic mixture feed concentration must be proportionally increased to maintain the optimal κ_L [36]. Generally speaking, one can say that, in order to attain the highest possible feed concentration (*i.e.* solubility concentration) at $\alpha_{D/L,int} = 1.9$, the low-affinity constant should be 2.5 over the solubility of this substrate. Note, the high-affinity constant is given by the low-affinity constant times $\alpha_{D/L,int}$. For our model system this implies that the affinity constants should decrease a factor of 140, so that K_L becomes 0.063 mM^{-1} and the racemic mixture feed concentration can be increased to 80 mM (*i.e.* solubility at 25°C).

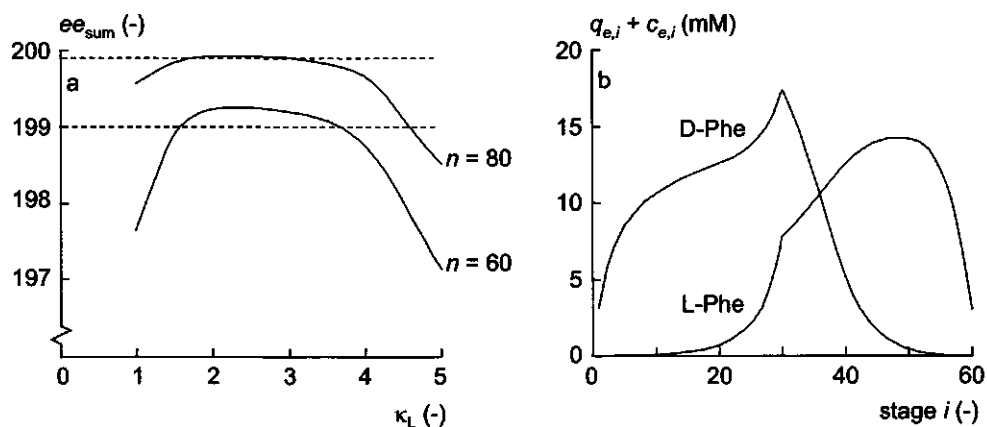


Figure 4. Cascade calculations using Langmuir equilibrium model, $\alpha_{D/L,int} = 1.9$, (a) effect of κ_L on cascade separation, ee_{sum} has been optimized for a range of κ_L using $\varphi_{B,i}$, where dotted lines represent $ee_{sum} = 199\%$ and 199.9% , respectively, (b) characteristic profiles of enantiomer concentrations ($n = 60$, $\kappa_L = 2.5$, $c_{F,e} = 40 \text{ mM}$).

For CLG and D,L-Phe, the reduction in affinity can be reached by:

- adjusting the hydrophobicity of the bulk phase to improve the preference of the enantiomers for the bulk phase [8,3].

- using another ion to form the ternary complex. Cu^{II} ions are known to form very stable ternary complexes [5,37]. Ternary complexes based on Zn^{II} , Co^{II} , and Ni^{II} have a lower stability than complexes based on Cu^{II} [38].

Of course, one could also develop another selector, possibly based on nonionic interactions. The combination of an increased selector and racemate feed concentration and a decreased affinity increases the feasibility of a separation process for D,L-Phe by enantioselective microheterogeneous media.

Process engineering

In addition to medium and selector engineering approaches, one could argue whether process engineering could offer alternatives. Therefore, we have studied the effect of the number of stages in the cascade n and the stage cuts of the bulk phase flow $\phi_{B,i}$.

Number of stages. Model calculations show that the width of the κ_L window depends on the enantioselectivity and the number of stages (Fig. 4a). Its position, of course, is a direct result of the required ee_{sum} constraint. Towards process optimization, the κ_L windows have been calculated for two ee_{sum} constraints (199% and 199.9%) and a series of $\alpha_{\text{D/L,int}}$: 1.9 (experimentally measured for our model system), 2.5, 5, and 10 (Fig. 5a). Based on the single stage calculations, it is not expected that a further increase of $\alpha_{\text{D/L,int}}$ above 10 will reduce the number of stages required to fulfill the ee_{sum} constraint [7]. The solid and dashed lines in Fig. 5a represent the intersections of the curves and the dotted lines of Fig. 4a indicating an ee_{sum} of 199% and 199.9%, respectively, for a range of n . As expected, the required number of stages increases upon increasing ee_{sum} and upon a decreasing enantioselectivity. Furthermore, at low enantioselectivities the separation is more sensitive to a deviation in κ_L , caused by the smaller distance between the extraction factor profiles of both enantiomers (Fig. 3). Consequently, more stages are needed to compensate this effect. The distance between the extraction profiles increases upon increasing enantioselectivity.

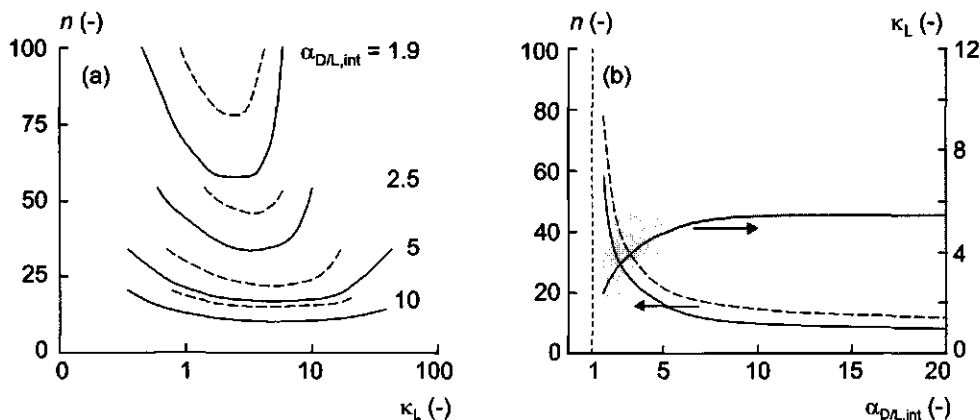


Figure 5. Cascade calculations using Langmuir equilibrium model, (a) required number of stages for a series of $\alpha_{D/L,int}$ and for an ee_{sum} of 199% (—) and 199.9% (---), (b) minimal number of stages n for an ee_{sum} of 199% (—) and 199.9% (---), and the coexisting value of κ_L . The vertical dotted line represent $\alpha_{D/L,int} = 1$.

Optimization of the number of stages is performed by plotting the minima of Fig. 5a as a function of the enantioselectivity (Fig. 5b). Indeed, the decrease in the number of stages required to reach 199% or 199.9% separation diminishes at $\alpha_{D/L,int} > 10$. Moreover, the optimal κ_L increases upon enantioselectivity. However, overdesigning the cascade by less than 5% more stages, allows a wide range of applicable κ_L values (gray area in Fig. 5b).

Of course, the number of stages alone is not sufficient to optimize the cascaded system. The costs of the system per kg of separated product should be minimized, under the condition that ee_{sum} satisfies the required purity.

Stage cuts. The stage cuts $\phi_{B,i} = \Phi_{B,i} / (\Phi_{B,i} + \Phi_{M,i})$ have a strong effect on the success of the separation in the cascade. This is shown by Storti *et al.* in simulated moving bed processes [39,40]. They have studied the effect of substrate affinity and feed composition on the flow ratios on both sides of the feeding stage in simulated moving bed processes. Similar to their results, we have found that a too high $\phi_{B,i}$ results in migration of all enantiomers with the bulk phase, so that $ee_{M,1} = 100\%$ and $ee_{B,n} = 0\%$. The reverse is the case when $\phi_{B,i}$ is too low ($ee_{M,1} = 0\%$ and $ee_{B,n} = 100\%$). Of course, in the cases where the $ee = 100\%$ there is no yield.

The optimal $\phi_{B,i}$ increases with $\alpha_{D/L,int}$ (Fig. 6a) and κ_L (not shown). Consequently, a larger membrane area per stage is required to separate the micelles from the bulk phase. On the other hand, the required number of stages decreases upon increasing $\alpha_{D/L,int}$. Hence, this

should be optimized. Moreover, the required number of chiral selector molecules (CS) per enantiomer entering the cascade decreases, since $\varphi_{M,i} = 1 - \varphi_{B,i}$ at a constant β of 1.

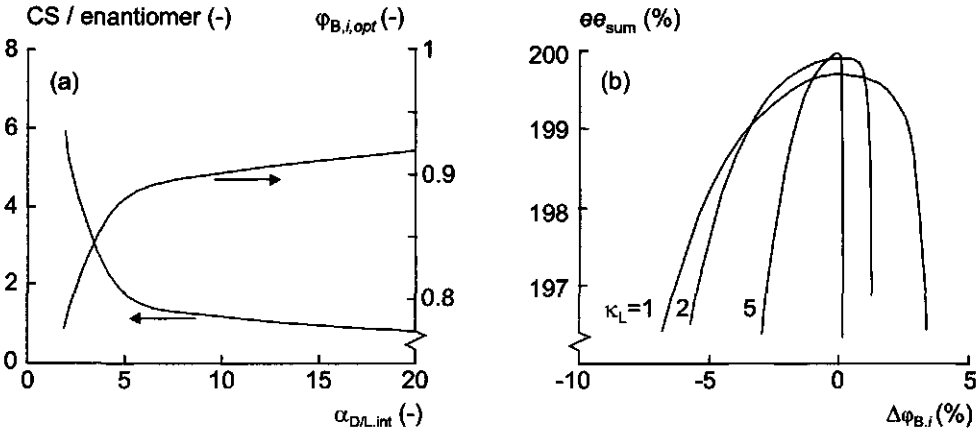


Figure 6. Cascade calculations using Langmuir equilibrium model, (a) number of chiral selector molecules entering the cascade per enantiomer and the coexisting optimal stage cut of the bulk phase ($\varphi_{B,i,opt}$), (b) sensitivity of ee_{sum} for deviation in $\varphi_{B,i}$ from $\varphi_{B,i,opt}$.

Since stage cuts are an important factor in the separation performance of the cascaded system, pump stability should be guaranteed. Fig. 6b shows that the sensitivity of ee_{sum} increases upon κ_L . Similar to our findings, Mazzotti *et al.* have calculated a decrease in robustness upon increasing κ_L , in their case upon increasing feed concentration [36]. The increased sensitivity at higher κ_L is also expressed by the V-shaped extraction factor profiles (see section 'Affinity of microheterogeneous media for the substrate'). Therefore, the $\Delta\varphi_{opt}$ -window satisfying the ee_{sum} criterion, should be maximized to improve the robustness of the system [39].

The concentration difference over the stages in the cascade can be reduced by a reflux, and therefore improve the separation, since it prevents the low affinity enantiomer to leave the system from stage 1 and facilitates it to leave the system from stage n . However, calculations ($n = 60$, $\alpha_{D/L,int} = 1.9$) show that the reflux ratios [33] of the high and low affinity enantiomers must be 2 and 10, respectively, to level the concentration profiles, which results in large regeneration flows.

So far, we have assumed that all $\varphi_{B,i}$ are the same for $i < m$ and for $i \geq m$, respectively. By tuning the stage cuts in each stage, the extraction factors can be set to values opposite from one. However, controlling all flows independently increases the system costs.

From dimensionless numbers back to system dimensions

In addition to the insight in the relation between the physical parameters describing the separation process, dimensionless numbers facilitate the scale-up of the separation process. For example, given one flow in the system the dimensionless stage cuts relate this flow to all other flows in the system. Table 5 shows the necessary system dimensions to separate a certain amount of enantiomers per day.

From case A it is concluded that the low racemic mixture concentration results in large flows through the system, so that a large membrane area is required. Moreover, the system is very large (6.5 m^3 per stage) as a consequence of the slow complexation, $3 \cdot 10^{-4} \text{ s}^{-1}$ [6]. In addition to the extra costs of a larger apparatus, large amounts of chiral media are present in the apparatus, 605 kg. Since it is expected that the chiral media will be the cost determining factor of the separation system, it is desired to improve the complexation kinetics. Note that the complexation rates of both Cu^{II} by hydroxyoximes in CTAB micelles [41] and D,L-Phe by N-decyl-L-hydroxyproline in emulsion liquid membranes [42] are only in order of seconds. If the amount of selector in the system is restricted to 1 kg (equal to the daily separated amount of racemic mixture), it is necessary to increase the complexation rate to 0.18 s^{-1} (case B) Accordingly, each stage has a volume of approximately 1 liter and requires 2.7 m^2 membrane.

Since the complexation is not limited by diffusion [6], it can be concluded that the complex formation itself is the rate limiting factor in the complexation process. Selector engineering is the apparent instrument to develop faster complexation processes.

Table 5. Required cascade dimensions in order to separate 1 kg of racemic mixture per day. The required dimensions for an ee_{sum} of 199% have been calculated for two cases. Case A represents the conditions under which the cascaded experiments have been conducted using the model system [7]. Case B represents a desired enantioselective medium that, compared to the model system: (i) contains a higher selector concentration (40 mM), (ii) has a lower affinity for the enantiomers ($K_L = 0.063 \text{ mM}^{-1}$) and (iii) performs faster. Parameters with a grey background have been fixed, others have been calculated using these constraints. For both cases: $n = 60$, $\alpha_{D/L,\text{int}} = 1.9$, $\beta = 1$, $\varphi_{B,1 < i < m} = 0.775$, $\varphi_{B,m \leq i \leq n} = 0.779$.

	A	B
productivity (kg / day)	1	1
racemic mixture feed (mM)	6.0	80 ^(c)
bulk phase flow into stage 1 (L / s)	0.50	$3.8 \cdot 10^{-2}$
system membrane area (m ²) ^(a)	$2.2 \cdot 10^3$	$1.6 \cdot 10^2$
complexation rate constant (s ⁻¹)	$3.6 \cdot 10^{-4}$	0.18
residence time (s)	$1.1 \cdot 10^4$	18
system volume (m ³) ^(b)	$3.9 \cdot 10^2$	$5.0 \cdot 10^{-2}$
selector in system (kg)	$6.1 \cdot 10^2$	1

^(a) UF experiments resulted in a permeate flux of $50 \text{ L} / \text{m}^2 \cdot \text{h}$ [7].

^(b) residence time = $3 / \text{complexation rate constant}$.

^(c) Phe solubility at 25 °C.

Concluding remarks

This study clearly proves the suitability of microheterogeneous media (in our case micelles) in cascaded ultrafiltration for molecular separations. The separation of D,L-Phe by cholesteryl-L-glutamate can be adequately described by Langmuir isotherms. The validated separation model can be used to predict the number of stages necessary to reach high purity products.

The different measured enantioselectivities for different amino acids, prompted the Laboratory of Organic Chemistry to do molecular modeling. Quantum mechanical calculations on model compounds show that subtle changes (*e.g.* due to a change in the number of coordinating water molecules), lead already to major changes in the overall structures. Therefore, in order to perform accurate calculations on large Cu^{II} bis-amino acids complexes, it is recommended to use QM/MM calculations. In this way, the metal ion and its direct surroundings are described by quantum mechanical methods, whereas other parts of the complex are described by molecular mechanics.

Model calculations show that the separation of enantiomers in a cascaded system is only successful within a certain κ -window (κ = enantiomer feed concentration multiplied by its affinity constant). Consequently, the productivity of the separation process can be improved by a reduction in affinity of the microheterogeneous media for the enantiomers. Moreover, the contribution of a higher enantioselectivity to separation decreases sharply at enantioselectivities higher than 10. Furthermore, the desired increase in selector concentration from tenths of mM to tens of mM shows that another media must be applied, due to the limited thermodynamic stability of micelles at high surfactant concentrations. So, medium engineering should focus on the development of separation media characterized by a high selector concentration and weak interactions with enantiomers. For this, one can think of polymerized micelles or dendrimers.

Ultrafiltration of microheterogeneous media in cascaded systems utilizes the benefits of chromatographic and distillation processes: preferential binding under mild conditions and counter-current flow of both the micellar phase and the bulk phase through the apparatus, respectively. Therefore, this concept provides a new basis for the development of large scale separation techniques.

Acknowledgements

The authors gratefully acknowledge financial support from the Dutch Technology Foundation (grant no. WCH44.3380), Akzo Nobel, and DSM. The authors wish to thank F. Leermakers and M.A. Cohen Stuart for the helpful discussions.

Nomenclature

A_{CS}	required area for selector/enantiomer complex	(nm^2)
$c_{e,i}$	unbound concentration in stage i	(mM)
$c_{F,e}$	enantiomer feed concentration (50% of racemic mixture)	(mM)
d_p	media particle diameter	(nm)
ee	enantiomeric excess	(%)
ee_{sum}	sum of $ee_{B,n}$ and $ee_{M,1}$	(%)
K_e	affinity constant	(mM^{-1})
n	number of stages	(-)
$q_{e,i}$	bound enantiomer concentration in stage i	(mM)
$q_{s,F}$	selector concentration in $\Phi_{M,n+1}$	(mM)

The enantiomer feed concentration ($c_{F,e}$) is half of the racemic mixture feed concentration.

Dimensionless numbers

$\alpha_{D/L,\text{int}}$	enantioselectivity	K_D / K_L
β	relative selector concentration	$q_{s,F} / c_F$
ϵ	volume fraction of media particles in solution	
$\Phi_{M,i}$	stage cut of micellar phase leaving stage i	$\Phi_{M,i} / (\Phi_{B,i} + \Phi_{M,i})$
$\Phi_{B,i}$	stage cut of bulk phase leaving stage i ($= 1 - \Phi_{M,i}$)	$\Phi_{B,i} / (\Phi_{B,i} + \Phi_{M,i})$
κ_L	relative affinity for the L-enantiomer	$K_L c_F$
$\Lambda_{e,i}$	extraction factor in stage i	$P_{e,i} (1 - \Phi_{B,i}) / \Phi_{B,i}$
$P_{e,i}$	partition factor in stage i	$(q_{e,i} + c_{e,i}) / c_{e,i}$

An apostrophe indicates a stage cuts of a flow entering a stage. The subscripts M, B, *e*, *i* and *m* represent the micellar phase, the bulk phase, the D- or L-enantiomer, the stage number and the feeding stage number, respectively.

References

- (1) Creagh, A. L.; Hasenack, B. B. E.; Van der Padt, A.; Sudhölter, E. J. R.; Van 't Riet, K. *Biotechnol. Bioeng.* **1994**, *44*, 690.
- (2) Overvest, P. E. M.; Van der Padt, A.; Keurentjes, J. T. F.; Van 't Riet, K. In *Surfactant-Based Separations: Science and Technology*; Scarnhorn, J. F.; Harwell, J. H., Eds.; ACS Symposium Series 740; American Chemical Society: Washington D.C., **1999**.
- (3) Overvest, P. E. M.; Van der Padt, A. *CHEMTECH* **1999**, *29*, no. 12, 17.
- (4) Overvest, P. E. M.; Van der Padt, A.; Keurentjes, J. T. F.; Van 't Riet, K. *Colloids and Surfaces A*, **2000**, *163*, 209.
- (5) Overvest, P.E.M.; de Bruin, T.J.M.; Sudhölter, E.J.R.; van 't Riet, K.; Keurentjes, J.T.F.; van der Padt, A. chapter 3.
- (6) Overvest, P. E. M.; Schutyser, M. A. I.; de Bruin, T. J. M.; Van 't Riet, K.; Keurentjes, J. T. F.; Van der Padt, A. chapter 4.
- (7) Overvest, P. E. M.; Hoenders, M. H. J.; Van 't Riet, K.; Keurentjes, J. T. F.; Van der Padt, A. chapter 5.
- (8) De Bruin, T. J. M.; Marcelis, A. T. M.; Zuilhof, H.; Rodenburg, L.M.; Niederländer, H.A.G.; Koudijs, A.; Overvest, P. E. M.; Van der Padt, A.; Sudhölter, E. J. R. for *Chirality* – accepted.
- (9) Gao, J. In *Reviews in Computational Chemistry*; Lipkowitz, K. B.; Boyd, D. B., Eds.; VCH: New York, **1996**; Vol. 7: pp 119-227.
- (10) Luzhkov, V.; Warshel, A. *J. Comp. Chem.* **1992**, *13*, 199.
- (11) Becke, A.D. *J. Chem. Phys.*, **1993**, *98*, 5648.
- (12) Stephens, P. J.; Devlin, F. J.; Chabalowski, C. F.; Frisch, M. J. *J. Phys. Chem.*, **1994**, *98*, 11623
- (13) De Bruin, T. J. M.; Marcelis, A. T. M.; Zuilhof, H.; Sudhölter, E. J. R. *Phys. Chem. Chem. Phys.* **1999**, *1*, 4157.

- (14) De Bruin, T. J. M.; Marcelis, A. T. M.; Zuilhof, H.; Sudhölter, E. J. R. Geometry and electronic structure of hydrated bis(glycinato)Cu^{II} complexes as studied by density functional B3LYP computations. On the problems of molecular mechanics, submitted.
- (15) De Bruin, T. J. M.; Marcelis, A. T. M.; Zuilhof, H.; Sudhölter, E. J. R. Enantioselectivity measurements of copper(II) amino acid complexes using isothermal titration calorimetry, submitted.
- (16) Evans, D. F.; Wennerström, H. *The colloidal domain*; VCH Publisher: New York, 1994.
- (17) Hebrant, M.; Toumi, C.; Tondre, C.; Roque, J. P.; Leydet, A.; Boyer, B. *Colloid and Polym. Sci.* 1996, 274, 453.
- (18) Wang, J.; Warner, I. M. *J. Chromatogr. A* 1995, 711, 297.
- (19) Overdevest, P. E. M.; Van der Padt, A. In *Proceedings of the 1998 Membrane Technology/Separation Planning Conference*; Business Communications Company, Inc.: Norwalk, 1999.
- (20) Goloub, T. P.; Koopal, L. K.; Bijsterbosch, B. H.; Sidorova, M. P. *Langmuir* 1996, 12, 3188.
- (21) Kawaguchi, T.; Hamanaka, T.; Mitsui, T. *J. Colloid Interf. Sci.* 1996, 96, 437.
- (22) Birdii, K. S. *Progr. Colloid & Polymer Sci.* 1985, 70, 23.
- (23) Hofland, H. E. J.; Bouwstra, J. A.; Verhoef, J. C.; Buckton, G.; Chowdry, B. Z.; Ponec, M.; Junginger, H. E. *J. Pharm. Pharmacol.* 1992, 44, 287.
- (24) Deroo, S. B.; Ollivon, M.; Lesieur, S. *J. Colloid Interf. Sci.* 1998, 202, 324.
- (25) Lawrence, M. J.; Lawrence, S. M.; Chauhan, S.; Barlow, D. J. *Chemistry and Physics of Lipids* 1996, 82, 89.
- (26) Shamsi, S. A.; Warner, I. M. *Electrophoresis* 1997, 18, 853.
- (27) Wang, J.; Warner, I. M. *Anal. Chem.* 1994, 66, 3773.
- (28) Chow, H.-F.; Mak, C. C. *J. Chem. Soc. Perkin Trans. 1* 1994, 2223.
- (29) Chang, H.-T.; Chen, C.-T.; Kondo, T.; Siuzdak, G.; Sharpless, K. B. *Angew. Chem. Int. Ed. Engl.* 1996, 35, 182.
- (30) Williams, C. C.; Shamsi, S. A.; Warner, I. M. In *Advances in chromatography*; Brown, P. R.; Grushka, E., Eds.; Marcel Dekker: New York, 1997.
- (31) Fréchet, J. M. J.; Hawker, C. J.; Wooley, K. L. *J. M. S. Pure Appl. Chem.* 1994, A31, 1627.
- (32) Jansen, J. F. G. A.; Van Brabander - van den Berg, E. M. M.; Meijer, E. W. *Science* 1994, 266, 1226.

- (33) Alders, L. *Liquid-liquid extraction*; Elsevier: Amsterdam, 1959.
- (34) Gentilini, A.; Migliorini, C.; Mazzotti, M.; Morbidelli, M. *J. Chromatogr. A* **1998**, *805*, 37.
- (35) Storti, G.; Baciocchi, R.; Mazzotti, M.; Morbidelli, M. *Ind. Eng. Chem. Res.* **1995**, *34*, 288.
- (36) Mazzotti, M.; Storti, G.; Morbidelli, M. *J. Chromatogr. A* **1997**, *769*, 3.
- (37) Brookes, G.; Pettit, L. D. *J. Chem. Soc. Dalton Trans.* **1977**, 1918.
- (38) Allenmark, S. *Chromatographic enantioseparation*; Ellis Horwood Limited: Chichester, 1991.
- (39) Storti, G.; Mazzotti, M.; Morbidelli, M.; Carrà, S. *AIChE J.* **1993**, *39*, 471.
- (40) Mazzotti, M.; Storti, G.; Morbidelli, M. *AIChE J.* **1994**, *40*, 1825.
- (41) Cierpiszewski, R.; Hebrant, M.; Szymanowski, J.; Tondre, C. *J. Chem. Soc. Dalton Trans.* **1996**, *92*, 249.
- (42) Pickering, P. J.; Chaudhuri, J. B. *Chem. Eng. Sci.* **1997**, *52*, 377.

Appendix

Nonionic surfactants used in separation experiments. Tween surfactants are characterized by a common head group of sorbitan and poly(ethylene oxide), where only the alkyl tail group differs in length (C_p -sorbitan- E_{20}). Brij surfactants differ both in tail as in head group length (C_pE_r).

trivial name	Chemical name	p
Tween 20	Polyoxyethylene(20) ^(a) sorbitan monolaurate	11
Tween 40	Polyoxyethylene(20) sorbitan monopalmitate	15
Tween 60	polyoxyethylene(20) sorbitan monostearate	17
Tween 80	polyoxyethylene(20) sorbitan monooleate	17
Brij 30	polyoxyethylene(4) lauryl ether	11
	polyoxyethylene(10) lauryl ether	11
Brij 35	polyoxyethylene(23) lauryl ether	11
Brij 56	polyoxyethylene(10) cetyl ether	15
Brij 58	polyoxyethylene(20) cetyl ether	15
Brij76	polyoxyethylene(10) stearyl ether	17
Brij 78	polyoxyethylene(20) stearyl ether	17

(a) length of hydrophilic head group as number (r) of ethylene oxide units.

SUMMARY

The fact that the mirror images of chiral compounds (enantiomers) can have different biological activities has forced pharmaceutical, food and agrochemical industries to develop methods for the production of optically pure compounds. Optically pure compounds can be directly obtained from the chiral pool or by (bio)chemical (total) synthesis. Additionally, the desired compounds can be separated from racemic mixtures. The production of these mixtures is more or less straightforward, although its separation is not, since their physical properties only differ in chiral media.

At Wageningen University a new enantiomer separation system is under development that is based on the ultrafiltration (UF) of enantioselective micelles containing chiral Cu^{II} -amino acid derivative selector molecules. The selector molecules preferentially form a ternary complex with one enantiomer of a pair of enantiomers, while unbound enantiomers can pass the membrane during the UF process. We have studied the separation of D-, and L-phenylalanine (Phe) enantiomers by UF of cholesteryl-L-glutamate (CLG) anchored in nonionic micelles. Since one single UF stage is inadequate for nearly complete (99+%) separations of both enantiomers, the separation has been studied in a cascaded system of multiple UF stages.

A two component Langmuir model is developed that predicts the competitive complexation at various pH. Both independent experiments and statistics show that nonselective complexation and membrane rejection of unbound enantiomers can be neglected if compared to the enantioselective complexation by CLG. It is shown that complexation only occurs at pH 7 and up. To design an economically attractive separation process, regeneration of D-Phe saturated micelles leaving the multistage system is inevitable. Regeneration, *i.e.* recovery of enantioselective micelles for reuse, is possible at $\text{pH} \leq 4$. To keep the salt production to a minimum, the shift in pH between the separation and the regeneration process must be minimized. Therefore, a separation process at pH 7 seems attractive.

The Linear Driving Force model describes both the complexation and decomplexation rates of enantiomers by the enantioselective micelles. The complexation is not instantaneous, characteristic complexation time approximates one hour. Decomplexation of both enantiomers is even slower, fortunately, a rapid exchange of bound L-Phe by unbound D-Phe improves the decomplexation rate of L-Phe. This exchange process can be described by a second order LDF model. Since the enantioselectivity is not kinetically controlled, it is expected that the selector effectiveness is fully attained when each stage is at equilibrium.

Using the previously estimates Langmuir isotherms a model has been developed that predicts the separation by enantioselective micelles in a cascade of UF stages. This separation model

has been validated by a cascaded system containing five stages and by simulating a cascade of 60 stages in a single stage bench scale system by controlling its enantiomer feed concentrations. In both systems, the model has proven its suitability to adequately describe the separation of both Phe enantiomers. This validated separation model has been used to optimize the number of stages necessary to reach high purity products.

Calculations with this validated model have shown that the following aspects can be effected to improve the performance of the counter-current separation system:

- An increase of $\alpha_{D/L,int}$ (intrinsic enantioselectivity) up to 10 strongly reduces the required number of stages to attain high purities of both enantiomers. Higher values of $\alpha_{D/L,int}$ do not greatly reduce the number of stages.
- A reduction in affinity allows to proportionally increase the feed concentration.
- The selector concentration should be in the same order as the enantiomer feed concentration. Hence, operating at high feed concentrations implies high selector concentrations. Reviewing several microheterogeneous media, such as micelles, vesicles, polymerized micelles, and dendrimers, has shown that only polymerized micelles and dendrimers can anchor sufficient chiral selectors in order to separate Phe enantiomers at their solubility concentration.
- Ultimately, the slow complexation rate is responsible for a large apparatus. Improving the complexation rate reduces the system volume and hence reduces the amount of chiral selectors present in the system.

This research has made clear that UF of enantioselective micelles in a cascaded system is a promising new technique to separate enantiomers at preparative scale. This concept exploits the advantageous aspects of chromatographic and distillation processes: preferential binding under mild conditions and counter-current flow, respectively. In general, this UF process can be applied for any aqueous solute separation, characterized by weak and fast substrate interactions and a high selector concentration.

SAMENVATTING

Het feit dat de spiegelbeelden van chirale componenten (enantiomeren) verschillende biologische activiteiten kunnen vertonen, hebben farmaceutische, voedingsmiddelen-, en agrochemische industrieën er toe gezet methoden te ontwikkelen die de productie van enantiomeer-zuivere stoffen op industriële schaal mogelijk maakt. Deze stoffen kunnen direct gewonnen worden uit de natuur of kunnen worden verkregen door (bio)chemische synthese. Daarnaast kunnen de gewenste chirale componenten gescheiden worden uit een racemaat (50/50 mengsel van beide spiegelbeeldmoleculen). De productie van een racemaat is min of meer eenvoudig, terwijl de scheiding daarvan dit niet is, omdat de verschillen tussen beide enantiomeren alleen tot uiting komen in een chirale omgeving.

Binnen Wageningen Universiteit is een nieuw enantiomeerscheidingsysteem in ontwikkeling dat gebaseerd is op ultrafiltratie (UF) van enantioselectieve micellen die chirale selectormoleculen (een Cu^{II} -aminozuurderivaat) bevatten. Deze selectoren vormen preferent een complex met één van beide typen enantiomeren, terwijl ongebonden enantiomeren het membraan kunnen passeren gedurende het filtratieproces. Micellen kunnen het membraan niet passeren. We hebben de scheiding bestudeerd van D- en L-fenylalanine (Phe) door cholesteryl-L-glutamaat selectoren (CLG), die verankerd zijn in ongeladen micellen. Omdat een enkele UF-eenheid niet toereikend is voor een bijna volledige scheiding (99⁺%) van beide enantiomeren, is de scheiding bestudeerd in een serie van UF-eenheden (meertraps).

Een Langmuir model is ontwikkeld die de concurrerende complexatie bij verschillende zuurgraden (pH) beschrijft. Zowel onafhankelijke experimenten als statistische analyse tonen aan dat niet-enantioselectieve complexatie en membraanrejectie van ongebonden enantiomeren verwaarloosd kan worden indien het vergeleken wordt met de selectieve complexatie door CLG. Aangetoond wordt dat complexatie alleen bij pH 7 en hoger plaatsvindt. Om een economisch aantrekkelijk scheidingsproces te ontwerpen, is regeneratie van verzadigde micellen, die het meertrapssysteem verlaten, onontkoombaar. Regeneratie, terugwinning van de enantioselectieve micellen voor hergebruik, is mogelijk bij pH 4 en lager. Om de zoutproductie tot een minimum te beperken, moet de pH stap tussen het scheidings- en het regeneratieproces geminimaliseerd worden. Daarom lijkt een scheidingsproces bij pH 7 aantrekkelijk.

Het *Linear-Driving-Force*-model beschrijft zowel de complexatie als decomplexatie snelheden van de enantiomeren door de enantioselectieve micellen. De complexatie is niet ogenblikkelijk, de karakteristieke complexatietijd benadert een uur. Decomplexatie van beide enantiomeren is zelfs trager, gelukkig, verbetert een snelle uitwisseling van gebonden L-Phe door ongebonden D-Phe de decomplexatiesnelheid van L-Phe. Dit uitwisselingsproces kan beschreven worden door een tweede orde LDF model. Omdat de enantioselectiviteit niet

snelheidsgecontroleerd is, wordt verwacht dat de selectoreffectiviteit ten volle benut wordt indien elke trap in evenwicht is.

Gebruikmakend voor de Langmuir-isothermen is een model ontwikkeld dat de scheiding door enantioselectieve micellen in een serie van UF-eenheden beschrijft. Dit scheidingsmodel is gevalideerd door een serie van vijf trappen en door een benadering van een serie van 60 trappen met een enkeltrapssysteem op werkbankschaal door sturing van de voedingsconcentraties van de enantiomeren. In beide systemen heeft het model bewezen de scheiding van beide enantiomeren adequaat te kunnen beschrijven. Dit gevalideerde scheidingsmodel is gebruikt om het aantal trappen te optimaliseren die nodig zijn om producten met hoge zuiverheid te verkrijgen.

Berekeningen met het gevalideerde scheidingsmodel hebben aangetoond dat de volgende aspecten gebruikt kunnen worden om de prestatie te verbeteren van het meertrapssysteem:

- Een toename van $\alpha_{D/L,int}$ (intrinsieke enantioselectiviteit) tot 10 reduceert het benodigde aantal trappen om producten met hoge zuiverheid te verkrijgen drastisch. Hogere waarden van $\alpha_{D/L,int}$ hebben nagenoeg geen effect op het benodigde aantal trappen.
- Een afname in affiniteit maakt een toename in racemaatvoedingsconcentratie mogelijk.
- De selectorconcentratie moet van dezelfde orde zijn als de voedingsconcentratie van een van beide enantiomeren (50% van de racemaatconcentratie). Verschillende microheterogene media bestudierend, zoals micellen, vesikels, gepolymeriseerde micellen en dendrimeren, heeft aangetoond dat van deze media alleen de twee laatst genoemde voldoende chiraalselectoren kunnen bevatten om Phe enantiomeren te kunnen scheiden bij de D,L-Phe oplosbaarheidsconcentratie (in de orde van 80 mM).
- Tenslotte leidt de lage complexatiesnelheid tot een groot systeem. Verhoging van de complexatiesnelheid reduceert het volume van het systeem en daarmee ook de hoeveelheid selectoren die aanwezig zijn in het systeem.

Dit onderzoek heeft duidelijk gemaakt dat UF van enantioselectieve micellen in een meertrapssysteem een veelbelovende nieuwe techniek is om op grote schaal enantiomeren te scheiden. Dit concept maakt gebruik van de voordelige aspecten van chromatografische en destillatieprocessen: preferente binding onder milde condities en het tegenstroomprincipe, respectievelijk. In het algemeen kan dit UF-proces toegepast worden voor iedere scheiding in waterachtige oplossingen, gekarakteriseerd door zwakke en snelle substraatinteracties en een hoge selectorconcentratie.

CURRICULUM VITAE

Pieter Everhardus Maria Overdevest werd op 16 september 1970 geboren te Wassenaar. In 1988 behaalde hij zijn HAVO diploma aan het St. Adelbert College eveneens te Wassenaar, gevolgd door het behalen van zijn VWO-B diploma in 1989. In datzelfde jaar begon hij met zijn studie aan de toenmalige Landbouwwuniversiteit Wageningen.

Na het behalen van de propaedeuse Moleculaire Wetenschappen met lof stapte hij over naar de studie Bioprocestechnologie. In juni 1995 studeerde hij met lof af met afstudeervakken in Proceskunde en Meet- Regel- en Systeemtechniek. Zijn stage periode bracht hij door bij Unilever Reseach Laboratorium te Vlaardingen bij dr. R. Soeterboek en dr. M.L.F. Giuseppin.

Vanaf mei 1995 tot en met augustus 1999 was hij als AIO werkzaam aan de sectie Proceskunde van Landbouwwuniversiteit Wageningen waar het onderzoek, zoals beschreven in dit proefschrift, werd uitgevoerd.

Vanaf november 1999 is hij werkzaam bij de groep Home and Personal Care van het Unilever Reseach Laboratorium te Vlaardingen.